



HAL
open science

Enveloped viruses distinct from HBV induce dissemination of hepatitis D virus in vivo

Jimena Pérez-Vargas, Fouzia Amirache, Bertrand Boson, Chloé Mialon, Natalia Freitas, Camille Sureau, Floriane Fusil, Cosset François-Loïc

► **To cite this version:**

Jimena Pérez-Vargas, Fouzia Amirache, Bertrand Boson, Chloé Mialon, Natalia Freitas, et al.. Enveloped viruses distinct from HBV induce dissemination of hepatitis D virus in vivo. *Nature Communications*, 2019, 10, pp.2098. 10.1038/s41467-019-10117-z . hal-02351240

HAL Id: hal-02351240

<https://hal.science/hal-02351240>

Submitted on 6 Nov 2019

HAL is a multi-disciplinary open access archive for the deposit and dissemination of scientific research documents, whether they are published or not. The documents may come from teaching and research institutions in France or abroad, or from public or private research centers.



L'archive ouverte pluridisciplinaire **HAL**, est destinée au dépôt et à la diffusion de documents scientifiques de niveau recherche, publiés ou non, émanant des établissements d'enseignement et de recherche français ou étrangers, des laboratoires publics ou privés.

ARTICLE

<https://doi.org/10.1038/s41467-019-10117-z>

OPEN

Enveloped viruses distinct from HBV induce dissemination of hepatitis D virus in vivo

Jimena Perez-Vargas¹ , Fouzia Amirache¹, Bertrand Boson¹, Chloé Mialon¹, Natalia Freitas¹, Camille Sureau², Floriane Fusil¹ & François-Loïc Cosset¹ 

Hepatitis D virus (HDV) doesn't encode envelope proteins for packaging of its ribonucleo-protein (RNP) and typically relies on the surface glycoproteins (GPs) from hepatitis B virus (HBV) for virion assembly, envelopment and cellular transmission. HDV RNA genome can efficiently replicate in different tissues and species, raising the possibility that it evolved, and/or is still able to transmit, independently of HBV. Here we show that alternative, HBV-unrelated viruses can act as helper viruses for HDV. In vitro, envelope GPs from several virus genera, including vesiculovirus, flavivirus and hepacivirus, can package HDV RNPs, allowing efficient egress of HDV particles in the extracellular milieu of co-infected cells and subsequent entry into cells expressing the relevant receptors. Furthermore, HCV can propagate HDV infection in the liver of co-infected humanized mice for several months. Further work is necessary to evaluate whether HDV is currently transmitted by HBV-unrelated viruses in humans.

¹ CIRI—Centre International de Recherche en Infectiologie, Univ Lyon, Université Claude Bernard Lyon 1, Inserm, U1111, CNRS, UMR5308, ENS Lyon, 46 allée d'Italie, F-69007 Lyon, France. ² Molecular Virology laboratory, Institut National de la Transfusion Sanguine (INTS), CNRS Inserm U1134, 6 rue Alexandre Cabanel, F-75739 Paris, France. Correspondence and requests for materials should be addressed to F.-L.C. (email: flcosset@ens-lyon.fr)

Hepatitis D virus (HDV) was discovered 40 years ago in the liver of individuals chronically infected with hepatitis B virus (HBV), a liver-specific pathogen present in ca. 250 million people. The HDV virion released in the extracellular milieu is an enveloped particle with an average diameter of 36 nm. It consists of a cell-derived lipid envelope harboring HBV surface proteins and coating an inner ribonucleoprotein (RNP)^{1–4}, which is composed of a multimer of ca. 70 copies of the HDV-encoded delta antigen (HDAg) protein^{5,6} that is associated to one copy of the small circular single-strand HDV RNA exhibiting self-annealing properties, conferring its rod-like conformation^{6,7}. Although HDAg was initially considered as a novel HBV antigen⁸, it was later shown to be associated with a small RNA as a transmissible and defective agent that uses the HBV envelope glycoproteins (GP) for its propagation, hence reflecting its nature of an obligate satellite of HBV. Indeed, HDV particles appear not to require specific cellular functions to promote egress of its RNP and to only rely on the budding mechanism provided by HBV envelope GPs, which hence offers the exclusive HBV contribution to the HDV life cycle. Their ensuing envelopment subsequently allows targeting and entry of HDV particles to human hepatocytes via mechanisms that depend on the same host entry factors than those used by HBV itself, i.e., through low-affinity attachment to cell surface heparan sulfate proteoglycans (HSPGs)^{9,10} and subsequent high-affinity engagement to the sodium taurocholate cotransporting polypeptide (NTCP)^{11,12}.

Noteworthy, the origin of HDV is currently unknown. The characterization of the HDAg-associated RNA, the HDV genome, revealed that it is unique among animal viruses and that it shares some properties with some plant agents called viroids^{13,14}. Indeed, the replication of its RNA involves the HDAg-mediated subversion of cellular RNA polymerase(s), such as Pol-II. Both genomic HDV RNA and antigenomic RNA (its replication intermediate) strands include ribozyme autocatalytic, self-cleaving elements. Interestingly, cells from highly divergent organisms express several HDV-like cellular ribozymes that play a role in many biological pathways^{15,16}. This has raised the possibility that HDV RNA originated from the cell transcriptome itself, in agreement with the finding that circular RNA species are abundant in cells¹⁷. Therefore, one possibility could be that the HDV RNA has emerged in HBV-infected hepatocytes subsequent to evolution of cellular circular RNA forms becoming autonomously replicative¹⁸ and for which the ribozyme and HDAg-coding RNA sequences may have arisen from the human transcriptome^{19,20}. Accordingly, that HBV, a strictly liver-tropic human pathogen, only provides RNP envelopment and transmission functions would therefore explain why HDV has been exclusively detected in the liver of HBV-infected patients. Alternatively, that HDV RNA can self-replicate in a much wider variety of cell types and species^{21–23} raises the theoretical possibility that it may be transmitted through unorthodox means. Furthermore, viruses closely related to HDV have been detected in non-human species in the absence of any hepadnavirus^{24,25}. Also, primary Sjögren's syndrome patients were reported to present HDV antigen and RNA in salivary glands in the absence of HBsAg or HBV antibodies²⁶.

Here, aiming to explore scenarios concerning the origin of HDV, we investigate the possibility that other, HBV-unrelated viruses could provide helper envelopment, budding, and entry functions. Our results indicate that HDV RNPs may exploit assembly functions provided by viruses from several alternative genera and families, including vesiculovirus, flavivirus, and hepacivirus, among other enveloped viruses. This compatibility allows efficient egress in the extracellular milieu of co-infected cells of HDV particles that appear to be infectious. This leads to

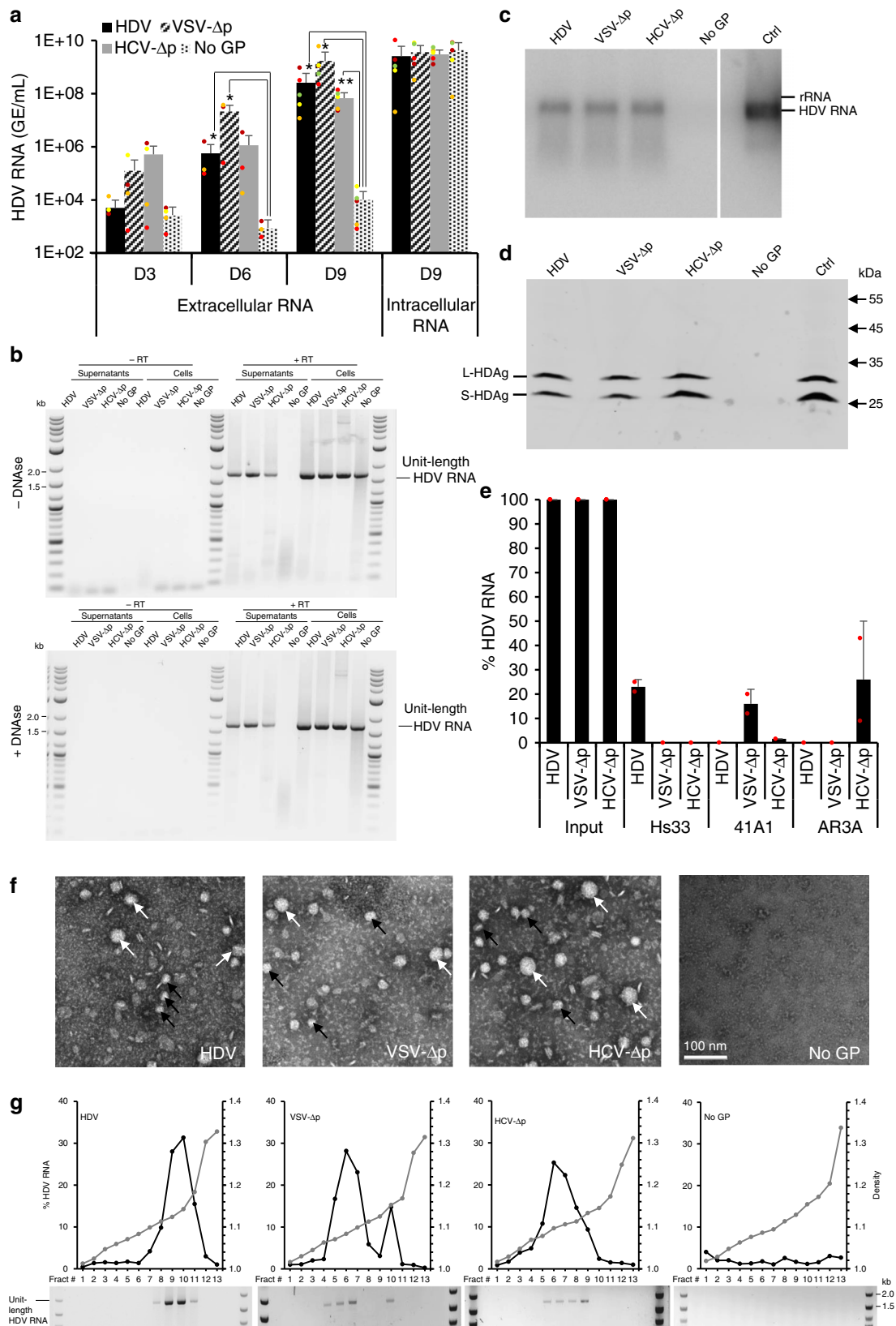
their subsequent entry into different cell types expressing the receptors targeted by the GPs of either virus genus and dissemination of HDV genome *in vivo* in experimentally infected humanized mice.

Results

HDV particle assembly with vesiculovirus and hepacivirus GPs. HDV particles were produced in Huh-7 cells by co-transfecting two plasmids, a first one providing the envelope GPs from HBV vs. alternative enveloped viruses, i.e., vesicular stomatitis virus (VSV) G protein and hepatitis C virus (HCV) E1E2 proteins, and a second one initiating the replication of the HDV RNA genome (pSVLD3²⁷) that encodes the HDV delta protein (HDAg). As controls, we co-transfected with pSVLD3 an “empty” plasmid that does not encode GPs (“No GP”) for assessing specific production, release, and infectivity of HDV particles. At 3, 6, and 9 days post transfection, the production of HDV particles was determined by quantifying by RT-qPCR of the HDV RNAs from the supernatants. While HDV RNAs accumulated at high levels in producer cells for all transfection conditions, reflecting its self-replication independently of GP expression, it was readily detected in the cell supernatants when the HBV GPs were co-expressed in transfected cells (Fig. 1a) with an over 4-log fold increase after day 3, in agreement with previous reports^{28,29}. In contrast, no significant HDV RNA secretion could be detected over the RT-qPCR threshold levels when pSVLD3 was transfected without GP (“No GP” control), confirming that HDV RNA release from cells requires co-expression of HBV GPs²⁹.

Strikingly, we found that the release of HDV RNAs could also be induced by envelope GPs from alternative viruses, as suggested by progressively increased secretion of extracellular HDV RNAs over time post transfection (Fig. 1a). Specifically, at day 9 post transfection, we detected high levels of HDV RNA in the supernatants of cells co-expressing these GPs and HDV RNAs, by up to 10⁹ GE/mL for VSV-G GP-expressing cells, i.e., ca. sixfold higher than for HBV GPs, and by ca. 5 × 10⁷ GE/mL for HCV-E1E2 GP-transfected cells (Fig. 1a). We confirmed that these extracellular RT-qPCR signals reflected bona fide HDV RNAs, as shown by strand-specific RT-PCR experiments that detected genomic HDV RNA at the expected size of 1.7 kb (Fig. 1b) and by northern blot experiments performed on pellets of ultracentrifuged supernatants from producer cells that revealed full-length HDV RNAs (Fig. 1c). Then, using a strand-specific RT-qPCR assay^{30,31} that specifically quantifies either genomic (gRNA) or antigenomic (agRNA) HDV RNAs (Supplementary Fig. 1f), we found a strong enrichment of HDV gRNA in the supernatants of cells transfected by pSVLD3 and either of these GP expression plasmids, as compared with lysates of producer cells (Supplementary Fig. 1a–c). The HDV gRNAs accounted for over 99% of HDV RNAs detected in the supernatants of these cells (Supplementary Fig. 1d–e), suggesting that VSV and HCV GPs induced extracellular release of genomic HDV RNA in a manner similar to HBV GPs.

Next, we sought to investigate the biochemical form of these extracellular genomic HDV RNAs. As shown in Fig. 1e, we found that immunoprecipitation of producer cell supernatants with antibodies against HBV, VSV, or HCV GPs could co-precipitate HDV RNAs in a GP-specific manner, which suggested that the latter are in the form of GP-associated RNPs. In agreement with this possibility, when we immunoblotted the pellets of ultracentrifuged producer cell supernatants with HDAg antibodies (Fig. 1d), we found similar levels and ratios of L- and S-HDAg for particles generated with HCV and VSV GPs as compared with “normal” HDV particles produced with HBV GPs. This suggested that the detected genomic HDV RNAs (Fig. 1a–c) are



incorporated as RNPs exhibiting wild-type properties. Of note, co-expression of HDV RNPs with HCV and VSV GPs did not induce higher cytotoxicity levels than those detected in cells producing “normal” HDV particles or in non-transfected cells (Supplementary Fig. 2), suggesting genuine processes of envelopment and production of these novel HDV particles. Altogether,

these results indicated that HDV can be enveloped by different types of viral surface glycoproteins, which induces secretion of HDV RNPs in the extracellular milieu.

To further characterize the non-HBV-induced HDV particles (Δp) coated with VSV-G or HCV-E1E2 envelope GPs, hereafter designated VSV- Δp and HCV- Δp , we incubated the supernatants

Fig. 1 Secretion of HDV particles is induced by surface glycoproteins from varied enveloped viruses. Huh-7 cells were co-transfected with pSVLD3 plasmid coding for HDV RNPs and plasmids coding for HBV, VSV, or HCV surface glycoproteins (GP), resulting in “HDV”, “VSV- Δ p”, and “HCV- Δ p” samples, respectively. As control, pSVLD3 was co-transfected with an empty plasmid (“No GP” samples). **a** At day 3, 6, or 9, extracellular HDV RNAs were quantified from cell supernatants by RT-qPCR. Intracellular HDV RNAs were quantified from cell lysates at day 9 post transfection. HDV RNA levels in GE (genome equivalent) are expressed as means ($n = 5$ independent experiments) per ml of cell supernatants for extracellular RNAs or, for intracellular RNAs, per mL of cell lysates containing 10^6 cells. **b** RNAs extracted from lysates and supernatants of transfected cells treated with RNase-free DNase, or not treated (-DNase), were reverse-transcribed using an antigenomic primer that detects HDV RNAs and then PCR-amplified with HDV-specific primers to reveal unit-length HDV genomic RNAs. As control, reverse transcriptase was omitted during processing of the samples (-RT). **c, d** In total, 2×10^7 HDV GEs from pellets retrieved after ultracentrifugation of cell supernatants on 30% sucrose cushions were analyzed by northern blot using a HDV-specific probe (**c**) or by western blot using an HDAg antibody (**d**). Control HDV RNAs (5×10^7 GE) (**c**) or HDAg from cell lysates (**d**) were loaded on the same gels (Ctrl). **e** Pelleted cell supernatants containing 10^9 HDV GEs (“Input”) immunoprecipitated with antibodies against HBsAg (Hs33 mAb), VSV-G (41A1 mAb), and HCV-E1E2 (AR3A mAb) glycoproteins, as indicated, were quantified by RT-qPCR after elution. The results are expressed as percentages of input values. **f** Electron microscopy of heparin bead-purified supernatants after elution and negative staining showing large (white arrows) and small (black arrows) particles. Scale bar: 100 nm. **g** HDV RNAs, from fractions from cell supernatant samples separated on equilibrium-density gradients, were analyzed by RT-qPCR, expressed as percentages of total HDV RNA contents, or by strand-specific RT-PCR that reveals HDV genome size (below each graph). Source data are provided as a Source Data file. Error bars correspond to standard deviation. Statistical analyses (Student’s *t*-test): $p < 0.05$ (*).

of Δ p-producer cells with heparin-coated beads and we examined the eluted material by electron microscopy. We observed two types of spheres with diameters of 35–40 and 25–30 nm (Fig. 1f). The small spheres likely corresponded to subviral particles since they were also detected when VSV-G and HCV-E1E2 were expressed alone, similar to HBV GPs (Supplementary Fig. 3c, 3d), whereas the large spheres, that were only detected when HDV RNA were transcribed along with either co-expressed GP (Supplementary Fig. 3a, 3b), could correspond to VSV- Δ p and HCV- Δ p particles. Next, the supernatants of Δ p-producer cells were subjected to equilibrium centrifugation on preformed iodixanol density gradients. Fractions collected from the gradients were assayed for density and HDV RNA by RT-qPCR (Fig. 1g). We found that HDV particles assembled with HBV GPs (noted “HDV” in the figures) exhibited a major peak of HDV RNAs at 1.12–1.14 g/mL, whereas HDV RNAs were detected at lower densities of 1.07–1.10 for VSV- Δ p and of 1.08–1.13 for HCV- Δ p (Fig. 1g). Finally, we found that these secreted HDV RNAs were genomic RNAs, as shown by strand-specific RT-PCR-binding assays (Fig. 1g, below density graphs). Altogether, these results indicated that heterologous envelope GPs can induce assembly of HDV particles, which are homogeneous and peak at densities likely reflecting the physicochemical features of the combination of HDV RNPs with these envelope GPs of different natures.

HDV assembled with heterologous envelope GPs is infectious.

To determine whether the HDV particles produced with VSV-G or HCV-E1E2 envelope GPs were infectious, we performed infection assays using HDV replication-permissive Huh-106, Huh-7, and 293T cells that express different sets of virus entry receptors. At 7 days post inoculation, i.e., corresponding to the plateau of HDV RNA replication^{29,32} (see below), the levels of infected cells and intracellular HDV RNAs were measured by counting HDAg-positive focus-forming units (FFU) via HDAg immunofluorescence (Fig. 2b, c) and by RT-qPCR (Fig. 2a), respectively. We found that the HDV particles produced with HBV envelope GPs could readily induce HDV RNA replication in inoculated Huh-106 cells expressing the HBV receptor, NTCP, but neither in Huh-7 nor in 293T cells, that are NTCP-negative, over the experimental thresholds provided by the “No GP” conditions, in agreement with previous studies^{12,33}. Importantly, we found that the VSV- Δ p and HCV- Δ p particles were infectious (Fig. 2a–c). First, through RT-qPCR detection of HDV RNA in inoculated cells, we found that VSV- Δ p could readily induce HDV RNA replication in the three cell types that all express the VSV-G receptor, LDLr^{34,35}, whereas HCV- Δ p could efficiently infect Huh-106 and Huh-7 cells but less efficiently 293T cells

(Fig. 2a), in line with the differential expression of HCV receptors in either cell type³⁶. Second, by using limiting dilution assays through immunofluorescence detection of HDAg (Fig. 2b), which indicated translation of HDV RNAs in inoculated cells, we confirmed that the levels of infectivity detected for the VSV- Δ p and HCV- Δ p particles were comparable to those of HBV GP-coated HDV particles. We deduced that all three particles type had similar specific infectivity, which is defined here by the ratio between the number of infectious viruses (measured in FFUs) and the amounts of viral RNA-containing particles (determined by RT-qPCR), with one infectious particle per 4000–7000 physical particles (Fig. 2d).

Next, to demonstrate that HDV RNA was transmitted by a bona fide HDV infectious process, we incubated producer cells with Lonafarnib, an inhibitor of prenylation that prevents HDV assembly^{37,38}, which requires RNP targeting to the ER membrane by farnesylation of L-HDAg³⁸. We found that Lonafarnib could readily inhibit production of HBV GP-coated HDV, VSV- Δ p, and HCV- Δ p particles (Fig. 3a) and hence, transmission and replication of HDV RNA in inoculated cells (Fig. 3b). These results indicated that farnesyl-mediated targeting to ER or other cell membranes is required for assembly of VSV- Δ p and HCV- Δ p particles, suggesting that they share with HDV the same early steps, leading to production of infectious particles. Through time-course analysis, we found that cells inoculated with VSV- Δ p and HCV- Δ p particles accumulated over time post infection both gRNA and agRNA (Fig. 3c), which indicated that HDV RNAs could be amplified in a typical manner following entry into cells. We show that this correlated with accumulation of genomic-size HDV RNA (Fig. 3d) as well as of S-HDAg and L-HDAg proteins (Fig. 3e) at similar levels and/or ratios than for HBV GP-coated HDV particles, which indicated that full-sized HDV genomes were replicated and translated in infected cells. Altogether, these results demonstrated that HDV particles coated with the envelope GPs of VSV and HCV induce functional entry into cells and, hence, are infectious.

Then, to establish if VSV- Δ p and HCV- Δ p enter in the cells through the same pathways as for the parental viruses (VSV and HCV), particles were pre-incubated with antibodies that are known to neutralize VSV and HCV before their inoculation onto Huh-106 cells. The results in Fig. 4a show that the Hs33 antibody targeting the HBsAg protein readily neutralized HDV particles bearing HBV GPs but not HDV particles bearing the other GPs. Conversely, the 41A1 antibody that blocks the entry of VSV³⁶ neutralized VSV- Δ p, whereas the AR3A antibody that neutralizes HCV³⁹ could only prevent infection of HCV- Δ p particles. Then, we sought to block the cell receptors used by either parental virus with specific inhibitors (Fig. 4b). We found that while taurocholic

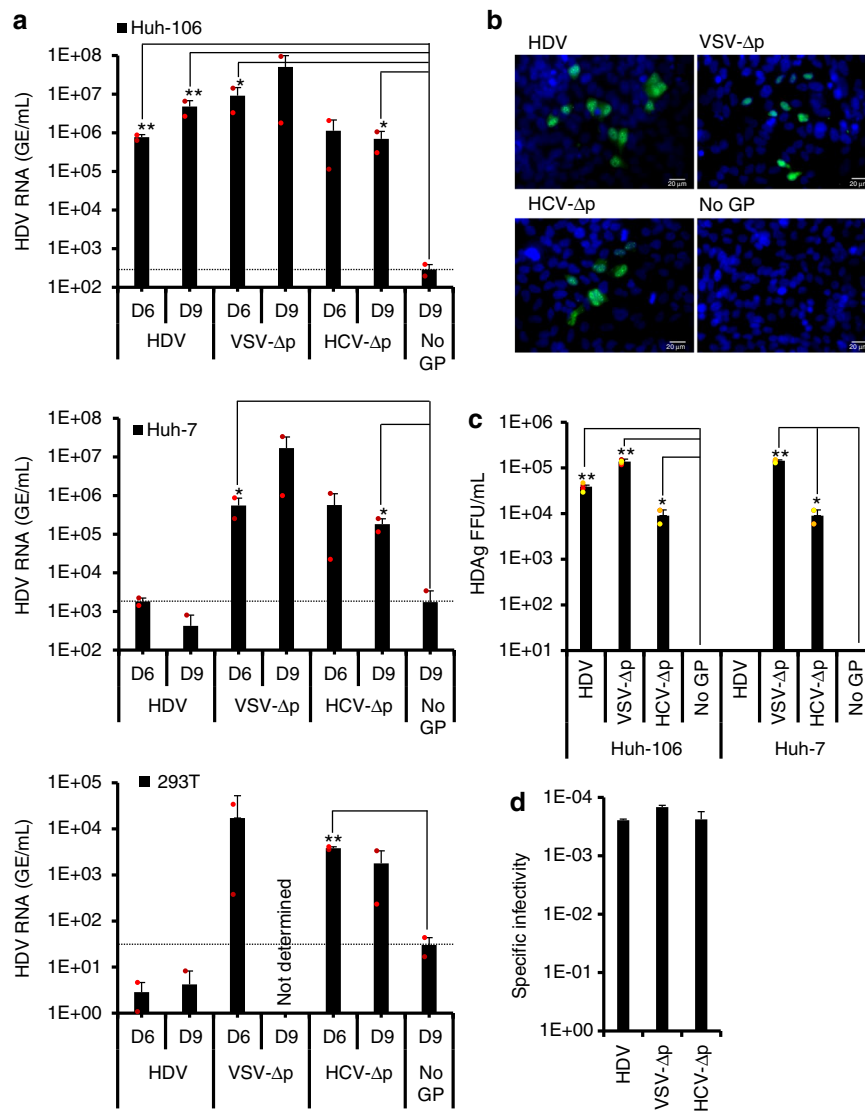


Fig. 2 HDV particles generated with heterologous envelope glycoproteins are infectious. **a** The infectivity of virus particles produced with HBV (HDV), VSV (VSV-Δp), HCV (HCV-Δp) glycoproteins, or with no envelope glycoprotein (No GP) and harvested at day 6 or 9 post transfection (see Fig. 1a) was determined in Huh-106 (NTCP-expressing Huh-7 cells), Huh-7, or 293T cells, as indicated. Infected cells were grown for 7 days before total intracellular RNA was purified. The results of HDV RNA quantification by RT-qPCR are expressed as means ($n = 2$ independent experiments) per mL of cell lysates containing 10^5 cells. Nd, not determined. The dotted lines represent the experimental thresholds, as defined with the “No GP” controls. **b, c** Huh-106 and Huh-7 cells infected by serial dilutions of supernatants containing the indicated virus particles harvested at day 9 post transfection (Fig. 1a) were fixed at 7 days post infection and stained by immunofluorescence with the SE1679 polyclonal anti-HDAg antibody before counting the foci of HDAg-positive cell colonies. The cells were counterstained with Hoechst to visualize the nuclei. Scale bars represent 20 μm (**b**). The results from colony counting are expressed as means ($n = 4$ independent experiments) of FFU per mL of cell supernatants (**c**). **d** The specific infectivity values of the indicated viruses determined in Huh-106 infected cells were calculated from the experiments shown in **c** using the infectious titers and the HDV RNA contents of the inoculums. The results show the ratios of HDAg-positive FFU induced by HDV RNA from the same inoculums. Source data are provided as a Source Data file. Error bars correspond to standard deviation. Statistical analyses (Student’s *t*-test): $p < 0.05$ (*); $p < 0.01$ (**)

acid (TCA) specifically inhibited infection of Huh-106 cells with HDV particles produced with HBV GPs, as expected¹², antibodies against LDLr and CD81 (i.e., one of the HCV receptors) blocked the entry of VSV-Δp and HCV-Δp particles, respectively, though LDLr antibodies exhibited some nonspecific levels of inhibition. Altogether, the results of virus-neutralization and receptor-blocking assays indicated that the conformation of the surface of VSV-Δp and HCV-Δp particles is similar to that of parental viruses and able to mediate GP-specific cell entry through their corresponding receptors.

Thereafter, we explored if HDV particles could be produced with envelope GPs from a broader set of enveloped viruses.

Hence, we co-transfected pSVLD3 with plasmids encoding the GPs from RD114 cat endogenous virus, murine leukemia virus (MLV), human immunodeficiency virus (HIV), avian influenza virus (AIV), lymphocytic choriomeningitis virus (LCMV), human metapneumovirus (HMPV), dengue virus (DENV), and West Nile virus (WNV), which did not prevent HDV RNA replication (Fig. 5a). We detected the secretion of HDV particles induced by the GPs from HMPV, DENV, and WNV at levels similar to those of HBV GPs and at lower levels with the GPs from LCMV, though not with the GPs from the other viruses (Fig. 5b). Importantly, while no infectivity could be detected in the supernatants from the latter GPs, HDV particles enveloped with

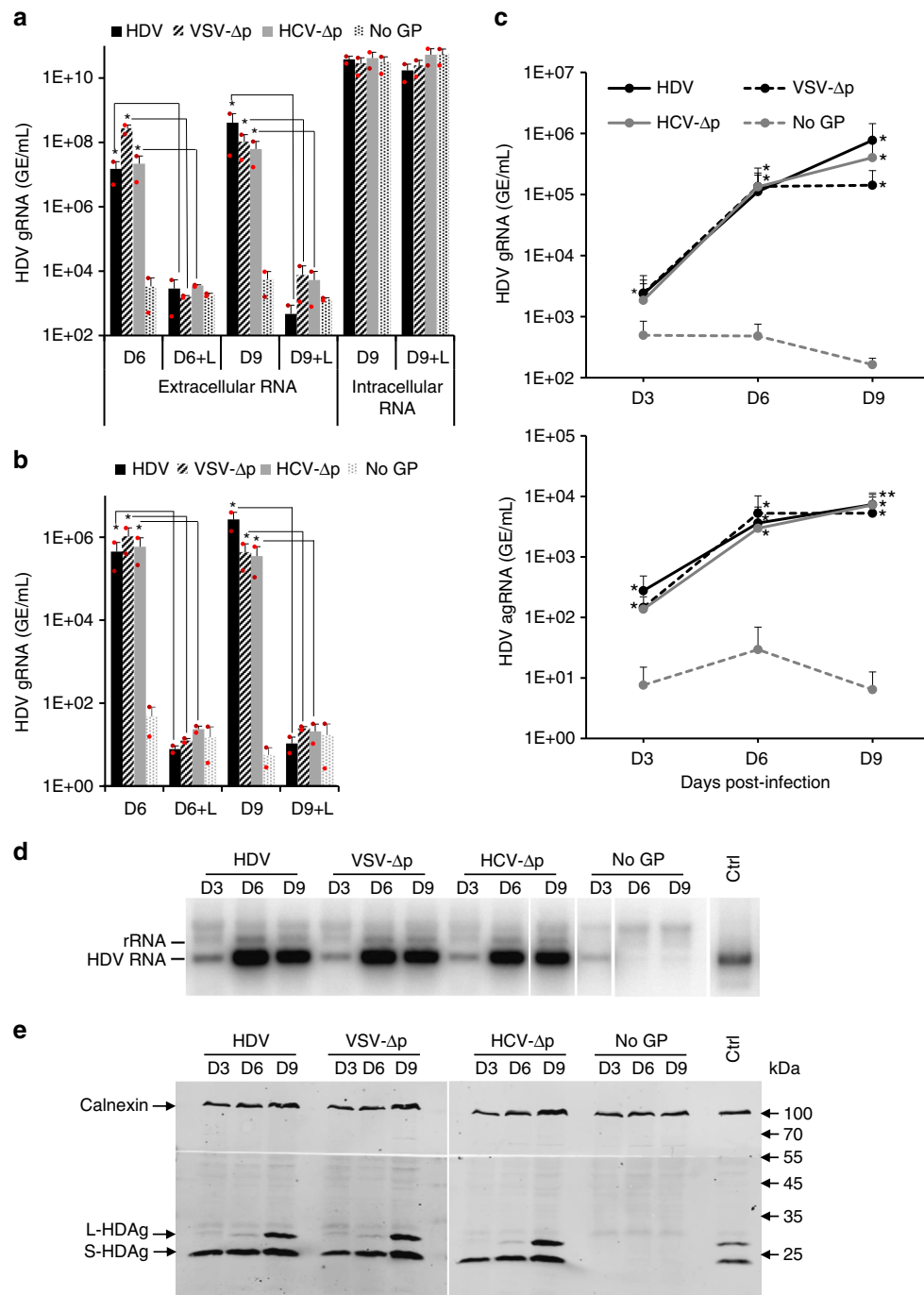


Fig. 3 HDV, VSV-Δp, and HCV-Δp particles share an early step of assembly and induce identical HDV markers in infected cells. Huh-7 cells were co-transfected with pSVLD3 plasmid coding for HDV RNPs and plasmids coding for HBV (HDV), VSV (VSV-Δp), or HCV (HCV-Δp) envelope glycoproteins. As control, pSVLD3 was transfected without envelope proteins (No GP). **a** The transfected cells were grown in the presence (or not) of 1 mM Lonafarnib (+L), a farnesyltransferase inhibitor, until collecting at day 6 or 9 post transfection (D6 vs. D6 + L and D9 vs. D9 + L) the cell supernatants, which were filtered and inoculated to Huh-106 cells. The RNAs from producer cells and supernatants were extracted and the HDV genomes (gRNAs) were quantified by a strand-specific RT-qPCR assay. The quantification of intracellular HDV RNAs in cells producing the HDV particles at day 9 post transfection is also shown. HDV RNA levels in GE (genome equivalent) are expressed as means ($n = 2$ independent experiments) per ml of cell supernatants for extracellular RNAs or, for intracellular RNAs, per ml of cell lysates containing 10^6 cells. **b** The inoculated cells were grown for 7 days before total intracellular RNA was purified. The results of HDV gRNA quantification by RT-qPCR are expressed as means ($n = 2$ independent experiments) per ml of cell lysates containing 10^6 cells. **c-e** Huh-106 cells inoculated with the indicated viral particles were harvested at different time points post infection. The RNAs were then extracted from the lysed cells. The HDV RNAs were quantified by genomic (gRNA) (upper panel) or antigenomic (agrRNA) (lower panel) strand-specific RT-qPCR assays and are expressed as means ($n = 4$ independent experiments) GE per ml of cell lysates containing 10^6 cells (**c**). The results of a northern blot experiment using $3 \mu\text{g}$ of total cellular RNA per well that were revealed with a HDV-specific probe (**d**). Intracellular proteins were extracted and analyzed by western blot using an HDAg antibody (**e**). Control HDV RNAs (5×10^7 GE) (**d**) or HDAg from cell lysates (**e**) were loaded on the same gels (Ctrl). Source data are provided as a Source Data file. Error bars correspond to standard deviation. Statistical analyses (Student's *t*-test): $p < 0.05$ (*); $p < 0.01$ (**)

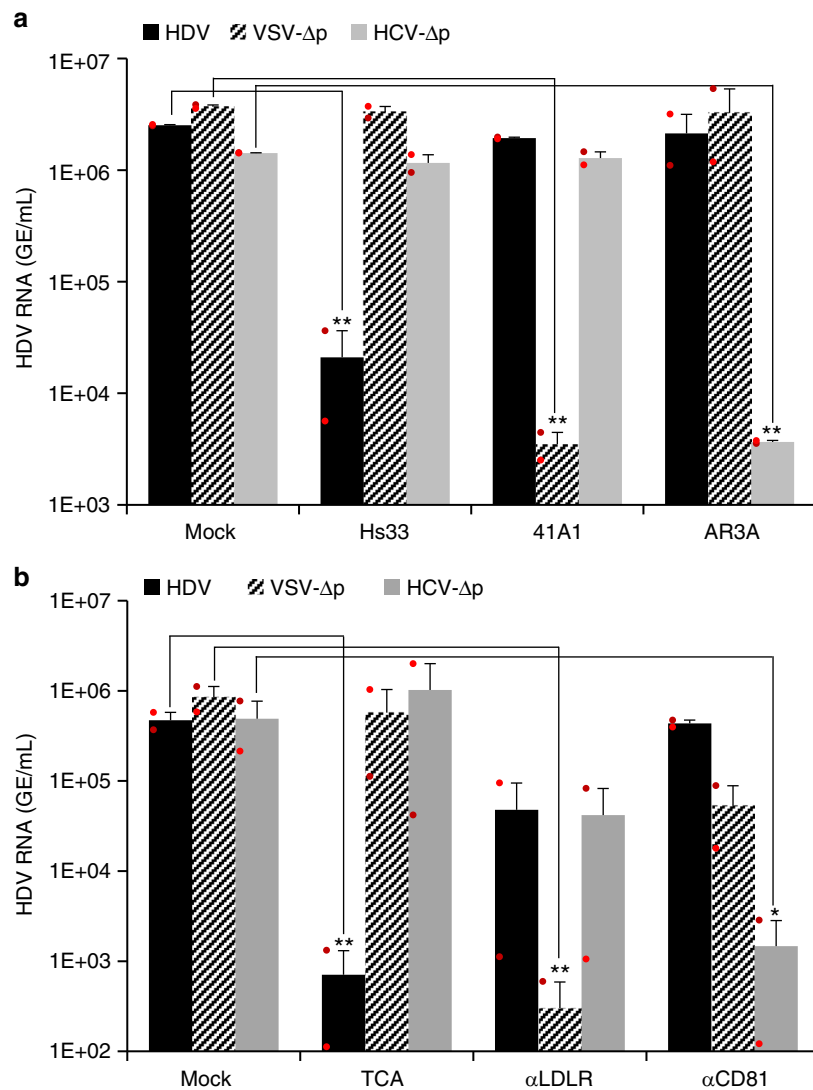


Fig. 4 Specific glycoprotein-receptor interactions mediate cell entry of HDV particles. **a** Similar inputs of virus particles produced with HBV (HDV), VSV (VSV-Δp), or HCV (HCV-Δp) glycoproteins were incubated for 1 h at 37 °C with 100 ng/mL of neutralizing monoclonal antibodies against HBV HBsAg (Hs33 mAb), VSV-G (41A1 mAb), and HCV-E1E2 (AR3A mAb) glycoproteins vs. no antibody (mock) before infection of Huh-106 cells. **b** Similar inputs of virus particles were used to infect Huh-106 cells that were pre-incubated for 1 h with compounds that block NTCP (TCA, taurocholic acid), LDLr (C7 mAb), and CD81 (JS-81 mAb) vs. no antibody (mock). Infected cells were grown for 7 days before total intracellular RNA was purified. The results of HDV RNA quantification by RT-qPCR are expressed as means ($n = 2$ independent experiments) per mL of cell lysates containing 10^6 cells. Source data are provided as a Source Data file. Error bars correspond to standard deviation. Statistical analyses (Student's *t*-test): $p < 0.05$ (*); $p < 0.01$ (**)

the former GPs were infectious. They exhibited high infectivity for those enveloped with DENV GPs (Fig. 5c), similar to HBV, VSV-G, and HCV GPs (Fig. 2), but intermediate or lower infectivity for particles assembled with LCMV, HMPV, and WNV.

Finally, to extend these findings, we determined if HDV particles could be produced from non-liver cells. Hence, the pSVLD3 plasmid was co-transfected with members of the above set of GP-expression plasmids in 293T human kidney cells. Similar to production in Huh-7 cells, we found that HDV RNA could replicate in 293T cells, and that infectious HDV particles could be efficiently assembled and secreted with the HBV, VSV, HCV, DENV, WNV, and HMPV GPs (Supplementary Fig. 4), indicating that assembly and release of functional HDV with heterologous GP is not cell-type restricted.

HDV coinfection with HCV or DENV rescues infectious HDV. Next, to validate and extend the results of expression assays to a

more relevant infectious context, we sought to determine if HCV-Δp and DENV-Δp particles could be produced after inoculation of live HCV or DENV to cells expressing intracellular HDV RNPs. Hence, we inoculated Huh-7.5 cells producing HDV RNAs with either cell culture-grown HCV (HCVcc) or DENV at two different MOIs, which were set at suboptimal values in order to prevent virus-induced cell death. As control, we performed HBV infection assays in Huh-106 cells producing HDV^{12,33}.

At 5 days post inoculation with HCV, we detected intracellular HCV-NS5A and HDAg in ca. 5–10% of co-infected cells (Supplementary Fig. 5a). HCV and HDV RNAs were then quantified by RT-qPCR from cell lysates and supernatants. As shown in Fig. 6a, we could readily detect intracellular HCV RNAs in cells replicating or not HDV RNA. Identical levels of intracellular HDV RNAs of genomic size were detected in HDV-expressing cells inoculated or not with HCV (Fig. 6a). Likewise, HCV RNAs were detected in supernatants of these cells at levels that were not affected by the presence of intracellular

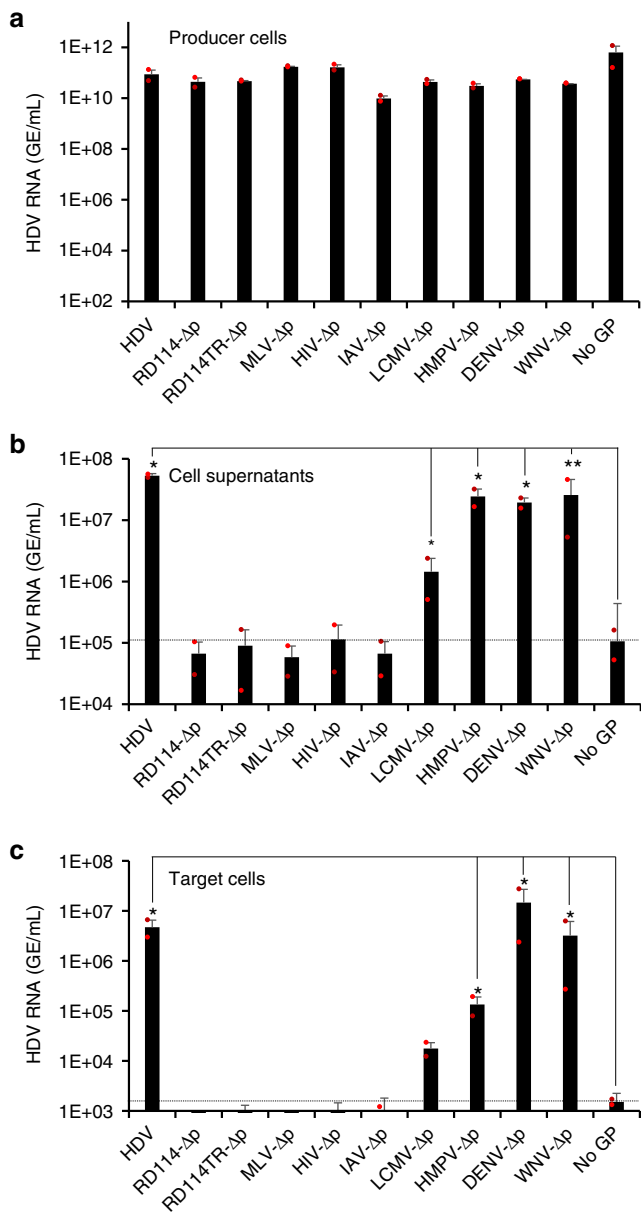


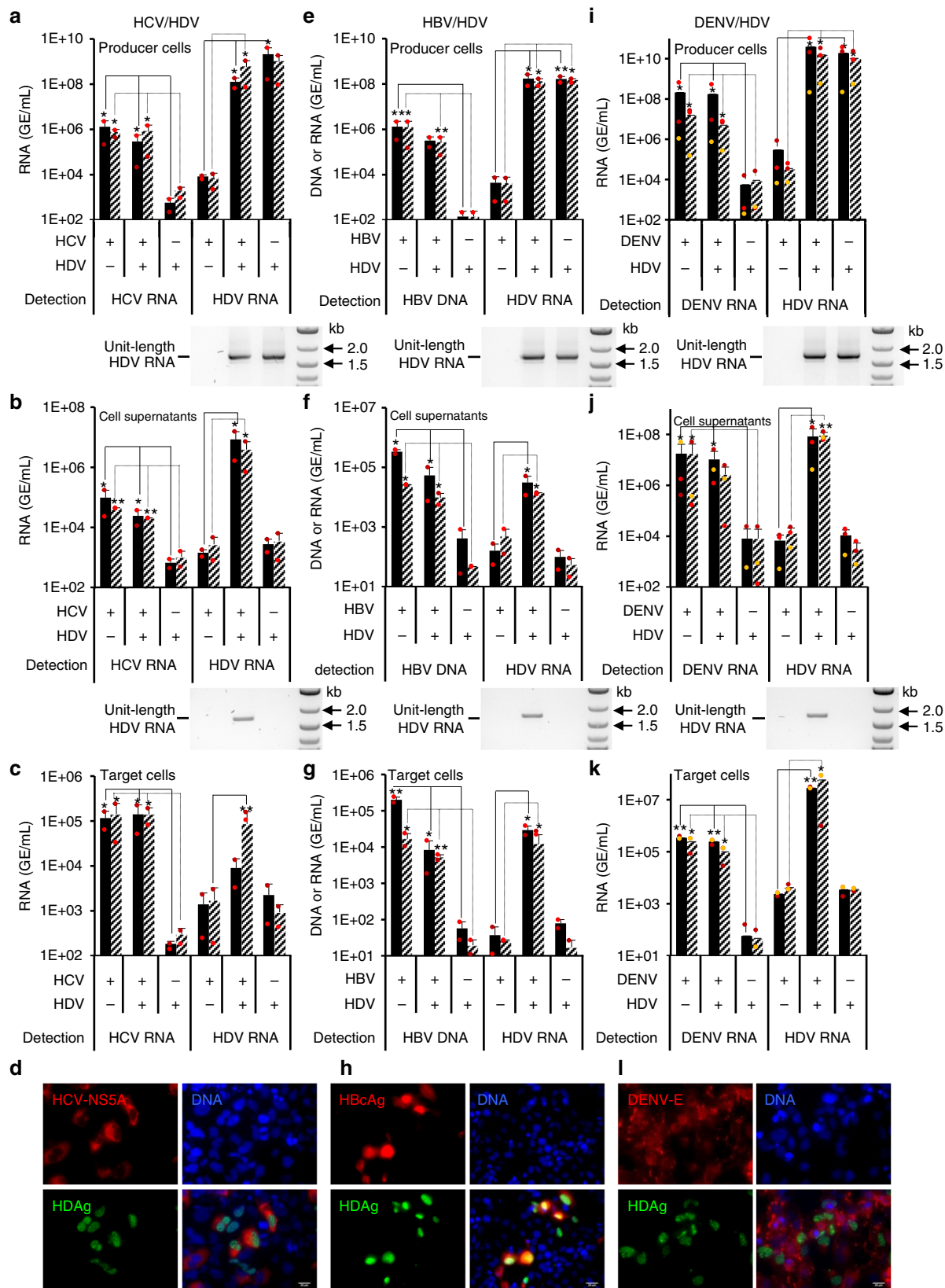
Fig. 5 Screening of surface glycoproteins from different enveloped viruses that allow production of infectious HDV particles. Huh-7 cells were co-transfected with pSVLD3 plasmid coding for HDV RNPs and plasmids coding for HBV glycoproteins (designated “HDV”) or for surface glycoproteins of the indicated enveloped viruses. The RD114TR GP is a cytoplasmic tail-modified variant of the RD114 GP that allows its trafficking to late endosomal compartments^{54,55}. As control, pSVLD3 was co-transfected with an empty plasmid (referred to as “No GP”). **a** The quantification of intracellular HDV RNAs in lysates of cells at day 9 post transfection is shown. HDV RNA levels in GE (genome equivalent) are expressed as means ($n = 2$ independent experiments) per mL of cell lysates containing 10^6 cells. **b** At day 9 post transfection, the cell supernatants were harvested, filtered, and the extracellular RNA was extracted and purified before quantifying HDV RNAs by RT-qPCR. HDV RNA levels in GE are expressed as means ($n = 2$ independent experiments) per mL of cell supernatants. **c** Huh-106 cells were incubated with the above supernatants. Infected cells were grown for 7 days before total intracellular RNA was purified. The results of HDV RNA quantification by RT-qPCR are expressed as means ($n = 2$ independent experiments) per mL of cell lysates containing 10^6 cells. The dotted lines represent the experimental thresholds, as defined with the “No GP” controls. Note that only supernatants containing secreted HDV RNAs (**b**) allow infectivity of HDV particles containing HBV (HDV), LCMV (LCMV-Δp), HPMV (HPMV-Δp), DENV (DENV-Δp), or WNV (WNV-Δp) GPs (**c**). Source data are provided as a Source Data file. Error bars correspond to standard deviation. Statistical analyses (Student’s *t*-test): $p < 0.05$ (*); $p < 0.01$ (**)

HDV RNA (Fig. 6b). Notably, we found that extracellular HDV RNAs could be readily detected only in the supernatants from cells co-infected with HDV and HCV (Fig. 6b), indicating that HCV infection can provide helper functions for assembly and secretion of HDV particles. These particles incorporated full-sized genomic HDV RNA, as shown by strand-specific RT-PCR assays (Fig. 6b, below the graphs). Next, we determined the infectivity of virus particles by measuring intracellular HCV and HDV RNAs in Huh-7.5 target cells 7 days after their inoculation with the producer cell supernatants. We detected HCV RNAs in these target cells, reflecting the presence of infectious HCV particles in the supernatants of HCV-(co)infected cells, at similar levels whether or not HDV genome was co-expressed in the producer cells. Importantly, we found that the HDV particles produced from HCV/HDV co-infected cells were infectious (Fig. 6c), as we could readily detect HDV RNAs in these target cells well over the experimental threshold provided by the control conditions. Corroborating these results, cells that were co-infected by both HCV and HDV or that were mono-infected by either virus were observed by immunofluorescence (Fig. 6d).

Noteworthy, the production and infectivity levels of HDV particles produced by HCV/HDV co-infected cells were similar to those of HDV particles produced with HBV as a co-infecting helper virus (Fig. 6e–h). Overall, this indicated that infectious HDV particles can be produced by coinfection with a non-HBV helper virus. To further address this, since DENV GPs could also provide helper functions for HDV RNP secretion (Fig. 5), we investigated HDV propagation from DENV/HDV co-infected Huh-7.5 cells (Fig. 6i; Supplementary Fig. 5a). We found that DENV coinfection could induce the replication and secretion of full-sized genomic HDV RNAs (Fig. 6i, j) at high levels, equivalent to those obtained via DENV GP co-expression (Fig. 5). This resulted in efficient HDV and DENV infection levels in Huh-7.5 target cells (Fig. 6k, l). Interestingly, similar results were obtained when DENV/HDV particles were inoculated in C6/36 *Aedes albopictus* mosquito cells that are permissive to DENV infection (Supplementary Fig. 6). We detected HDV (and DENV) RNAs in DENV/HDV-infected C6/36 cells (Supplementary Fig. 6d, 6e), which indicated entry and replication of HDV RNA in insect cells, though at lower levels than for Huh-7.5 cells (Supplementary Fig. 6a, 6b). Moreover, these DENV/HDV-infected C6/36 cells allowed HDV RNP assembly, secretion, and transmission to both Huh-7.5 and C6/36 naive cells (Supplementary Fig. 6f, 6g).

Overall, these results indicated that infectious HDV particles could be assembled in cells co-infected with different viruses other than HBV, and that replication and infectivity of co-infecting virus seem not affected by HDV replication.

HCV/HDV coinfection can disseminate in vivo. We then sought to demonstrate that HCV could propagate HDV RNPs in vivo. We generated cohorts of liver-humanized mice (HuHep-mice) derived from the FRG mouse model⁴⁰ (Fig. 7a). We retained the animals that displayed >15 mg/mL of human serum albumin (HSA), which corresponded to 40–70% of human hepatocytes in the liver⁴¹. In agreement with previous reports^{41,42}, these animals supported HBV (Group#1) and HCV (Group#5) infection for several months (Fig. 7b; see



Supplementary Fig. 7a for individual mice). In contrast, inoculation of HuHep-mice with “helper-free” HDV, i.e., HDV particles produced with HBV GP-expression plasmid (Fig. 1), did not lead to HDV viremia, as shown by RT-qPCR values in infected animal sera that were identical to those detected in the non-infected HuHep-mice control group (Group#9: HDV vs.

Group#10: Mocks; Supplementary Fig. 7a). The other groups of HuHep-mice (5–8 animals each) were inoculated with either “helper-free” HDV followed by HCV 4 weeks later (Group#7), HCV followed by “helper-free” HDV (Group#6), or both HCV and “helper-free” HDV simultaneously (Group#8). HDV RNAs were detected in animals of the three latter groups within a few

Fig. 6 HDV RNA-producing cells infected with HCV and DENV secrete infectious HDV particles. Huh-7.5 (**a, i**) or Huh-106 (**e**) cells producing HDV RNAs were inoculated with high (black bars) vs. low (hatched bars) MOIs of live HCV (MOI = 0.01 and 0.1 FFU/cell; **a**), HBV (MOI = 20 and 200 GE/cell; **e**) or DENV (MOI = 0.01 and 0.1 FFU/cell; **i**) particles. Supernatants and lysates from these cells were harvested at day 5 (HCV, DENV) and day 7 (HBV) post infection. HDV-expressing cells without subsequent infection (referred to as “HDV”) as well as naive cells only infected with HCV, HBV, or DENV, as indicated in legends below each graph, were used as controls. Supernatants from HCV/HDV (**b**), HBV/HDV (**f**), or DENV/HDV (**j**) co-infected cells or corresponding control cells were used to infect Huh-7.5 (**c, k**) or Huh-106 (**g**) cells. Infection levels were assessed at day 7 post infection. Nucleic acids present in filtered cell supernatants (**b, f**, and **j**) and lysates of producer (**a, d**, and **g**) or target cells (**a, f**, and **i**) were extracted and purified for quantification of HDV (**a-c**, **e-g**, and **i-k**) and HCV RNA (**a-c**), HBV DNA (**e-g**), or DENV (**i-k**) RNA by qPCR. The results expressed in GE (genome equivalent) are displayed as means ($n = 2$ (**a-c**, **e-g**) or $n = 3$ (**i-k**) independent experiments) per mL of cell supernatants for extracellular nucleic acids or, for intracellular nucleic acids, per mL of cell lysates containing 10^6 cells. Extracted RNAs were reverse-transcribed and were PCR-amplified with HDV-specific primers to reveal the size of transcribed HDV genomes (HDV RNA unit length), as shown below the graphs. Huh-7.5 (**d, i**) or Huh-106 (**h**) cells co-infected with HDV and HCV (**d**), HBV (**h**), or DENV (**i**) were fixed 7 days after infection, stained for HDAg and HCV-NS5A, HDAg and HBcAg, and HDAg and DENV-E, respectively, and counterstained with Hoechst to visualize the nuclei. HDAg (green channel), HCV-NS5A, HBcAg, DENV-E (red channels), and nuclei (blue channel) were then visualized by immunofluorescence. Scale bars represent 20 μm . Source data are provided as a Source Data file. Error bars correspond to standard deviation. Statistical analyses (Student's *t*-test): $p < 0.05$ (*); $p < 0.01$ (**)

weeks after inoculation. All HCV-positive animals of these groups were also positive for HDV (Fig. 7b; Supplementary Fig. 7a) and secreted HDV RNA of genomic size was detected in the sera (see examples for two animals/group in Supplementary Fig. 7b). We obtained qualitatively comparable results in HuHep-mice co-infected with HDV and HBV (Fig. 7a, b, Group#2, #3, and #4; Supplementary Fig. 7a, 7b). Of note, similar results were obtained in another cohort of HuHep-mice in which HDV was inoculated 1 week after HCV (Supplementary Fig. 8). Altogether, these results indicated that HDV can be propagated *in vivo* by different virus types, including HCV.

Discussion

Satellite viruses are scarcely found in animal viruses in contrast to their profusion in plant viruses. Only two representative satellite viruses are known currently in human viruses and include HDV and adeno-associated virus (AAV), which uses helper functions of e.g., adenovirus or herpes simplex virus at the level of replication of its genome, unlike for HDV. Indeed, HDV has been described as a satellite virus of HBV, a liver-specific human pathogen that provides its surface GPs to induce envelopment and secretion of HDV RNPs, as well as transmission to other cells via HBV cell entry factors. *In vivo*, HDV has been found to be associated with HBV in >5–10% of the ca. 250 million HBV-infected individuals⁴³ worldwide.

A specific feature of HBV is the assembly and secretion of different types of viral particles. While the three HBV envelope GPs, S-HBsAg, M-HBsAg, and L-HBsAg, induce the secretion of bona fide virions incorporating HBV capsid and DNA genome through the ESCRT assembly and budding machinery in cellular multivesicular bodies (MVB)^{44,45}, they also induce a particularly abundant formation of HBV nucleocapsid-free subviral particles (SVPs) at a pre-Golgi membrane that are subsequently exported through the cell secretory pathway⁴⁶. The latter type of particles is exploited by HDV through a process allowing binding of its RNP to a cytosolic determinant of the HBV envelope GPs^{29,38,47–49}. Hence, as HBV SVPs outnumber by ca. 4 orders of magnitude of the HBV virions⁵⁰, HDV RNPs are particularly efficiently coated and secreted with the HBV envelope GPs, with titers that can reach up to 10^{11} HDV virions per mL of serum, and are consequently transmitted to the liver, which explains why HDV and HBV share tropism to human hepatocytes.

Yet, genetically, HDV belongs to a group of infectious agents that are related to plant viroids and that are completely distinct from HBV. As HDV efficiently replicates in different tissues and species²³, here we raised the hypothesis that it may have arisen from and/or conceivably still infects hosts independently of HBV. To formally address this possibility, we questioned whether different

enveloped viruses, totally unrelated to HBV and HDV themselves, could provide both assembly and entry functions to HDV particles. By testing GPs from ten different virus genera, we demonstrate that HDV RNPs could be enveloped by GPs from six of these non-HBV particles and could produce infectious HDV particles.

The nature of the determinant(s) and mechanism(s) allowing HDV assembly with these unconventional GPs remains to be unraveled. Noteworthy, a farnesylation signal located at the C-terminus of L-HDAg anchors the HDV RNP to the ER membrane³⁸, the site where, by definition, envelope GPs are generally synthesized and translocated. Such early assembly events of HDV production seem also to be used for assembly of HDV RNP with alternative GPs, such as VSV-G and HCV-E1E2 GPs, since inhibition of this pathway by Lonafarnib, a farnesyltransferase inhibitor that is currently in phase-IIa clinical trial⁵¹, could readily prevent production and transmission of HDV, VSV- Δp , and HCV- Δp particles (Fig. 3). As for conventional HDV particles assembly, i.e., associated with HBV GPs, S-HBsAg is necessary and sufficient for assembly of HDV, although incorporation of L-HBsAg is required for infectivity⁵². Previous studies have described a crucial determinant of HDV envelopment, consisting of a conserved tryptophan-rich motif present in the cytosolic side of the S-HBsAg that acts as an HDV matrix domain and binds a poorly conserved proline-rich C-terminal sequence located before the farnesylation site of L-HDAg⁴⁸. Yet, such a tryptophan-rich motif is likely not present in the heterologous GPs that induce efficient HDV release, such as e.g., VSV-G, HCV-E1E2, and DENV-PrME, inferring that a specific interaction between HDV RNP and these envelope GPs is highly improbable. Rather, this indicates that besides such specific HDV/HBV interaction allowing HDV transmission and subsequent pathogenesis, other determinant(s) of envelopment of HDV RNPs must exist.

How viruses in general exploit or subvert cellular envelopment processes and machineries is of major interest. Budding mechanisms vary widely for different virus families and there are few common principles that govern these events. Particularly, the assembly and budding of enveloped virus particles is a complex and multistep process that involves the simultaneous recruitment of viral proteins, surface GPs and inner structural proteins, and nucleic acids to varying assembly sites. Such sites can be localized either at the plasma membrane (e.g., HIV) or in the lumen of diverse intracellular membranes (e.g., HCV, DENV), such as the ER as well as the nuclear envelope, the intermediate or pre-Golgi compartment, the Golgi cisternae and trans-Golgi network, and the endosomes. Alternatively, assembly sites can be generated via specific virus-induced membranous structures or compartments⁵³. Accordingly, a critical determinant of GP incorporation in the envelopes of retrovirus particles allows intracellular trafficking of GP and colocalization with nucleocapsids, although

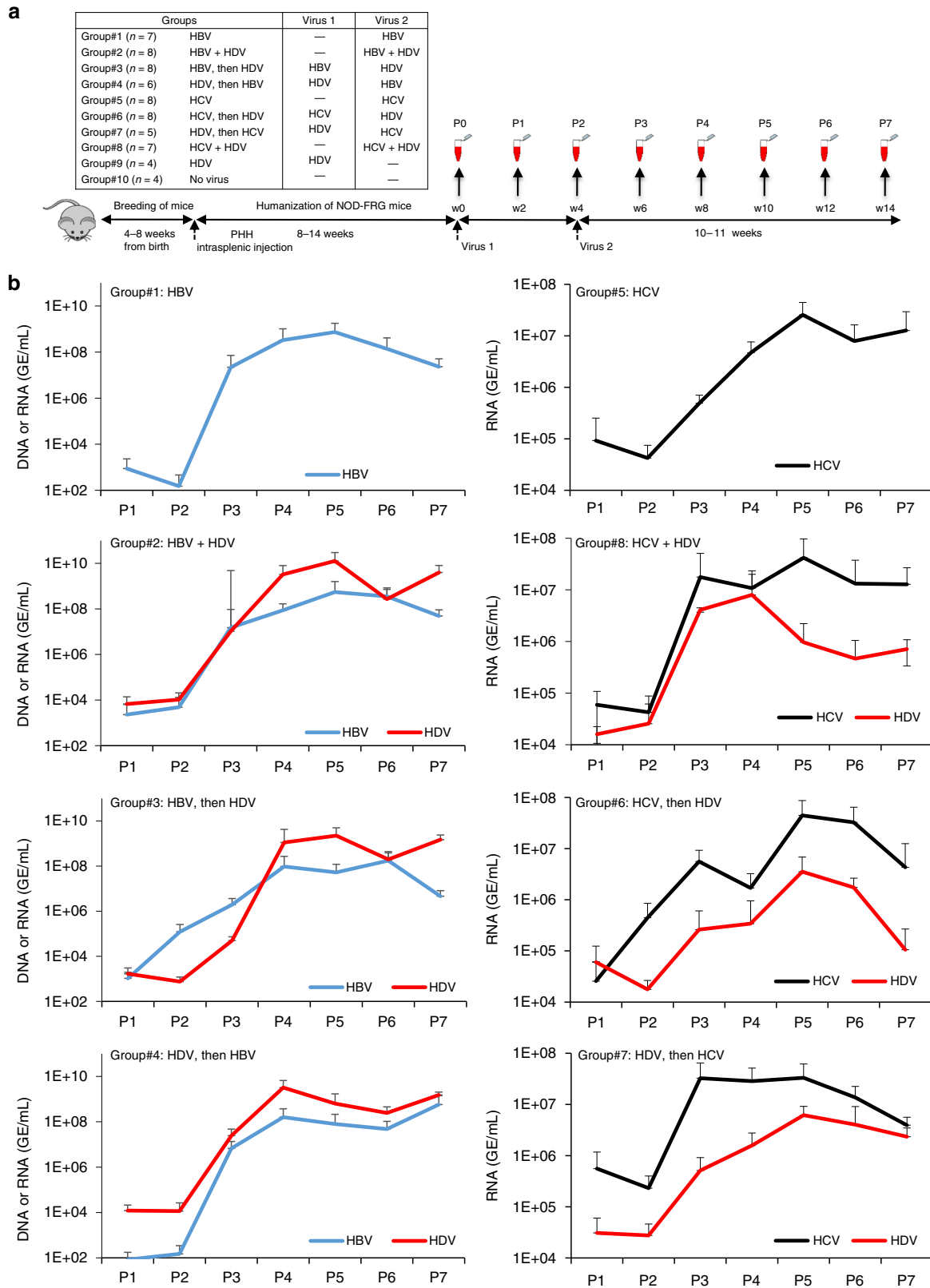


Fig. 7 HCV propagates HDV particles in vivo. Four- to eight-week-old NOD-FRG mice were engrafted with primary human hepatocytes (PHH). After ca. 2–3 months, the animals displaying HSA levels >15 mg/mL were split into 10 different groups ($n = 4$ to $n = 8$ independent animals) that were infected with HDV (10^7 GE/mouse) and/or HCV (1.5×10^5 FFU/mouse) or HBV (10^8 GE/mouse), as shown in the schedule (a). At different time points post infection, blood samples (50 μ l) were collected and the viremia in sera was monitored by qPCR on the genomes of the indicated viruses (GE/mL of serum) (b). The graphs show the mean results of viremia of HDV (red lines), HBV (blue lines), and HCV (black lines). See results of individual mice as well as of control groups, inoculated with HDV only (Group#9: HDV) or with PBS (Group#10: Mocks) in Supplementary Fig. 7. Source data are provided as a Source Data file. Error bars correspond to standard deviation

signals modulating direct as well as indirect interactions of the GP cytoplasmic tails with nucleocapsid components have been described^{54,55}. Thus, different scenarios could explain how HDV RNPs may incorporate non-HBV glycoproteins. Besides factors allowing colocalization and/or interactions between GP and nucleocapsids, the budding and subsequent envelopment of viral particles requires the curvature and scission of the host membrane concomitant with the inclusion of nucleocapsid components. The driving force for budding can be provided by the nucleocapsid itself, via specific inner structural proteins (e.g., Gag precursor of HIV) that “pushes” a virion membranous bud through the cytoplasmic side of a membrane. Alternatively, budding can be driven by an envelope GP that, by forming a symmetric lattice (e.g., prME GP of flaviviruses) or alternatively, a cellular vesiculation (e.g., G protein of VSV), “pulls” the membrane, creates a bud in which the nucleocapsid can be incorporated. Although there are many subtle variations and/or combinations between these two main models⁵⁶, it is intriguing that the enveloped viruses that induce an efficient release of HDV particles (this report) are known to form subviral particles, i.e., nucleocapsid-free vesicles coated with envelope GPs, which typically pertain to the “pull” model of virion assembly/budding. Indeed, in addition to their own infectious particles, HBV⁴⁶, VSV⁵⁷, HCV^{58,59}, DENV⁶⁰, and WNV⁶¹ can release their GPs in sediment, vesicular forms, which, at least for HBV, HCV and flaviviruses are assembled and released in the ER lumen or ER-derived compartment. Conversely, the GPs from retroviruses such as RD114, MLV or HIV, and influenza virus are released from the plasma membrane and/or late endosomes upon incorporation at the surface of infectious virions⁵⁴ but they have not been described to form SVPs, a characteristic compatible with their inability to assemble HDV particles (Fig. 5). It is puzzling that VSV-G, which induces the formation of infectious virions from the plasma membrane⁶², allows efficient HDV particles release. Yet, we cannot exclude that formation of VSV-G subviral particles may also occur in the lumen of the ER or, alternatively, that HDV RNP could be targeted beneath the plasma membrane, in addition to that of the ER.

Importantly, we show that the formation of infectious HDV particles with unconventional GPs could also occur via coinfection with live viruses different from HBV, as shown by their release from HCV/HDV or DENV/HDV co-infected cells. We presume that this occurs through the same mechanisms of HDV RNP assembly and envelopment in SVPs formed by either virus type, as proposed above. Noteworthy, our results reveal that HDV particles can be propagated by HCV in experimentally co-infected mice, indicating that, in this *in vivo* setting at least, HDV can be a satellite of a virus genus totally unrelated to HBV. This raises the possibility that in nature, HDV could be associated with different virus types, including human viral pathogens, which could possibly favor previously unappreciated HDV transmission scenarios and modulate their pathogenicity. Indeed, hepatitis D is a most aggressive form of hepatitis that affects ca. 15–20 million persons worldwide, with high disparities around the world⁴³. While the clinical course of acute HDV infection is hardly distinguishable from acute hepatitis B⁶³, chronic HDV infection worsens liver diseases caused by HBV, even though HBV replication is often suppressed^{64–66}. Longitudinal cohort studies have shown that chronic hepatitis D induces a threefold higher risk of progression to cirrhosis as compared with patients infected by HBV only⁶⁷. HDV replicates in hepatocytes and the pathologic changes it induces are limited to the liver, which are characterized by hepatocyte necrosis and inflammatory infiltrates that may correlate with intrahepatic replication levels⁶⁸. Thus, since HDV RNA can persist in the liver in the absence of HBV for at least 6 weeks⁶⁹, its propagation could be triggered upon superinfection

by other hepatitis viruses such as HCV as well as other viral infections. Why HDV infection in patients has not been reported in association with HCV infection is uncertain and raises interesting scenarios. It is possible that direct or indirect (e.g., immune-mediated) interference mechanisms may impede in the long-term HDV/HCV co-infections *in vivo*, though this may occur in different contexts. For example, HDV-induced activation of the innate immune response, which is known to have little/no effect on HDV itself^{70,71}, may impact several markers of coinfection, such as for HCV that is interferon-sensitive in contrast to HBV^{72,73}. Thus, what might determine eventual successful vs. sporadic transmission and propagation of HDV with non-HBV helper viruses would reside in the balance between biochemical and virological compatibility of HDV RNP with the GPs of these helper viruses vs. potential immunological mechanisms of interference, though the immune status of individuals, such as immune suppression, may also favor transmission of such HDV co-infections. Overall, our demonstration that unconventional cell transmission of HDV is experimentally possible *in vivo* warrants that studies be conducted in infected individuals.

Methods

Cells. Huh-7⁴⁹ hepatocarcinoma and Huh-106³³ (a subclone of NTCP-expressing Huh-7 cells) were grown in William’s E medium (Invitrogen, France) supplemented with nonessential amino acids, 2 mM L-glutamine, 10 mM HEPES buffer, 100 U/mL of penicillin, 100 µg/mL of streptomycin, and 10% fetal bovine serum (FBS). Huh-7.5 cells (kind gift of C Rice) and 293T kidney (ATCC CRL-1573) cells were grown in Dulbecco’s modified minimal essential medium (DMEM, Invitrogen) supplemented with 100 U/mL of penicillin, 100 µg/mL of streptomycin, and 10% FBS. The C6/36 *Aedes albopictus* cells (ATCC CRL-1660) were grown in DMEM medium supplemented with 100 U/mL of penicillin, 100 µg/mL of streptomycin, L-glutamine, and 10% FBS at 28 °C.

Plasmids. pSVLD3 plasmid encodes HDV RNP^{27,29}. Plasmids pT7HB2.7 for HBV²⁹, phCMV-VSV-G for vesicular stomatitis virus (VSV), phCMV-JFH1-E1E2 for hepatitis C virus (HCV), phCMV-RD114 and phCMV-RD114TR for cat endogenous virus, phCMV-MLV-A for amphotropic murine leukemia virus (MLV), phCMV-HIV for human immunodeficiency virus (HIV), phCMV-NA and phCMV-HA for avian influenza virus (AIV), phCMV-LCMV for lymphocytic choriomeningitis virus (LCMV), phCMV-FgsHMPV for human metapneumovirus (HMPV), phCMV-PrME for dengue virus (DENV), and West Nile virus (WNV) encode the envelope surface glycoproteins of the indicated viruses^{36,74,75}.

Antibodies. The HDAg antigen was detected with the SE1679 rabbit polyclonal antibody for western-blot and immunofluorescence experiments. The human anti-E2 AR3A³⁹ (kind gift from M Law), mouse anti-VSV-G 41A1⁵⁸, and mouse anti-HBsAg Hs33 (Cat # GTX41723, GeneTex) monoclonal antibodies (mAb) were used in neutralization and immunoprecipitation assays. The mouse anti-CD81 JS-81 (Cat # 555675 BD Pharmingen) and anti-LDLr C7 (Cat # sc-18823, Santa Cruz Biotechnology) mAbs were used for receptor-blocking experiments. The mouse anti-DENV-E 3H5 mAb (kind gift from P Desprès), the mouse anti-NS5A 9E10 mAb (kind gift of C Rice), and the human anti-HBcAg (from an anti-HBcAg-positive and anti-HBsAg-negative patient) serum were used for immunofluorescence.

HDV particle production and infection. Huh-7 cells were seeded in 10-cm plates at a density of 10⁶ cells per plate and were transfected with a mixture of 2.5 µg of pSVLD3 plasmid and 10 µg of plasmid, allowing the expression of surface envelope glycoproteins of the above-mentioned viruses²⁹ using FuGENE 6 transfection reagent (Promega). Transfected cells were grown for up to 9 days in primary hepatocyte maintenance medium containing 2% FBS and 2% DMSO to slow cell growth⁷⁶. Supernatants of virus-expressing cells were separated from the producer cells, filtered through 0.45-µm-pore filters, and were analyzed by RT-qPCR for detection of HDV RNA²⁸, using the methodologies and primers described below. These supernatants were also used for infection experiments in Huh-106 and other target cells, which were seeded in 48-well plates at a density of 1.5 × 10⁴ cells per well.

Transfected or infected cells were cultured in primary hepatocyte maintenance medium containing 2% FBS and 2% DMSO following infection to slow cell growth. Infectivity of viral particles was assessed 7 days post infection by RT-qPCR of HDV RNA isolated from cell lysates or by determining focus-forming units in ethanol-fixed plates using HDAg antibodies. For neutralization and receptor-blocking experiments, 100 ng/mL of antibodies were incubated with virus particles for 1 h at 37 °C before addition to the cells.

For purification of viral particles, 10 mL of producer cell supernatants were harvested, filtered through a 0.45- μ m filter, and centrifuged at 32,000 rpm for 4 h at 4 °C on a 30% sucrose cushion with a SW41 rotor and Optima L-90 centrifuge (Beckman). Pellets were resuspended in 100 μ L of TNE (50 mM Tris-HCl, pH 7.4, 100 mM NaCl, and 0.1 mM EDTA) prior to use for immunoprecipitation and western blot of HDAG or for northern blot of RNAs.

For inhibition of farnesyltransferase in producer cells, we used Lonafarnib (Sigma-Aldrich), an inhibitor of prenylation that prevents HDV assembly^{37,38}. Following transfection with pSVLD3 plasmid and GP expression plasmid, as described above, Huh-7 cells were maintained in a daily-changed medium supplemented with 0.2% DMSO and 400 mM DTT alone or in the presence of 1 mM Lonafarnib. The cell supernatants were used for infection experiments in Huh-106 as described above.

RT-qPCR detection of HDV RNAs. Total RNA from serum, filtrated cell supernatant, or from virus producer or infected cells washed with phosphate-buffer saline (PBS) was extracted with TRI Reagent according to the manufacturer's instructions (Molecular Research Center) and treated with RNase-free DNase (Life Technologies). RNAs were reverse-transcribed using random oligonucleotide primers with iScript cDNA synthesis kit (Bio-Rad) before quantification by qPCR, as described below.

For strand-specific HDV RNA RT-qPCR^{30,31}, extracted RNAs were reverse-transcribed with High-Capacity cDNA Reverse Transcription kit (Applied Biosystems) to amplify either genomic or antigenomic cDNAs by using primers DSg: 5'-CCGGCTACTCTCTTTCCCTTCTCTCGTC for genomic-sense cDNA synthesis and DSag: 5'-CACCGAAGAAGGAAGGCCCTGGAGAACA for antigenomic-sense cDNA synthesis. The qPCR assay was then performed, as described below.

The genomic and antigenomic HDV RNAs used as standards for this strand-specific RT-qPCR assay were obtained by *in vitro* transcription of HDV DNA amplicons flanked by T7 promoters. The full-length HDV amplicons were amplified by PCR from pSVLD3 plasmid with primers T7HD 687–706: 5'-CAATTCTAATACGACTCACTATAGGGAGAA GGCCGGCATGGTCCCAGCC TC (with T7 promoter sequences) and HDVgR: 5'-ATCAGGTAAGAAAGGA TGGAACGCGGACCC for the amplicon allowing synthesis of the genomic HDV RNA standards and, for the amplicon allowing synthesis of the antigenomic HDV RNA standards, with primers HDVgF: 5'-GGCCGGCATGGTCCCAGCCTC and AgT7HD 685–656: 5'-CAATTCTAATACGACTCACTATAGGGAGAAA TCAGGT AAGAAAGGATGGAACGCGGACCC (with T7 promoter sequence). Either amplicon was transcribed from T7 promoters using a commercially available kit according to the manufacturer's instructions (RiboMAX™ Express T7, Promega). The full-length linear RNAs were treated with RNase-free DNase, followed by RNA purification (GeneJET RNA purification kit, Thermo Fisher Scientific) and quantified using a Nanodrop device (Thermo Fisher Scientific). These artificial genomic or antigenomic HDV RNAs were diluted in RNase-free water and stored at –80 °C in single-use aliquots and were used as calibration standards for strand-specific HDV RNA RT-qPCR^{31,32,77}. The copy numbers in genomic or antigenomic HDV RNAs extracted from cells or supernatants were quantified using 10-fold dilution series of either genomic or antigenomic HDV RNA standards processed in parallel. We deduced that 10⁶ HDV RNA molecules (genomic or antigenomic) are equal to 1 pg of the corresponding HDV RNA standard. The specificity of the strand-specific RT-qPCR assay was investigated by the quantification of genomic and antigenomic RNA standards (artificial RNA) with the correct primer and the respective opposite primer (genomic primer on antigenomic HDV RNA standard and vice versa) (Supplementary Fig. 1f). Unspecific reverse transcription with the opposite primer occurred, though in a very limited extent (<0.000001%).

The following specific oligonucleotides were then used for HDV cDNA quantification:^{31,32} forward (Kuo F: 5'-GGACCCCTTCAGGAACA) and reverse (Kuo R: 5'-CCTAGCATCTCTCTATCGTAT) primers. The qPCR was performed using FastStart Universal SYBR Green Master (Roche Applied Science) on a StepOne Real-Time PCR System (Applied Biosystems).

As an internal control of extraction, *in vitro*-transcribed exogenous RNAs from the linearized Triplescript plasmid pTRI-Xef (Invitrogen) were added into the samples prior to RNA extraction and quantified with specific primers (Xef-1a 970L20: 5'-CGACGTTGTCACCGGGCAGC and Xef-1a 864U24: 5'-ACCAGGCATGGTGGTTACCTTTGC). All values of intracellular HDV RNAs were normalized to GAPDH gene transcription. For GAPDH mRNA quantification, we used as forward primer, hGAPDH 83U: 5'-AGGTGAA GGTCGGAGTCAACG and as a reverse primer, hGAPDH 287 L: 5'-TGGAAG ATGGTGATGGGATTTTC.

RT-PCR assays. Total RNA from cells or supernatants was extracted with TRI Reagent according to the manufacturer's instructions (Molecular Research Center). RNAs were reverse-transcribed with SuperScript III reverse transcriptase kit (Invitrogen) using a strand-specific primer HDV gRNA: 5'-ATCAGGTAAGAAAGGA TGGAACGCGGACCC that detects the genomic HDV RNA and allows amplification of antigenomic-sense cDNA. The reverse-transcribed cDNA products were used to perform a PCR using the following specific oligonucleotides to amplify the unit-length HDV genome: forward (HDVgF: 5'-GGCCGGCATGGTCCCAGCCTC) and

reverse (HDVgR: 5'-ATCAGGTAAGAAAGGATGGAACGCGGACCC) primers. The PCR bands were visualized on propidium iodide-stained agarose gels.

Northern blots. The purified RNA was subjected to electrophoresis through a 2.2 M formaldehyde, 1.2% agarose gel, and transferred to a nylon membrane. The membrane-bound RNA was hybridized to a ³²P-labeled RNA probe specific for genomic HDV RNA⁴⁹. Quantification of radioactive signals was achieved using a phosphorimager (BAS-1800 II; Fuji). Uncropped and unprocessed scans of all blots are provided in the Source Data file.

Western blots. The proteins from pelleted cell supernatants or extracted from total cell lysates were denatured in Laemmli buffer at 95 °C for 5 min and were separated by sodium dodecyl sulfate polyacrylamide gel electrophoresis and then transferred to nitrocellulose membranes (GE Healthcare). Membranes were blocked with 5% nonfat dried milk in PBS and incubated at 4 °C with the SE1679 rabbit anti-HDAG serum at a 1/500 dilution in PBS–0.01% milk, followed by incubation with a IRDye secondary antibody (LI-COR Biosciences). Membrane visualization was performed using an Odyssey infrared imaging system CLx (LI-COR Biosciences). Uncropped and unprocessed scans of all blots are provided in the Source Data file.

Immunoprecipitation of HDV particles. For immunoprecipitation, 50 μ L of Dynabeads Protein G (Thermo Scientific) bound with 10 μ g of anti-HBsAg Hs33, anti-E2 AR3A, or anti-VSV-G 41A1 mAbs were incubated for 1 h at room temperature with purified virus particles. The beads were then washed three times with 1 mL of PBS with 0.02% Tween-20. The RNA was extracted from the complex with TRI Reagent and detected by RT-qPCR.

Equilibrium-density gradients. One milliliter of cell supernatant containing virus particles harvested at 9 days post transfection was loaded on top of a 3–40% continuous iodixanol gradient⁵⁸ (Optiprep, Axis Shield). Gradients were centrifuged for 16 h at 4 °C in Optima L-90 centrifuge (Beckman). Thirteen fractions of 900 μ L were collected from the top and used for refractive index measurement and RNA quantification, as described above.

Electron microscopy. One milliliter of cell supernatant containing virus particles harvested at 9 days post transfection was mixed with 100 μ L of heparin-agarose beads (Sigma) preequilibrated with 10 mM Tris-HCl and 100 mM NaCl buffer (pH 8). Unbound particles were washed off five times with 10 mM Tris-HCl, 200 mM NaCl buffer (pH 8), and the particles were eluted from the heparin-agarose beads with 10 mM Tris-HCl, 800 mM NaCl buffer (pH 8). For negative staining in electron microscopy, 5 μ L of sample solution was applied onto a glow-discharged EM grid coated with amorphous carbon. After 1 min of sample adsorption, the excess solution was blotted away using a piece of filter paper and the grid was put onto a drop of 1% (w/v) sodium silicotungstate staining solution. After 30 s, excess stain solution was blotted away as before and the grid was dried in air. The samples were examined using a transmission electron microscope Philips CM120 operating at 120 kV.

Coinfection assays. Huh-7.5 cells seeded in six-well plates at a density of 8 × 10⁴ cells per well producing HDV RNAs were superinfected 3 days later cells with Jc1 HCVcc, HBV, or DENV live, helper virus particles^{78,79}. Lysates and supernatants of infected cells were harvested at 5 days post infection from the producer cells and were analyzed by qPCR for detection of HDV²⁸, HCV⁵⁸, HBV⁷⁸, and DENV nucleic acids. The supernatants containing HDV and either helper virus particles were used for infection experiments in relevant target cells. Infectivity was assessed at 7 days later by qPCR of HDV (see above) and of helper virus RNAs or DNAs isolated from cell lysates, using the following specific oligonucleotides: for HCV, forward HCV U147: 5'-TCTGCGGAACCGGTGAGTA and reverse HCV L277: 3'-TCAGGCAGTACCACAAGGC primers; for HBV, forward HBV-SUF: 5'-TCCCAGAGTGAGAGGCCTGTA and reverse HBV-SUR: 5'-ATCCTCGAGAA GATGACGATAAGG primers; and for DENV, forward DENV NSF: 5'-ACCT GGGAAAGAGTGATGGTTATGG and reverse DENV NSR: 5'-ATGGTCTCTGG TATGGTGCTCTGG primers.

Immunofluorescence. Producer or infected cells were fixed with 4% paraformaldehyde (Sigma-Aldrich, France) for 15 min and permeabilized with 0.1% Triton X-100 (Sigma-Aldrich) for 7 min. Fixed cells were then saturated with 3% bovine serum albumin (BSA)/PBS for 20 min and incubated for 1 h with primary antibodies diluted in 1% BSA/PBS at the following dilutions:⁸⁰ anti-HDAG SE1679 rabbit polyclonal serum, 1/500; anti-DENV-E 3H5 mAb, 1/800; anti-NS5A 9E10 mAb, 1/1,000; and anti-HBcAg serum, 1/500. After three washes with 1% BSA/PBS, cells were incubated for 1 h with the corresponding secondary antibodies (Molecular Probes, The Netherlands) at a 1/1000 dilution: donkey anti-rabbit Alexa Fluor 488 (Cat # A-21206); donkey anti-mouse Alexa Fluor 555 (Cat # A-31570); and goat anti-human Alexa Fluor 555 (Cat # A-21433) sera. Cells were washed three times with PBS and then stained for nuclei with Hoechst 33342 (Molecular Probes) for 5 min. After two washes in PBS, cells were imaged with an Axiovert

135 M microscope (Zeiss, Germany) equipped with a DC350FX camera (Leica, Germany), and images were analyzed with the ImageJ software (imagej.nih.gov).

In vivo experiments. All experiments were performed in accordance with the European Union guidelines for approval of the protocols by the local ethics committee (Authorization Agreement C2EA-15, “Comité Rhône-Alpes d’Ethique pour l’Expérimentation Animale”, Lyon, France—APAFIS#1570-2015073112163780). Primary human hepatocytes (PHH, Corning, BD Gentest) were intrasplenically injected into FRG mice⁴⁰, a triple-mutant mouse knocked out for fumarylacetoacetate hydrolase (*fah*^{-/-}), recombinase-activating gene 2 (*rag2*^{-/-}), and interleukin 2 receptor gamma chain (*IL2rg*^{-/-}), 48 h after adeno-uPA conditioning^{41,42}. Mice were subjected to NTBC cycling during the liver repopulation process⁴¹. Mice with human serum albumin (HSA) levels > 15 mg/mL, as determined using a Cobas C501 analyzer (Roche Applied Science), were inoculated with virus preparations by intraperitoneal injection. Sera were collected at different time points before and after infection. Mice were killed 10–14 weeks post infection.

Statistical analysis. Data are shown as means ± standard deviations. Statistical analyses were performed using two-sample Student’s t tests assuming unequal variance. The p-values are represented according to the following convention: *p* > 0.05 (nonsignificant, ns); *p* < 0.05 (*); *p* < 0.01 (**).

Reporting summary. Further information on research design is available in the Nature Research Reporting Summary linked to this article.

Data availability

The datasets generated during this study are available from the corresponding author upon reasonable request. The source data underlying figures and Supplementary Figures are provided as a Source Data file.

Received: 19 July 2018 Accepted: 22 April 2019

Published online: 08 May 2019

References

- Gudima, S., Chang, J., Moraleda, G., Azvolinsky, A. & Taylor, J. Parameters of human hepatitis delta virus genome replication: the quantity, quality, and intracellular distribution of viral proteins and RNA. *J. Virol.* **76**, 3709–3719 (2002).
- Bonino, F. et al. Delta hepatitis agent: structural and antigenic properties of the delta-associated particle. *Infect. Immun.* **43**, 1000–1005 (1984).
- He, L. F. et al. The size of the hepatitis delta agent. *J. Med. Virol.* **27**, 31–33 (1989).
- Rizzetto, M. et al. delta Agent: association of delta antigen with hepatitis B surface antigen and RNA in serum of delta-infected chimpanzees. *Proc. Natl Acad. Sci. USA* **77**, 6124–6128 (1980).
- Ryu, W. S., Netter, H. J., Bayer, M. & Taylor, J. Ribonucleoprotein complexes of hepatitis delta virus. *J. Virol.* **67**, 3281–3287 (1993).
- Lin, B. C., Defenbaugh, D. A. & Casey, J. L. Multimerization of hepatitis delta antigen is a critical determinant of RNA binding specificity. *J. Virol.* **84**, 1406–1413 (2010).
- Zuccola, H. J., Rozzelle, J. E., Lemon, S. M., Erickson, B. W. & Hogle, J. M. Structural basis of the oligomerization of hepatitis delta antigen. *Structure* **6**, 821–830 (1998).
- Rizzetto, M. et al. Immunofluorescence detection of new antigen-antibody system (delta/anti-delta) associated to hepatitis B virus in liver and in serum of HBsAg carriers. *Gut* **18**, 997–1003 (1977).
- Lamas Longarela, O. et al. Proteoglycans act as cellular hepatitis delta virus attachment receptors. *PLoS ONE* **8**, e58340 (2013).
- Schulze, A., Gripon, P. & Urban, S. Hepatitis B virus infection initiates with a large surface protein-dependent binding to heparan sulfate proteoglycans. *Hepatology* **46**, 1759–1768 (2007).
- Yan, H. et al. Sodium taurocholate cotransporting polypeptide is a functional receptor for human hepatitis B and D virus. *Elife* **1**, e00049 (2012).
- Ni, Y. et al. Hepatitis B and D viruses exploit sodium taurocholate cotransporting polypeptide for species-specific entry into hepatocytes. *Gastroenterology* **146**, 1070–1083 (2014).
- Denniston, K. J. et al. Cloned fragment of the hepatitis delta virus RNA genome: sequence and diagnostic application. *Science* **232**, 873–875 (1986).
- Wang, K. S. et al. Structure, sequence and expression of the hepatitis delta (delta) viral genome. *Nature* **323**, 508–514 (1986).
- Riccitelli, N. & Luptak, A. HDV family of self-cleaving ribozymes. *Prog. Mol. Biol. Transl. Sci.* **120**, 123–171 (2013).
- Webb, C. H., Riccitelli, N. J., Ruminski, D. J. & Luptak, A. Widespread occurrence of self-cleaving ribozymes. *Science* **326**, 953 (2009).
- Memczak, S. et al. Circular RNAs are a large class of animal RNAs with regulatory potency. *Nature* **495**, 333–338 (2013).
- Taylor, J. M. Host RNA circles and the origin of hepatitis delta virus. *World J. Gastroenterol.* **20**, 2971–2978 (2014).
- Brazas, R. & Ganem, D. A cellular homolog of hepatitis delta antigen: implications for viral replication and evolution. *Science* **274**, 90–94 (1996).
- Salehi-Ashtiani, K., Luptak, A., Litovchick, A. & Szostak, J. W. A genomewide search for ribozymes reveals an HDV-like sequence in the human CPEB3 gene. *Science* **313**, 1788–1792 (2006).
- Chang, J., Gudima, S. O., Tarn, C., Nie, X. & Taylor, J. M. Development of a novel system to study hepatitis delta virus genome replication. *J. Virol.* **79**, 8182–8188 (2005).
- Bichko, V., Netter, H. J. & Taylor, J. Introduction of hepatitis delta virus into animal cell lines via cationic liposomes. *J. Virol.* **68**, 5247–5252 (1994).
- Polo, J. M. et al. Transgenic mice support replication of hepatitis delta virus RNA in multiple tissues, particularly in skeletal muscle. *J. Virol.* **69**, 4880–4887 (1995).
- Hetzel U., et al. Identification of a novel deltavirus in Boa Constrictors. *MBio* **10**, e00014-19 (2019).
- Wille M., et al. A divergent hepatitis D-like agent in birds. *Viruses* **10**, 720 (2018).
- Weller, M. L. et al. Hepatitis delta virus detected in salivary glands of Sjogren’s syndrome patients and recapitulates a sjogren’s syndrome-like phenotype in vivo. *Pathog. Immun.* **1**, 12–40 (2016).
- Kuo, M. Y., Chao, M. & Taylor, J. Initiation of replication of the human hepatitis delta virus genome from cloned DNA: role of delta antigen. *J. Virol.* **63**, 1945–1950 (1989).
- Freitas, N., Cunha, C., Menne, S. & Gudima, S. O. Envelope proteins derived from naturally integrated hepatitis B virus DNA support assembly and release of infectious hepatitis delta virus particles. *J. Virol.* **88**, 5742–5754 (2014).
- Sureau, C. The use of hepatocytes to investigate HDV infection: the HDV/HepaRG model. *Methods Mol. Biol.* **640**, 463–473 (2010).
- Li, Y. J., Macnaughton, T., Gao, L. & Lai, M. M. RNA-templated replication of hepatitis delta virus: genomic and antigenomic RNAs associate with different nuclear bodies. *J. Virol.* **80**, 6478–6486 (2006).
- Freitas, N. et al. Hepatitis delta virus infects the cells of hepadnavirus-induced hepatocellular carcinoma in woodchucks. *Hepatology* **56**, 76–85 (2012).
- Gudima, S. et al. Assembly of hepatitis delta virus: particle characterization, including the ability to infect primary human hepatocytes. *J. Virol.* **81**, 3608–3617 (2007).
- Verrier, E. R. et al. A targeted functional RNA interference screen uncovers glypican 5 as an entry factor for hepatitis B and D viruses. *Hepatology* **63**, 35–48 (2016).
- Amirache, F. et al. Mystery solved: VSV-G-LVs do not allow efficient gene transfer into unstimulated T cells, B cells, and HSCs because they lack the LDL receptor. *Blood* **123**, 1422–1424 (2014).
- Finkelshtein, D., Werman, A., Novick, D., Barak, S. & Rubinstein, M. LDL receptor and its family members serve as the cellular receptors for vesicular stomatitis virus. *Proc. Natl Acad. Sci. USA* **110**, 7306–7311 (2013).
- Bartosch, B., Dubuisson, J. & Cosset, F. L. Infectious hepatitis C virus pseudo-particles containing functional E1-E2 envelope protein complexes. *J. Exp. Med.* **197**, 633–642 (2003).
- Bordier, B. B. et al. In vivo antiviral efficacy of prenylation inhibitors against hepatitis delta virus. *J. Clin. Invest.* **112**, 407–414 (2003).
- O’Malley, B. & Lazinski, D. W. Roles of carboxyl-terminal and farnesylated residues in the functions of the large hepatitis delta antigen. *J. Virol.* **79**, 1142–1153 (2005).
- Law, M. et al. Broadly neutralizing antibodies protect against hepatitis C virus quasispecies challenge. *Nat. Med.* **14**, 25–27 (2008).
- Azuma, H. et al. Robust expansion of human hepatocytes in *Fah*^{-/-}/*Rag2*^{-/-}/*Il2rg*^{-/-} mice. *Nat. Biotechnol.* **25**, 903–910 (2007).
- Calattini, S. et al. Functional and biochemical characterization of hepatitis C virus (HCV) particles produced in a humanized liver mouse model. *J. Biol. Chem.* **290**, 23173–23187 (2015).
- Bissig, K. D. et al. Human liver chimeric mice provide a model for hepatitis B and C virus infection and treatment. *J. Clin. Invest.* **120**, 924–930 (2010).
- Ciancio, A. & Rizzetto, M. Chronic hepatitis D at a standstill: where do we go from here? *Nat. Rev. Gastroenterol. Hepatol.* **11**, 68–71 (2014).
- Lambert, C., Doring, T. & Prange, R. Hepatitis B virus maturation is sensitive to functional inhibition of ESCRT-III, Vps4, and gamma 2-adaptin. *J. Virol.* **81**, 9050–9060 (2007).
- Watanabe, T. et al. Involvement of host cellular multivesicular body functions in hepatitis B virus budding. *Proc. Natl Acad. Sci. USA* **104**, 10205–10210 (2007).

46. Patient, R. et al. Hepatitis B virus subviral envelope particle morphogenesis and intracellular trafficking. *J. Virol.* **81**, 3842–3851 (2007).
47. O'Malley, B. & Lazinski, D. A hepatitis B surface antigen mutant that lacks the antigenic loop region can self-assemble and interact with the large hepatitis delta antigen. *J. Virol.* **76**, 10060–10063 (2002).
48. Komla-Soukha, I. & Sureau, C. A tryptophan-rich motif in the carboxyl terminus of the small envelope protein of hepatitis B virus is central to the assembly of hepatitis delta virus particles. *J. Virol.* **80**, 4648–4655 (2006).
49. Blanchet, M. & Sureau, C. Analysis of the cytosolic domains of the hepatitis B virus envelope proteins for their function in viral particle assembly and infectivity. *J. Virol.* **80**, 11935–11945 (2006).
50. Chai, N. et al. Properties of subviral particles of hepatitis B virus. *J. Virol.* **82**, 7812–7817 (2008).
51. Koh, C. et al. Oral prenylation inhibition with lonafarnib in chronic hepatitis D infection: a proof-of-concept randomised, double-blind, placebo-controlled phase 2A trial. *Lancet Infect. Dis.* **15**, 1167–1174 (2015).
52. Sureau, C. & Negro, F. The hepatitis delta virus: replication and pathogenesis. *J. Hepatol.* **64**, S102–S116 (2016).
53. Romero-Brey I., Bartenschlager R. Endoplasmic Reticulum: the favorite intracellular niche for viral replication and assembly. *Viruses* **8**, E160 (2016).
54. Sandrin, V. & Cosset, F.-L. Intracellular vs. cell surface assembly of retroviral pseudotypes is determined by the cellular localization of the viral glycoprotein, its capacity to interact with Gag and the expression of the Nef protein. *J. Biol. Chem.* **281**, 528–542 (2006).
55. Bouard, D. et al. An acidic cluster of the cytoplasmic tail of the RD114 virus glycoprotein controls assembly of retroviral envelopes. *Traffic* **8**, 835–847 (2007).
56. Welsch, S., Muller, B. & Krausslich, H. G. More than one door - Budding of enveloped viruses through cellular membranes. *FEBS Lett.* **581**, 2089–2097 (2007).
57. Miyahara, A. Preparation of vesicular stomatitis virus-G (VSV-G) conjugate and its use in gene transfer. *Cold Spring Harb. Protoc.* **2012**, 453–456 (2012).
58. Denolly, S. et al. The amino-terminus of the hepatitis C virus (HCV) p7 viroporin and its cleavage from glycoprotein E2-p7 precursor determine specific infectivity and secretion levels of HCV particle types. *PLoS Pathog.* **13**, e1006774 (2017).
59. Scholtes, C. et al. High plasma level of nucleocapsid-free envelope glycoprotein-positive lipoproteins in hepatitis C patients. *Hepatology* **56**, 39–48 (2012).
60. Konishi, E. & Fujii, A. Dengue type 2 virus subviral extracellular particles produced by a stably transfected mammalian cell line and their evaluation for a subunit vaccine. *Vaccine* **20**, 1058–1067 (2002).
61. Hanna, S. L. et al. N-linked glycosylation of west Nile virus envelope proteins influences particle assembly and infectivity. *J. Virol.* **79**, 13262–13274 (2005).
62. Swintek, B. D. & Lyles, D. S. Plasma membrane microdomains containing vesicular stomatitis virus M protein are separate from microdomains containing G protein and nucleocapsids. *J. Virol.* **82**, 5536–5547 (2008).
63. Smedile, A. et al. Influence of delta infection on severity of hepatitis B. *Lancet* **2**, 945–947 (1982).
64. Giersch, K. & Dandri, M. Hepatitis B and delta virus: advances on studies about interactions between the two viruses and the infected hepatocyte. *J. Clin. Transl. Hepatol.* **3**, 220–229 (2015).
65. Krogsgaard, K. et al. Delta-infection and suppression of hepatitis B virus replication in chronic HBsAg carriers. *Hepatology* **7**, 42–45 (1987).
66. Smedile, A. et al. Infection with the delta agent in chronic HBsAg carriers. *Gastroenterology* **81**, 992–997 (1981).
67. Fattovich, G. et al. Influence of hepatitis delta virus infection on progression to cirrhosis in chronic hepatitis type B. *J. Infect. Dis.* **155**, 931–935 (1987).
68. Negro, F. et al. Chronic HDV (hepatitis delta virus) hepatitis. Intrahepatic expression of delta antigen, histologic activity and outcome of liver disease. *J. Hepatol.* **6**, 8–14 (1988).
69. Giersch, K. et al. Persistent hepatitis D virus mono-infection in humanized mice is efficiently converted by hepatitis B virus to a productive co-infection. *J. Hepatol.* **60**, 538–544 (2014).
70. Alfaiate, D. et al. HDV RNA replication is associated with HBV repression and interferon-stimulated genes induction in super-infected hepatocytes. *Antivir. Res.* **136**, 19–31 (2016).
71. Zhang, Z. et al. Hepatitis D virus replication is sensed by MDA5 and induces IFN-beta/lambda responses in hepatocytes. *J. Hepatol.* **69**, 25–35 (2018).
72. Lutgehetmann, M. et al. Hepatitis B virus limits response of human hepatocytes to interferon-alpha in chimeric mice. *Gastroenterology* **140**, 2074–2083 (2011). 2083 e2071-2072.
73. Mutz, P. et al. HBV bypasses the innate immune response and does not protect HCV from antiviral activity of interferon. *Gastroenterology* **154**, 1791–1804 e1722 (2018).
74. Sandrin, V. et al. Lentiviral vectors pseudotyped with a modified RD114 envelope glycoprotein show increased stability in sera and augmented transduction of primary lymphocytes and CD34+ cells derived from human and nonhuman primates. *Blood* **100**, 823–832 (2002).
75. Levy, C. et al. Virus-like particle vaccine induces cross-protection against human metapneumovirus infections in mice. *Vaccine* **31**, 2778–2785 (2013).
76. Sainz, B. Jr. & Chisari, F. V. Production of infectious hepatitis C virus by well-differentiated, growth-arrested human hepatoma-derived cells. *J. Virol.* **80**, 10253–10257 (2006).
77. Giersch, K. et al. Both interferon alpha and lambda can reduce all intrahepatic HDV infection markers in HBV/HDV infected humanized mice. *Sci. Rep.* **7**, 3757 (2017).
78. Lucifora, J. et al. Direct antiviral properties of TLR ligands against HBV replication in immune-competent hepatocytes. *Sci. Rep.* **8**, 5390 (2018).
79. Boson, B., Granio, O., Bartenschlager, R. & Cosset, F. L. A concerted action of hepatitis C virus p7 and nonstructural protein 2 regulates core localization at the endoplasmic reticulum and virus assembly. *PLoS Pathog.* **7**, e1002144 (2011).
80. Boson, B. et al. Daclatasvir prevents hepatitis C Virus infectivity by blocking transfer of the viral genome to assembly sites. *Gastroenterology* **152**, 895–907 e814 (2017).

Acknowledgements

We thank Massimo Levrero and Fabien Zoulim for helpful discussions and critical reading of this paper. We thank Christelle Granier and Solène Denolly and all the members of our laboratory for their support and encouragement. We are grateful to Philippe Desprès for the 3H5 DENV-E antibody, Mansun Law for the AR3A HCV-E2 antibody, and Charles Rice for the Huh-7.5 cells and the 9E10 HCV-NS5A antibody. We thank the Plateforme de Thérapie Génique in Nantes (France) for the production of the in vivo-certified lots of adeno-uPA vector. We thank Jean-François Henry, Nadine Aguilera and Jean-Louis Thoumas from the animal facility (PBES, Plateau de Biologie Experimentale de la Souris, UMS3444/CNRS, US8/ Inserm, ENS de Lyon, UCBL), and Anaïs Ollivier for her technical help in handling of mice. We acknowledge the contribution of the ANIRA-Genetic Analysis facility of SFR Biosciences (UMS3444/CNRS, US8/Inserm, ENS de Lyon, UCBL) for technical assistance and support. We thank Didier Décimo for support with the BSL3 facility. We thank Christelle Fabrer-Boulé from the electron microscopy studies at the “Centre Technologique des Microstructures (CTμ)” at UCBL. We thank N. Gadot (Plateforme Anatomopathologie Recherche, Centre Léon Bérard, F-69373 Lyon, France) for the IHC analyses. This work was supported by the French “Agence Nationale de la Recherche sur le SIDA et les hépatites virales” (ANRS) and the LabEx Ecofect (ANR-11-LABX-0048) of the “Université de Lyon”, within the program “Investissements d’Avenir” (ANR-11-IDEX-0007) operated by the French National Research Agency (ANR).

Author contributions

J.P.-V. and F.-L.C. conceived the study. J.P.-V., F.A., B.B., C.M., F.F. and F.-L.C. designed and performed experiments. J.P.-V., F.A., B.B., N.F., C.S., F.F. and F.-L.C. analyzed the data. J.P.-V. and F.-L.C. wrote the paper with contributions from all authors.

Additional information

Supplementary Information accompanies this paper at <https://doi.org/10.1038/s41467-019-10117-z>.

Competing interests: The authors declare no competing interests.

Reprints and permission information is available online at <http://npg.nature.com/reprintsandpermissions/>

Journal peer review information: *Nature Communications* thanks the anonymous reviewer (s) for their contribution to the peer review of this work. Peer reviewer reports are available.

Publisher's note: Springer Nature remains neutral with regard to jurisdictional claims in published maps and institutional affiliations.



Open Access This article is licensed under a Creative Commons Attribution 4.0 International License, which permits use, sharing, adaptation, distribution and reproduction in any medium or format, as long as you give appropriate credit to the original author(s) and the source, provide a link to the Creative Commons license, and indicate if changes were made. The images or other third party material in this article are included in the article's Creative Commons license, unless indicated otherwise in a credit line to the material. If material is not included in the article's Creative Commons license and your intended use is not permitted by statutory regulation or exceeds the permitted use, you will need to obtain permission directly from the copyright holder. To view a copy of this license, visit <http://creativecommons.org/licenses/by/4.0/>.

© The Author(s) 2019

Enveloped viruses distinct from HBV induce dissemination of hepatitis D virus *in vivo*

Authors: Jimena Perez-Vargas¹, Fouzia Amirache¹, Bertrand Boson¹, Chloé Mialon¹, Natalia Freitas¹, Camille Sureau², Floriane Fusil¹, and François-Loïc Cosset^{1*}

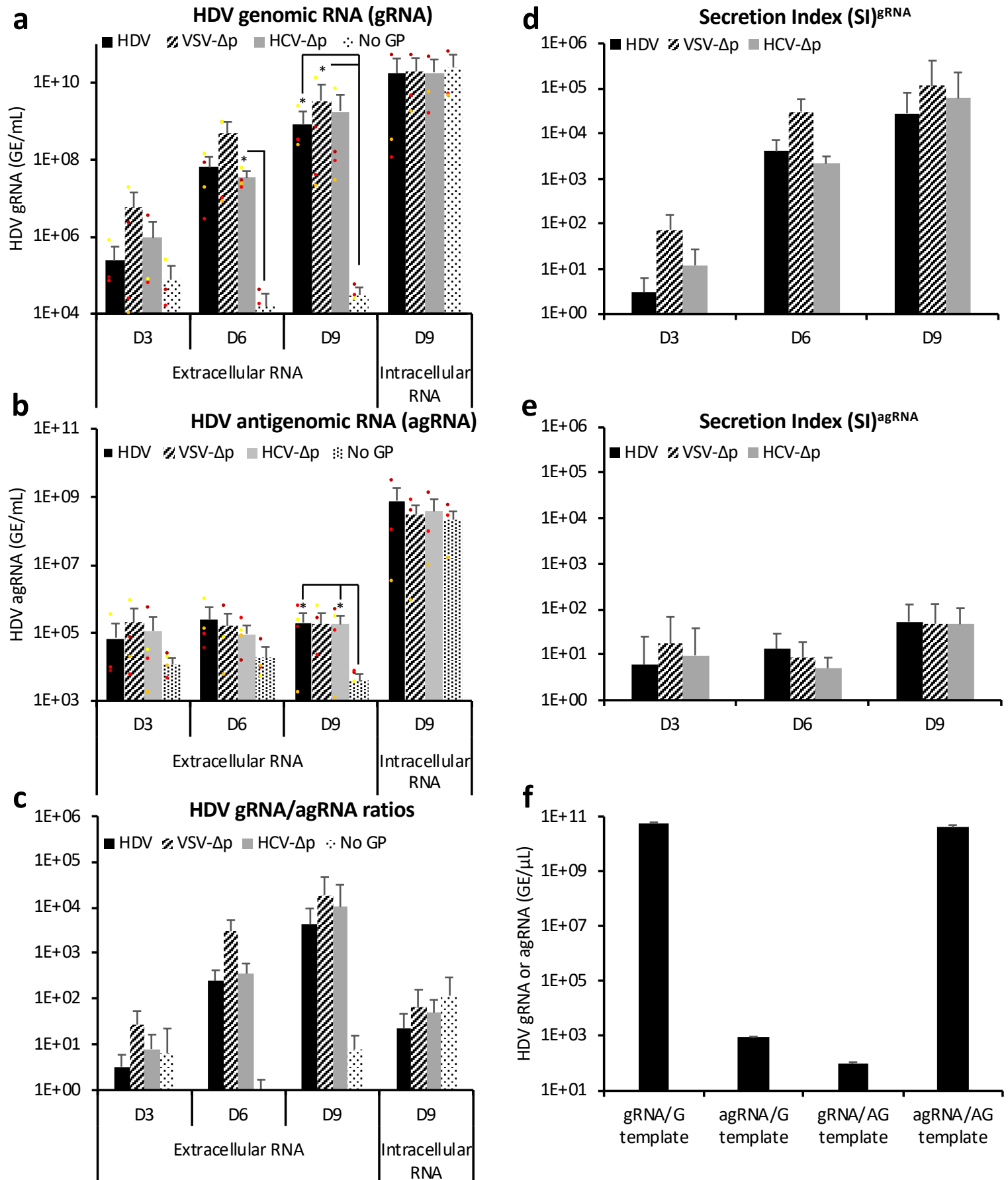
Affiliations :

¹CIRI – Centre International de Recherche en Infectiologie, Univ Lyon, Université Claude Bernard Lyon 1, Inserm, U1111, CNRS, UMR5308, ENS Lyon, 46 allée d'Italie, F-69007, Lyon, France.

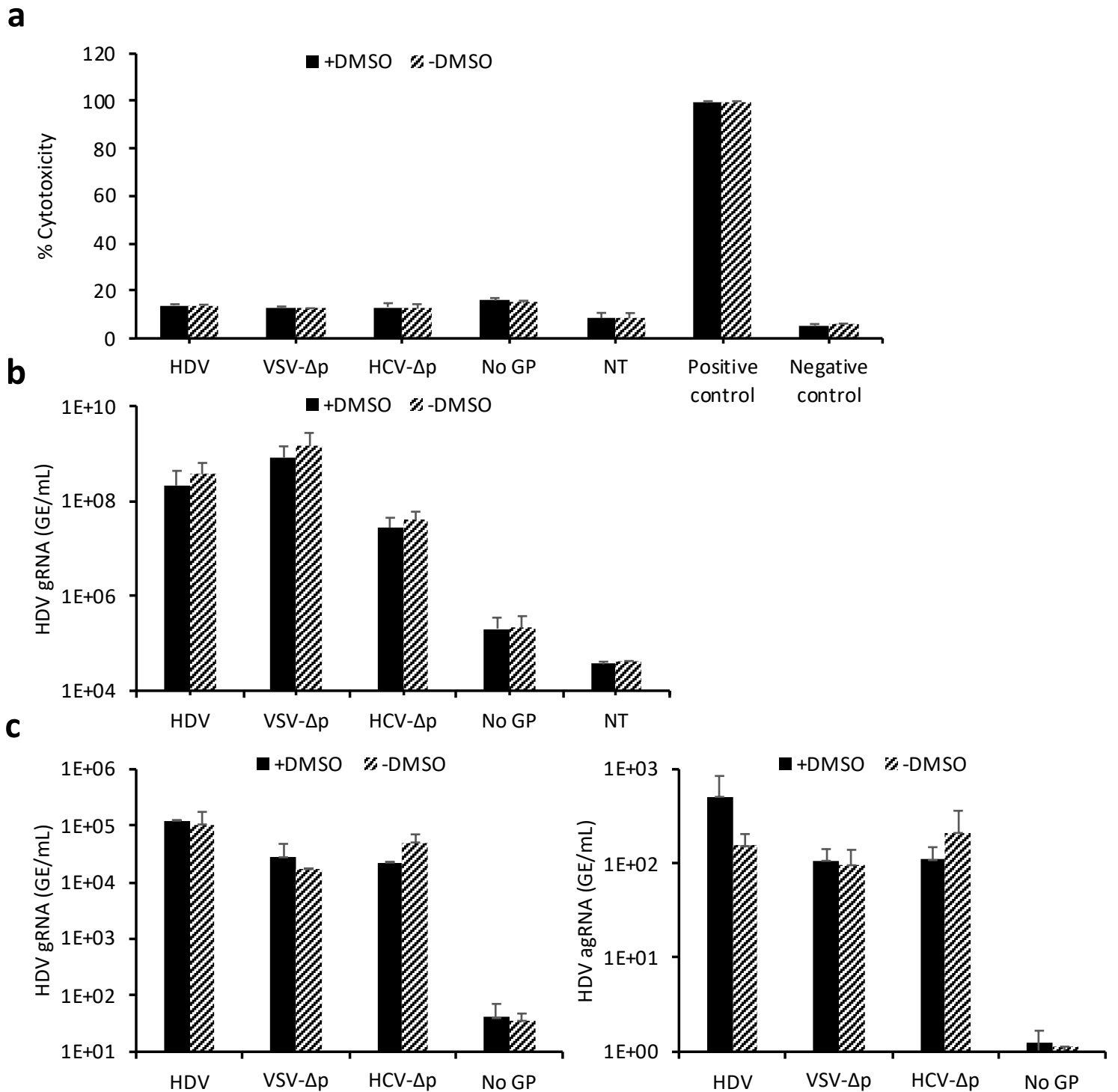
²Molecular Virology laboratory, Institut National de la Transfusion Sanguine (INTS), CNRS Inserm U1134, 6 rue Alexandre Cabanel, F-75739 Paris, France.

***Correspondence:** François-Loïc Cosset. CIRI – International Center for Infectiology Research. E-mail: fcosset@ens-lyon.fr

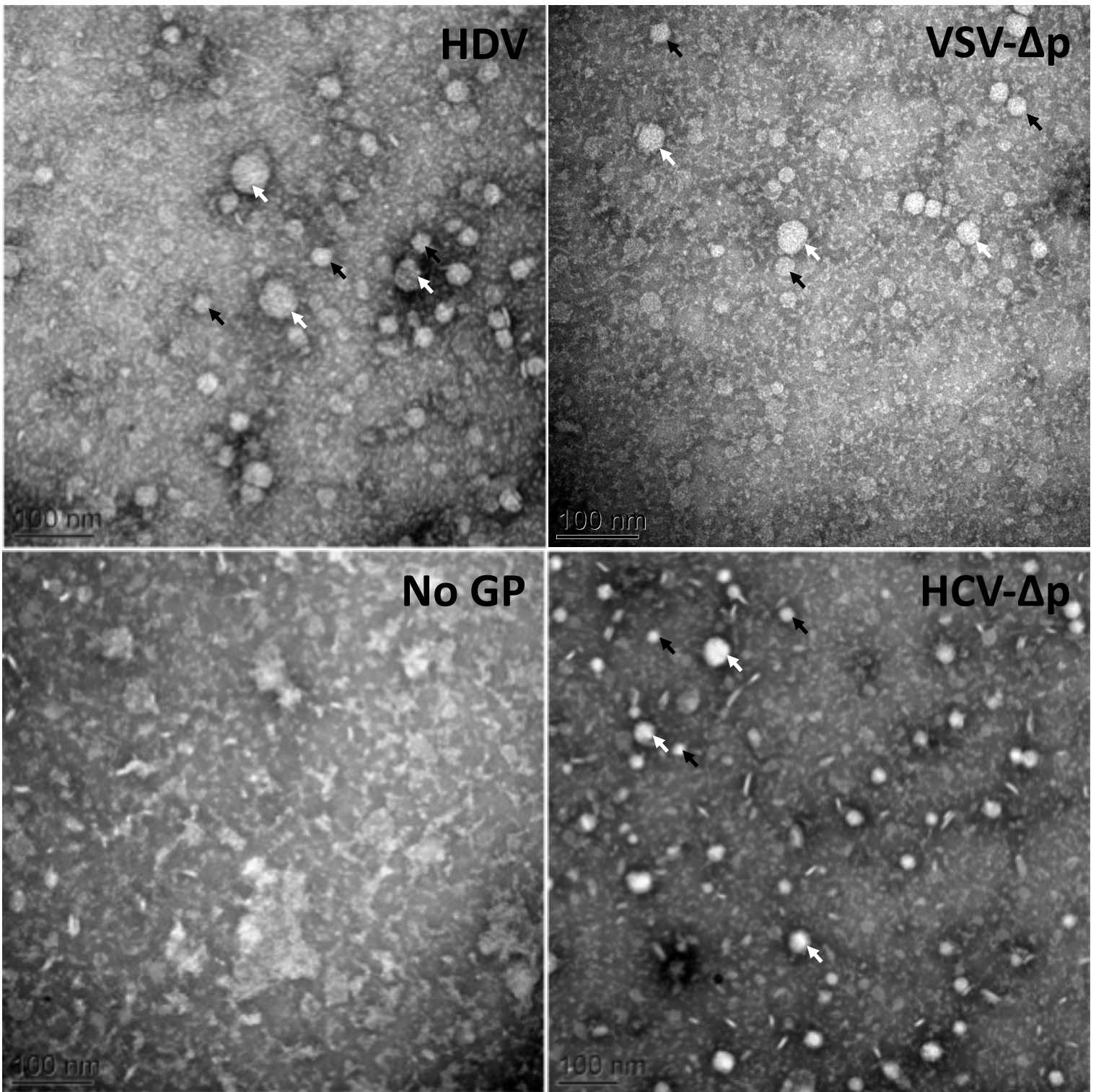
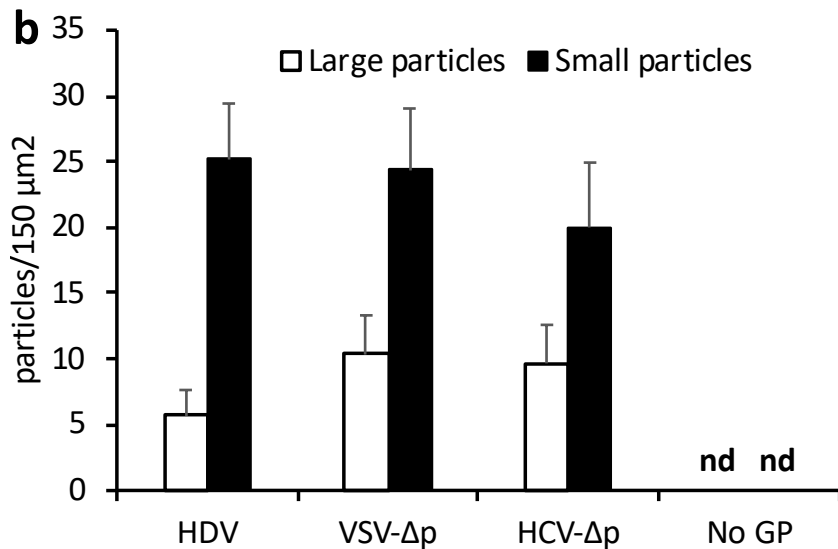
Supplementary Information



Supplementary Figure 1. Quantification of genomic and antigenomic HDV RNAs in lysates and supernatants of cells producing HDV, VSV-Δp, and HCV-Δp particles. (a, b) Huh-7 cells were co-transfected with pSVLD3 plasmid coding for HDV RNPs and plasmids coding for either HBV, VSV or HCV surface glycoproteins (GP), resulting in “HDV”, “VSV-Δp”, and “HCV-Δp” samples, respectively. As control, pSVLD3 was co-transfected with an empty plasmid (“No GP” samples). At day 3, 6 or 9, extracellular HDV RNAs were quantified from cell supernatants by using a strand-specific RTqPCR assay for genomic (gRNA) (a) and anti-genomic (agRNA) (b) HDV RNAs. Intracellular HDV gRNA and agRNA RNAs were quantified from cell lysates at day 9. HDV RNAs in GE (genome equivalent), per ml of cell supernatants for extracellular RNAs or, for intracellular RNAs, per ml of cell lysates containing 10^6 cells. No significant increase of HDV agRNAs over time post-transfection could be detected in the supernatants (b), in sharp contrast to the extracellular HDV gRNAs that increased by up to 1,000-fold (a). (c) The enrichment of HDV gRNAs in secreted particles is reflected by calculating the gRNA/agRNA ratios in HDV, VSV-Δp or HCV-Δp particles from the supernatants and in cell lysates. Particularly, at day 9 post-transfection, the gRNA/agRNA ratios in particles are up to 800-fold higher than the gRNA/agRNA ratios in the cell lysates. (d, e) “Secretion Indexes” (SI) were calculated for HDV gRNAs (SI^{gRNA}) (d) and for HDV agRNAs (SI^{agRNA}) (e) by normalizing extracellular RNAs detected in cell supernatants for HDV, VSV-Δp or HCV-Δp to the “No GP” condition. (f) The strand-specific RTqPCR assay allowing quantification of gRNAs or agRNAs was calibrated and validated using either 10^{11} genomic (G) or antigenomic (AG) HDV RNA standards that had been transcribed *in vitro* as templates to detect unspecific quantification. The results indicate specific detection of either template and very low detection of opposite templates. Error bars correspond to standard deviation. Statistical analyses (Student’s t-test): $p < 0.05$ (*).

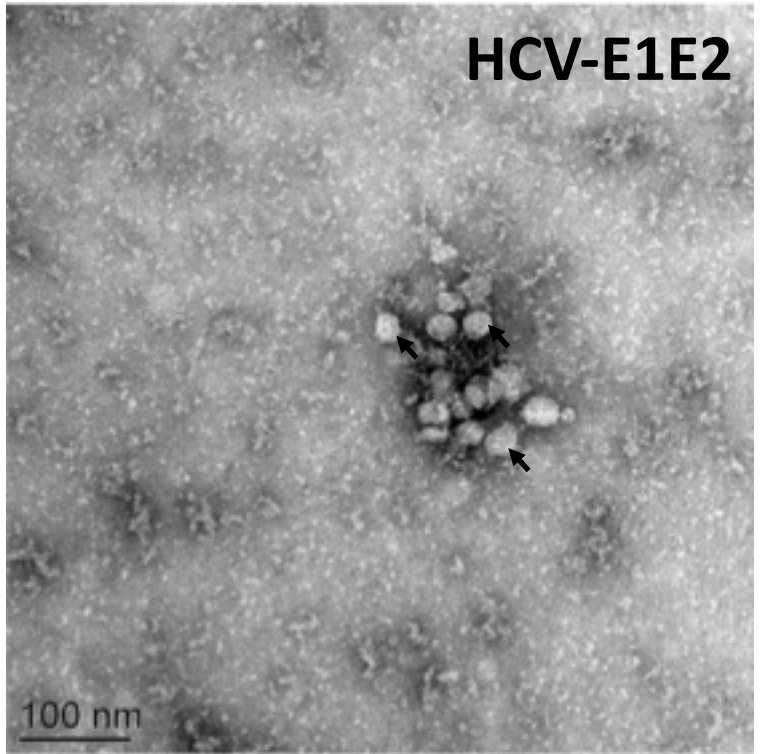
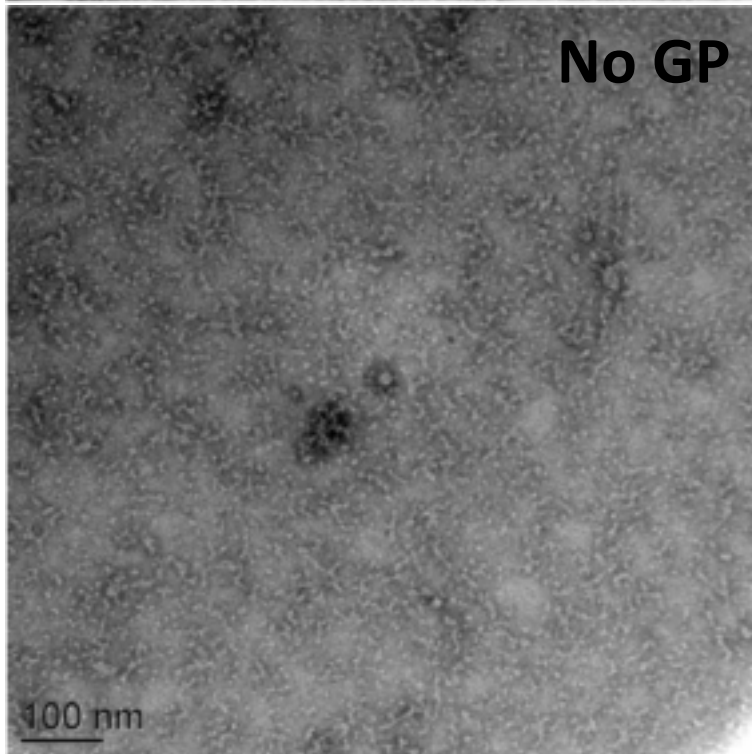
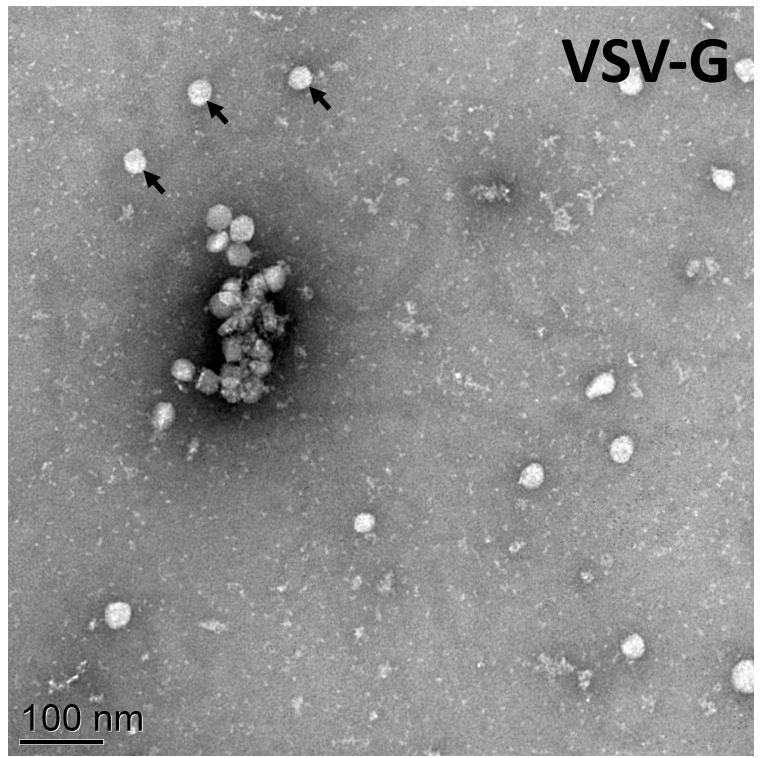
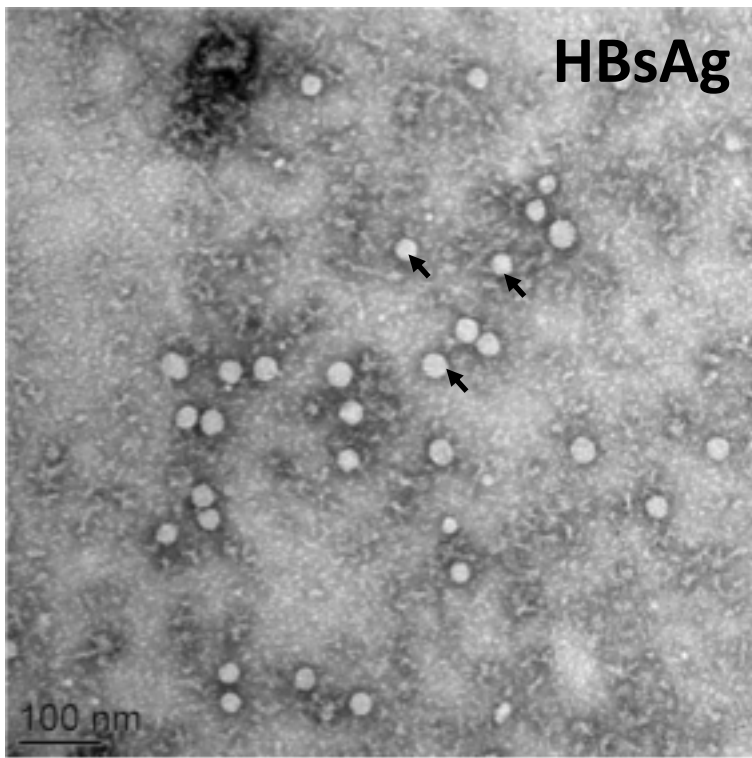


Supplementary Figure 2. DMSO supplementation in producer cell culture media does not affect production of HDV particles. Huh-7 cells were co-transfected with pSVLD3 plasmid coding for HDV RNPs and plasmids coding for either HBV “HDV”, VSV “VSV-Δp” or HCV “HCV-Δp” envelope glycoproteins (GP). As control, Huh-7 cells were transfected with pSVLD3 plasmid without envelope proteins (No GP) or were not transfected (NT). (a-c) The cells were cultured for 6 days in primary hepatocyte maintenance medium (see Methods section) containing (+DMSO), or not (-DMSO), 2%DMSO to slow cell growth, as indicated. Cell toxicity assessment was performed with the LDH (Pierce Cytotoxicity Assay Kit) using the indicated positive and negative controls of the kit (a). The cell supernatants were then filtered and the extracellular RNA was extracted and purified before quantifying HDV gRNAs by strand-specific RTqPCR (b). Huh-106 cells were inoculated with the above supernatants. Infected cells were grown for 7 days before total intracellular RNA was purified (c). The quantification of intracellular viral nucleic acids in lysates of infected cells were normalized with GAPDH RNAs. The results of HDV gRNAs quantification by strand-specific RTqPCR assays are expressed in GE (genome equivalent) and are displayed as means per mL of cell supernatants for extracellular nucleic acids or, for intracellular nucleic acids, per mL of cell lysates containing 10^6 cells. Source data are provided as a Source Data file. Error bars correspond to standard deviation.

a**b**

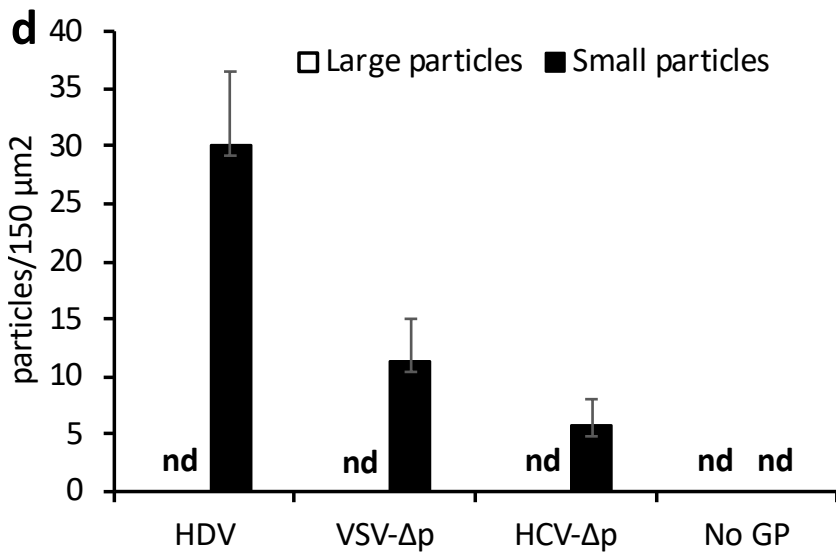
Supplementary Figure 3. Electron microscopy analysis of HDV particles produced with VSV and HCV glycoproteins.

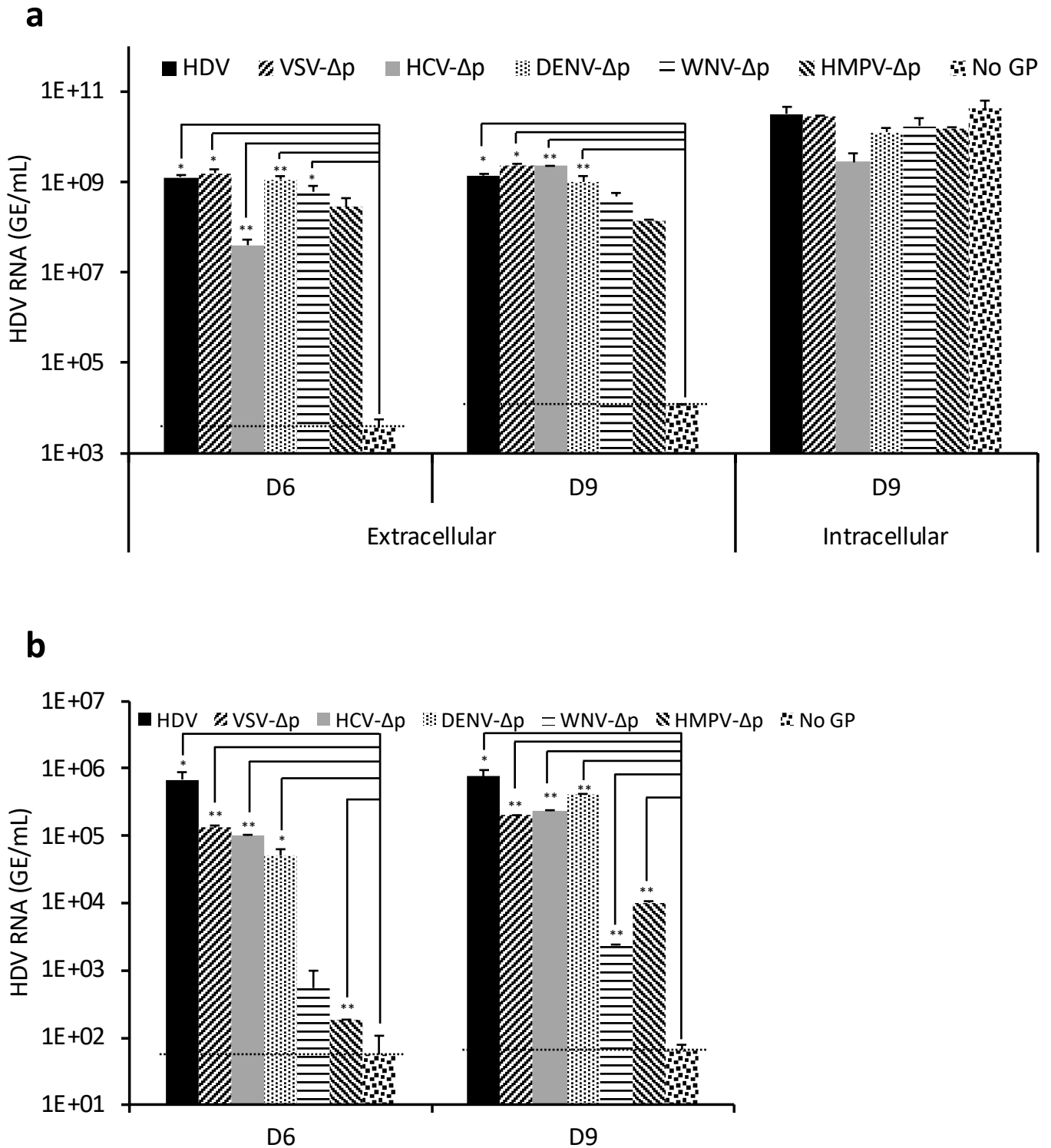
Huh-7 cells were co-transfected with pSVLD3 plasmid coding for HDV RNPs and plasmids coding for either HBV “HDV”, VSV “VSV-Δp” or HCV “HCV-Δp” envelope glycoproteins (GP) (a) or were only transfected with plasmids encoding the above GPs, as indicated (c). As controls, an empty plasmid was co-transfected with pSVLD3 (a) or transfected alone (c) (referred to as “No GP”). At day 6 post-transfection, the cell supernatants were harvested, filtered and purified on heparin beads. Particles were eluted and observed by electron microscopy after negative staining. The scale bars represent 100 nm. The panels in (a) show examples of particles produced by co-transfection of pSVLD3 plasmid and plasmids encoding HBsAg (HDV), VSV-G (VSV-Δp), or HCV-E1E2 (HCV-Δp) while the panels in (c) show examples of particles produced by transfection of plasmids encoding either GP alone. Note that large, *i.e.*, with diameters of 35-40 nm (white arrows) and small, *i.e.*, with diameters of 25-30 nm (black arrows) particles can be detected in (a) whereas only small particles can be detected in (c). See quantification of either particle type (b, d). nd, not detectable. Source data are provided as a Source Data file. Error bars correspond to standard deviation.

c

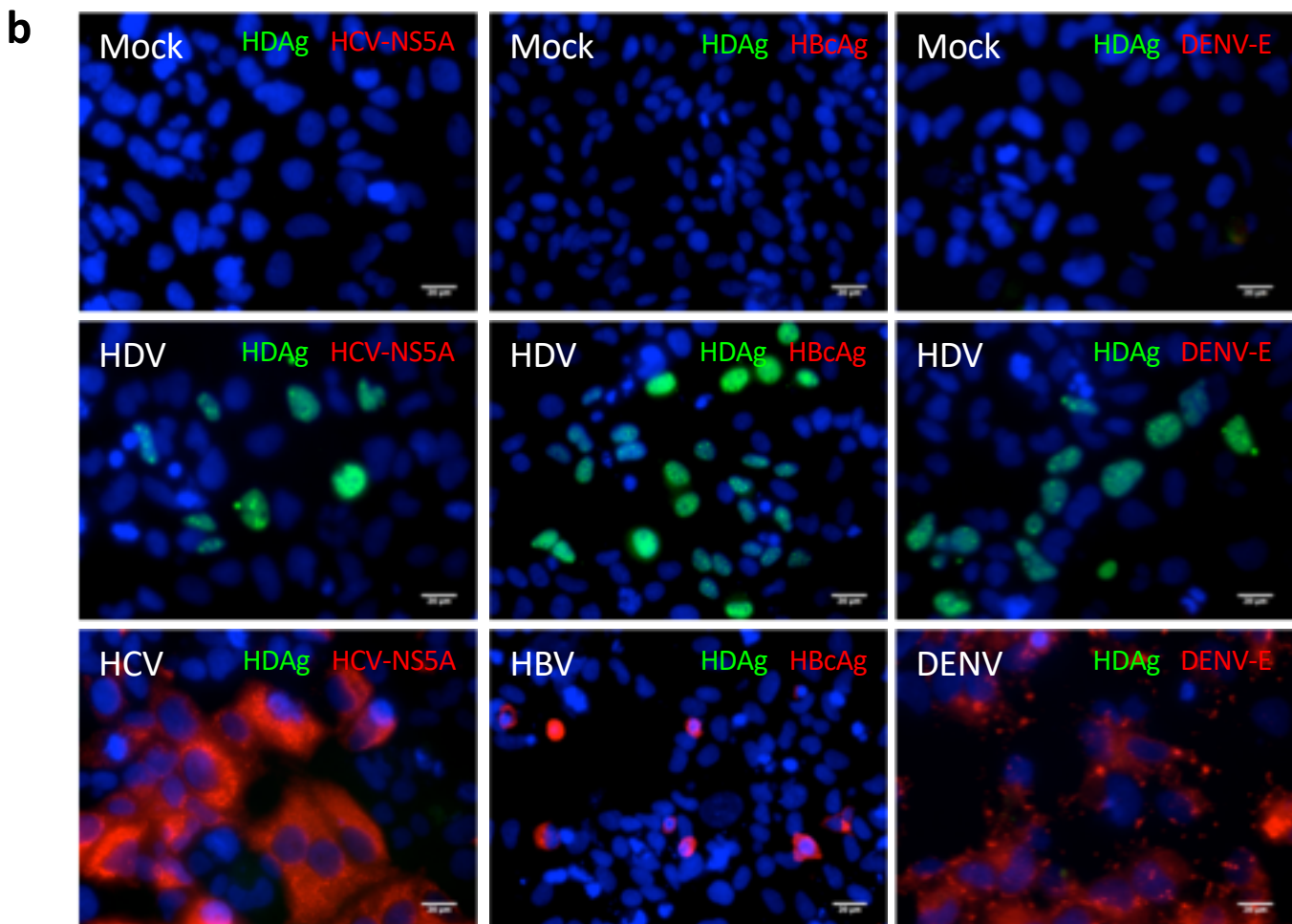
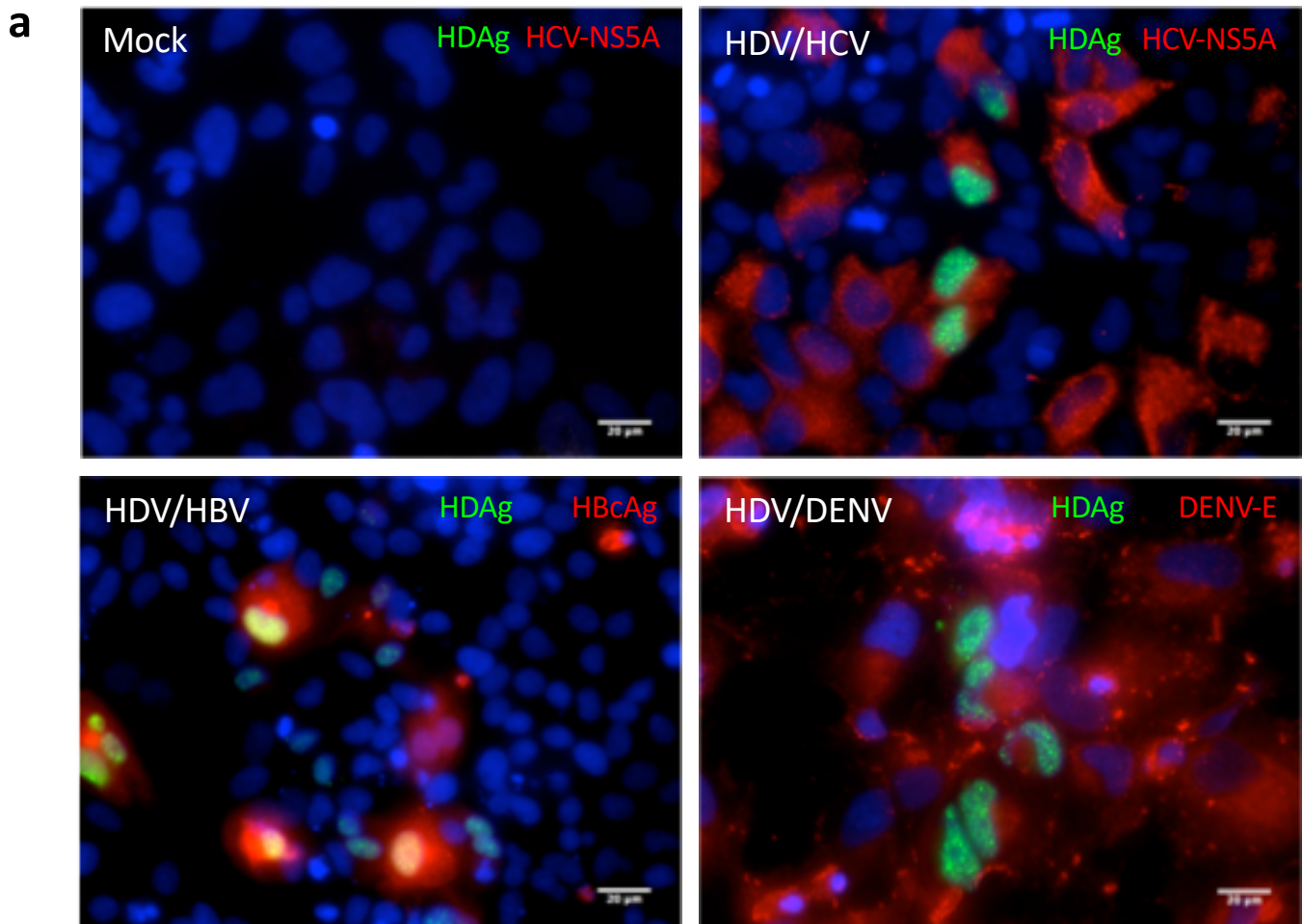
Supplementary Figure 3. Electron microscopy analysis of HDV particles produced with VSV and HCV glycoproteins.

(continued)

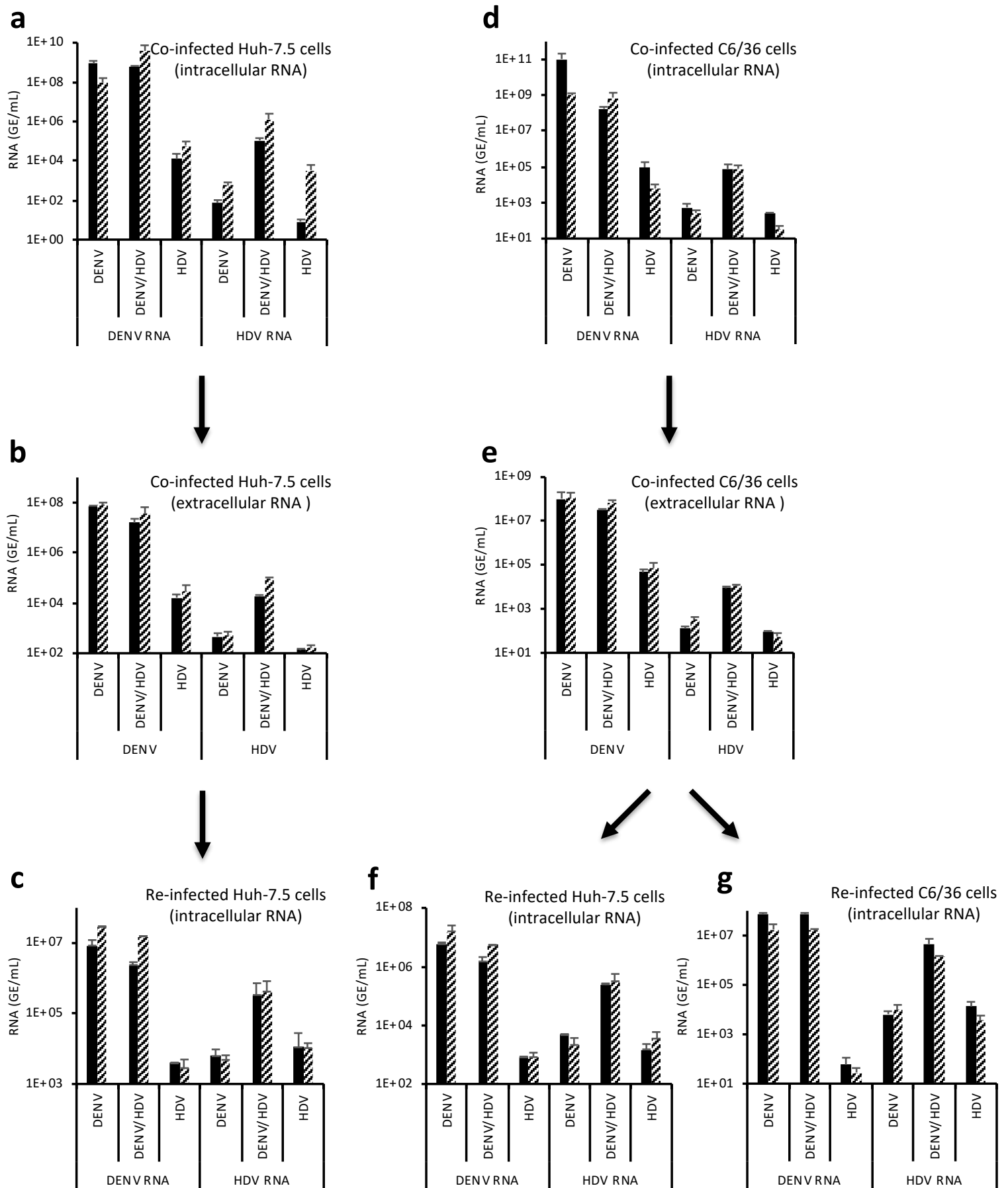




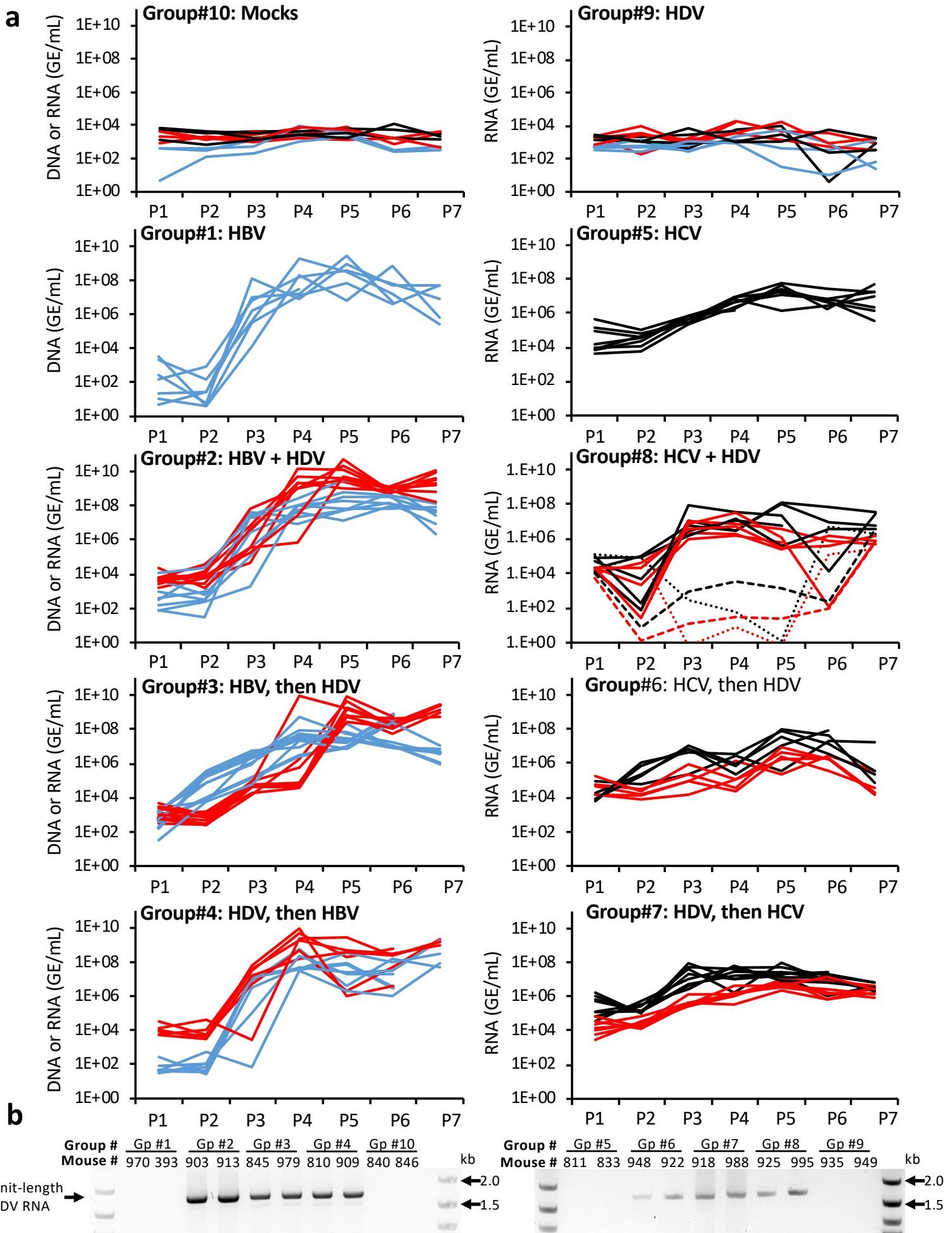
Supplementary Figure 4. Secretion and infectivity of HDV particles enveloped with different GP from 293T cells. (a) Cell culture media from 293T cells were harvested at day 6 or 9, as indicated, upon co-transfection of pSVLD3 plasmid coding for HDV RNPs and plasmids coding for HBV (HDV), VSV (VSV-Δp), HCV (HCV-Δp), DENV (DENV-Δp), WNV (WNV-Δp) or HMPV (HMPV-Δp) envelope glycoproteins. As control, pSVLD3 was transfected without envelope proteins (No GP). The cell supernatants were filtered and the extracellular RNA was extracted and purified before quantifying HDV RNAs by RTqPCR. The quantification of intracellular HDV RNAs in cells producing the HDV particles at day 9 post-transfection and normalized with GAPDH RNAs are also shown. HDV RNAs in GE (genome equivalent)/mL are expressed as means (N=5 independent experiments) per ml of cell lysates containing 10^6 cells. (b) The infectivity of virus particles present in the cell supernatants that were harvested at day 6 or 9 post-transfection was determined in Huh-106 (NTCP-expressing Huh-7 cells) cells. Infected cells were grown for 7 days before total intracellular RNA was purified. The results of HDV RNAs quantification by RTqPCR are expressed as means after normalization with GAPDH RNAs. The dotted lines represent the experimental thresholds, as defined with the "No GP" controls. Source data are provided as a Source Data file. Error bars correspond to standard deviation. Statistical analyses (Student's t-test): $p < 0.05$ (*); $p < 0.01$ (**).



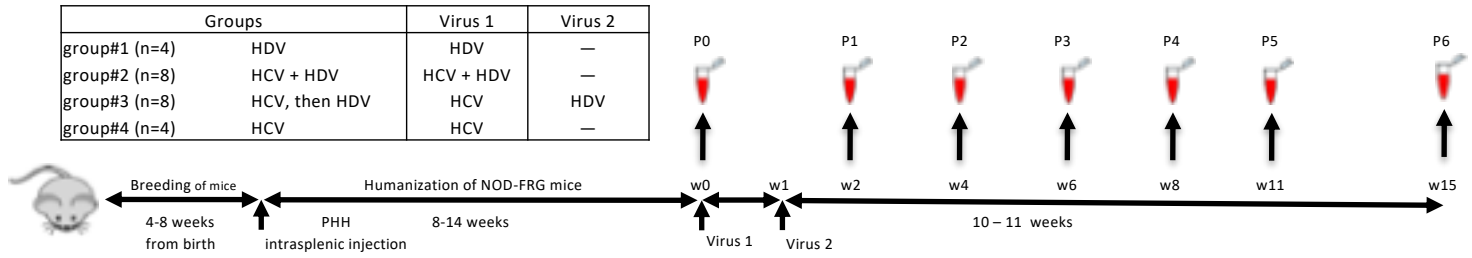
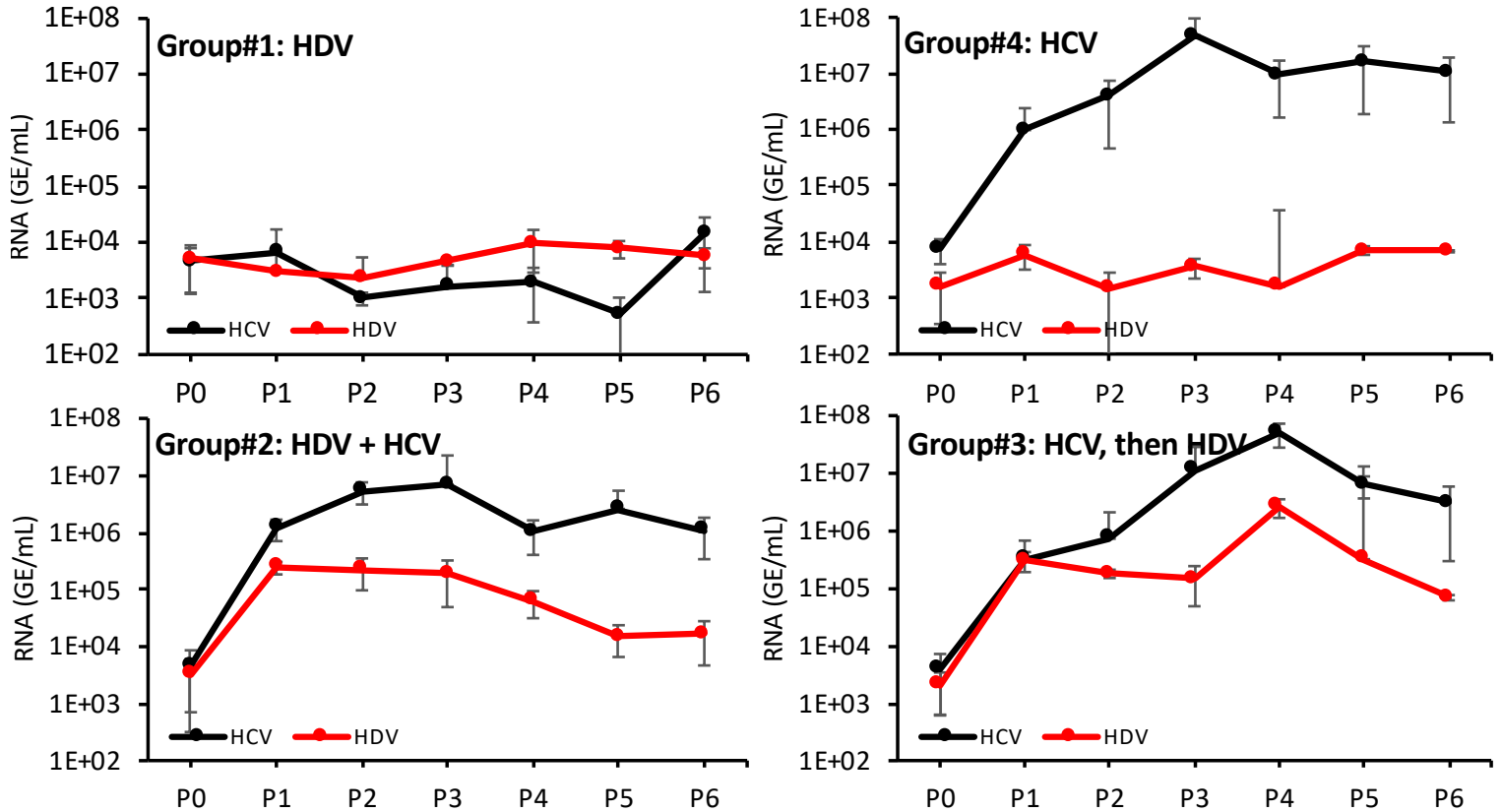
Supplementary Figure 5. Immunofluorescence of HDV RNA-expressing cells superinfected with HBV, HCV and DENV. (a) mock-infected cells (Mock) or cells expressing HDV RNAs that were inoculated with live HCV (HDV/HCV), HBV (HDV/HBV) or DENV (HDV/DENV) viruses were fixed, stained for HDV and HCV-NS5A, HDV and HBcAg and HDV and DENV-E, as indicated, counterstained with Hoechst to visualize the nuclei. HDV (green channel), HCV-NS5A, HBcAg, DENV-E (red channels) and nuclei (blue channel), and were then visualized by immunofluorescence. Scale bars represent 20 μ m. (b) Controls of immunofluorescence staining. Mock-infected cells (top row), HDV-expressing cells (middle row) and HCV-, HBV- or DENV-infected cells (bottom row) were stained for HDV (green), nuclei (blue) and HCV-NS5A (red, left column), HBcAg (red, middle column) or DENV-E (red, right column), and visualized by immunofluorescence. Scale bars represent 20 μ m.



Supplementary Figure 6. HDV/DENV productively infect and propagate in C6/36 mosquito cells. Huh-7.5 (a) or C6/36 (d) cells were inoculated with low (black bars) vs. high (hatched bars) inputs of HDV/DENV (MOI=0.01 and 0.1 FFU/cell for HDV and DENV, respectively) particles, that were purified from HDV/DENV co-infected cells (see Figure 6). Supernatants and lysates from these cells were harvested at day 5 post-infection. The supernatants from HDV/DENV co-infected Huh-7.5 (b) or C6/36 (e) cells were used, respectively, to re-infect naïve Huh-7.5 (c) cells or both Huh-7.5 (f) and Huh-106 (g) cells. Infection levels were assessed at day 7 post-infection. The nucleic acids present in filtered cell supernatants (b, e) as well as in lysates of producer cells (a, d) and target cells (c, f, g) were extracted and purified for quantification of HDV and DENV RNA by RTqPCR. The quantification of intracellular RNAs in cell lysates were normalized with GAPDH RNAs. The results expressed in GE (genome equivalent) are displayed as means per mL of cell supernatants for RNAs or, for intracellular RNAs, per mL of cell lysates containing 10^6 cells. Source data are provided as a Source Data file. Error bars correspond to standard deviation.



Supplementary Figure 7. HCV propagates HDV particles *in vivo*. NOD-FRG mice, engrafted with primary human hepatocytes (PHH) for two months and displaying HSA levels >15 mg/mL, which corresponded to 40-70% human hepatocytes as assessed by FAH staining (data not shown), were split in different groups that were infected with HDV (10^7 GE/mouse), HBV (10^8 GE/mouse) and/or HCV (1.5×10^5 FFU/mouse), as shown in the schedule of Figure 7a. (a) At different time points post-infection, blood samples (50 μ l) were collected and the viremia in sera was monitored by qPCR on genomes of the indicated viruses (GE/mL of serum). The graphs show the results of viremia of HDV (red lines), HBV (blue lines) and HCV (black lines) in individual mice from all groups as well as from control groups, inoculated with PBS (Mocks; Group#10) or with HDV only (HDV; Group#9). Note the results from two identified mice of Group#8 as displayed in the small (mouse #902) and large (mouse #978) dotted lines that show correlation between HCV and HDV viremia. (b) Reverse-transcribed RNAs from sera from co-infected animals were PCR-amplified with HDV-specific primers to reveal the size of transcribed and secreted HDV genomes (HDV RNA unit-length). The results from two mice per group are shown here.

a**b**

Supplementary Figure 8. 2nd study of HDV propagation *in vivo* by HCV. 4-8 weeks old NOD-FRG mice were engrafted with primary human hepatocytes (PHH). After ca. 2-3 months, the animals displaying HSA levels >15 mg/mL were split in 4 groups (N=4 to N=8 independent animals, see Table) that were infected with HDV (10^7 GE/mouse) and/or HCV (1.5×10^5 FFU/mouse), as shown in the schedule (a). At different time points post-infection, blood samples (50 μ l) were collected and the viremia in sera was monitored by qPCR on the genomes of the indicated viruses (GE/mL of serum) (b). The graphs show the mean results of viremia of HDV (red lines) and HCV (black lines). Source data are provided as a Source Data file. Error bars correspond to standard deviation.

Reviewers' Comments:

Reviewer #1:

Remarks to the Author:

NCOMMS-18-21856

Hepatitis delta virus (HDV) has long been known to co-infect people in a manner dependent on the hepatitis B virus and, indeed, was discovered based on its association with severe hepatitis in HBV patients. This dependence is due to the need for the hepadnavirus envelope to release infectious particles containing the HDV RNA and protein enveloped by the hepadnavirus surface antigen. Perez-Vargas et al describe results indicating that HDV might be able to use the envelope proteins of other viruses to produce infectious particles. The observations involve combinations of cell culture based experiments in which infectious HDV was found to be released from cells co-expressing the envelope of other viruses besides HBV, as well as experiments using mice with "humanized" livers in which HDV spread occurred via HCV rather than HBV, although at much lower levels. The authors findings not only have the potential to dramatically expand our understanding of the egress of HDV RNA-protein complexes from cells but also imply that HDV might affect the pathogenesis of numerous other viruses, as it is known to do for Hepatitis B virus. Thus, the potential impact of this study is quite large. However, given this potential impact, it is imperative that several weaknesses in the cell-culture based experiments several be addressed to convincingly demonstrate that the authors' conclusions are correct. These weaknesses (addressed specifically below), in addition to inconsistencies in some of the data and the use of somewhat unorthodox cell culture conditions undermine confidence in the robustness of the experimental results.

Major points

1. The conclusion that infectious HDV particles are secreted from cells expressing VSV or HCV glycoproteins is indeed suggested by the results in Figs. 1 and 2; however, there are concerns. The biggest is that the purported secreted viral particles are not characterized sufficiently and the characterization that is provided - immunoprecipitation - raises questions about their identity. The immunoprecipitation of the particles is very inefficient - less than 10%. This inefficiency is masked by the log representation of the graph in Fig. 1B. There is no need for a log representation in this figure; it should be changed. It seems possible that the observed release of what are presumed to be enveloped particles might be just HDV RNPs. Further analysis of the particles, in particular determining whether the RNA is genome, antigenome or some combination of both, would help to conclude one way or the other. In addition, in Fig. 1B, the authors suggest a very unusual HDAG composition for the HDV particles released from cells co-expressing different virus glycoproteins (even for regular "HDV"). Numerous studies of HDV particles obtained from cells, infected animals and patients consistently show similar amounts of S-HDAg and L-HDAg. The authors, from labeling of the immunoblot, propose that the particles consist mostly of L-HDAg, with very little S-HDAg present (except following immunoprecipitation with anti-VSV G antibody). There is no discussion of this highly unusual HDAG composition. On the other hand, without showing specific L-HDAg and S-HDAg controls on the immunoblot, it is possible the electrophoresis is not resolving the two species (that is, the labeling is incorrect) and that it is not possible to determine the relative amounts of S-HDAg and L-HDAg from the blot shown.

2. A second major concern is that the authors have not conclusively shown that the particles they have obtained are actually infectious. Several additional experiments are necessary to prove that the authors are observing actual infections rather than, for example, adherence of material to cells. A time course showing accumulation of HDV RNA and protein over several days following incubation would be more convincing than a single time point on day 7. Also more convincing would be demonstration of

antigenomic RNA accumulation (assuming that the released RNA is genome) and an increase with time in the amount of L-HDAg, which only occurs during replication.

3. The authors included 2% DMSO in the cell cultures used to produce HDV particles and for infection experiments. The stated purpose was to retard cell growth. However, this treatment is unnecessary (2% DMSO is not typically included in experiments used to produce HDV nor to analyze infection in Huh 106 cells) and its use here raises questions about the generality of the results. Perhaps 2% DMSO is somewhat toxic (it does retard cell growth) and leads to the release of HDV from cells stressed by expression of certain viral glycoproteins. At least some of the production and infection experiments should be repeated in the absence of DMSO.

Additional points

1. There was considerable variability between some similar experiments, or unexplained inconsistencies. In Fig. 3, for example, the levels of HDV RNA detected in mock infected cells varied by almost 10-fold between panel A and panel B. While the RNA analyses suggest that HDV obtained from cells expressing VSV G replicates to 10-fold higher levels than HDV with an HBV envelope (Fig 2A), the immunofluorescence analysis shows approximately 5 times more cells positive for HDV with the HBV envelope (Fig. 2C).
2. Page 3, second paragraph, second sentence. The statement that HDV does not meet the criteria for the definition of a virus is overstated. HDV is a satellite virus, with HBV as the only known helper.
3. Figure 5. The legend describes black and gray bars, there are only solid black and hashed bars.
4. Supplemental Fig. 1; Group 9. According to the table in Fig. 6, only 4 animals were in this group, yet there are about 9 lines on the graph. There is no indication of what the colors represent in this graph nor on any of the others in this figure.

Reviewer #2:

Remarks to the Author:

Perez-Vargas et al. report that hepatitis D virus (HDV), which was thought to be a cognate satellite virus of hepatitis B Virus (HBV), may be enveloped by the surface glycoproteins (GPs) from a variety of viruses for its assembly and the release. The authors also found that the production and infection of HDV is not restricted to liver cells, but is restricted by the GPs enveloping HDV and the corresponding receptors expressed on cells. The authors performed various cell culture and animal experiments to support their observations. Co-expression of HDV RNPs and individual viral GP (HBV, VSV, HCV, etc) in hepatoma cell lines led to release of infectious HDV particles. The infection of different GP-enveloped HDV could be blocked by antibodies to the corresponding viral envelop proteins. Notably, in both HBV or HCV infected mice HDV viremia was detected, confirming the observations in a physiologically relevant experimental system.

Based on these lines of evidence, the authors propose that HDV may have an origin independent of HBV, and could potentially be propagated by viruses other than HBV. The authors observation is surprising, given the scarcity of literature hinting HDV infection in the absence of an HBV infection. The authors have carved a unique angle to investigate the HDV propagation and provided both cell culture and animal evidences to support their hypothesis, which if proven true will enrich our understanding of HDV origin and the interplay of different viruses. However, several issues need to be addressed to further validate their hypothesis.

Major issues:

1. In figure 1 and figure 4, the key plasmid pSVLD3 was first developed in the Taylor lab (Kuo, et al, 1989, J. Virol) as a trimer of HDV genome and used for HDV replication. However, as it was indicated later (Taylor, 2006, Curr Top Microbiol Immunol), that the unit-length genomic or antigenomic HDV

RNA was mostly DNA-directed rather than RNA-directed, and since this does not recapitulate the authentic HDV replication, an improved construct was made to have slightly larger than one unit length to produce RNA-derived transcripts (Lazinski & Taylor, 1994, J. Virol). The data produced in Figure 1 and 4 may not hold if the production of HDV RNPs is formed in way that deviates from the authentic mechanism. Two methods could be used: 1) NTCP expressing cells/cell lines expressing various viral GPs is infected by recombinant HBV enveloped HDV virus to test if infectious HDV particles is secreted, and 2) use the improved constructs to validate the findings.

2. In figure 1a, the release of virus through cell death should be ruled out.

Minor issues:

1. Figure 1b, the VSV- Δ p 41A1 has a different pattern, e.g, much more s-HDAg and a 55 kDa band. A discussion of the difference, cause, and implication would be helpful.

2. Figure 2c should include light-field or nuclei staining.

3. Figure 5, it is not clear what is the HDV-RNA expressing cell, what construct is used to drive HDV-RNA expression?

4. Is there any explanation why the HDV infection is not reported to be dependent on HCV, if HCV propagates HDV indeed rather efficiently?

5. At numerous occasions the authors refer to "data not shown". This reviewer regards it as important to show all data relevant to the study in the manuscript

6. Page 4: "While HDV was expressed..." rephrase as RNA is not expressed but transcribed or in this case replicated. Proteins are expressed.

7. Page 8, line: please correct/spell out the mutant alleles in the FRG mice: fumarylacetoacetate hydrolase (fah-/-), recombinase activating gene 2 (rag2-/-), interleukin 2 receptor gamma chain (IL2RgNULL)

8. Page 12: subheading, delta particle NOT particles

Reviewer #3:

Remarks to the Author:

The origin of HDV attracts many interesting speculations. Current study proposed it coming from cellular circular RNAs that captured by HBV envelopes, so it is possible other viruses also enabling the packaging of naked HDV RNPs. They tested several viruses, such as HCV, dengue, HIV, et al, and showed HCV, denge and WNV, among others, could package the HDV RNPs into their envelope proteins and pass the HDV into next round of infections in cell cultures or in human hepatocyte chimera mice.

Though the results appeared to be interesting, their validation of pseudo-typed HDV and its infections is incomplete and many basic HDV RNA and proteins analysis are missing.

The comments are for authors' reference.

1. The claimed of packaging of HDV RNP by HBV Surface proteins, or by VSV or HCV GPs are interesting by in vitro co-transfection. This finding is supported by their immune-precipitation of these

pseudo-typed HDVs, using anti-HBs or anti-VSV or anti-HCV GP. However, the validation of these packaged HDV falls far behind. To confirm the packaged HDV RNP, the authors only showed an ambiguous detection of so-called HDV large HDAg, but not HDV RNA. It is essentially to include a HDV virus packaged by HBV surface protein as a positive control. Such virion has to contain the HDV small delta antigen, and genomic HDV RNA, other than the so-called large HDAg. A Northern blot to confirm an intact, full-sized HDV RNA is required. The RT-PCR quantitation cannot distinguish the viral genomic vs. antigenomic HDV RNAs, either about the size. (In fact, the large HDAg detected in western blot appeared to be suspicious. Other HDAg-specific antibody is required, as it is difficult to understand why no small HDAg is co-packaged).

2. The packaging of HDV RNP by HBsAg required specific isoprenylation of large HDAg. Do the rescue of HDV RNPs require the same modification or not? This can be easily studied by using isoprenylation inhibitor currently available.

3. The authors tried to band the VSV or HCV GP-packaged HDV virions by CsCL gradient analysis. They succeeded in identifying the putative pseudo-typed HDV in unique density fractions. Again, their only data based upon RT-PCR assay for HDV RNA. Northern and western blots to show HDV genomic RNA and both large and small delta antigens are essential. Finally, as the HDV virions are so abundant, it is necessary to do a simple EM study for these fractions to visualize the size, distribution of these pseudo-type HDV particles.

4. In their co-infection experiments, though HCV or other viruses appeared able to rescue the intracellular HDV RNPs and resulted in efficient next round infections, the data are not comprehensive. The authors relied only HDV RNA quantification by RT-PCR, however, they failed to provide either northern blot or western blot to show the simultaneous presence of HDV RNA or delta antigens. These are easily to show, as the HDV RNA titers are so high by their data. Besides, it is important to document the co-presence of HDAg and HCV antigen or dengue virus antigen in the same human hepatocytes from the chimera mice. Without these collaborating data, the HDV RNA RT-PCR seems shaky. It should be pointed that currently there is no approved HDV RNA assays, and many in-house assays suffer from varying or inconsistent performance.

5. Finally, the HCV or dengue virus infections in humanized chimera mice took a lot of effort and showed intriguing results. Other than insufficient virological data as mentioned in point 3, the authors may need to study the natural HCV/HDV coinfection in human intravenous drug abusers who frequently co-infected by HBV/HDV/HCV. Do these patients carry HDV RNA within HCV envelope?

Dr. François-Loïc Cosset
Scientific and Executive Director

International Center for Infectiology Research
21 Avenue Tony Garnier
69365 LYON, France
<http://ciri.inserm.fr>



December 2nd, 2018

Dear Reviewers

Please find enclosed our revised manuscript entitled “Enveloped viruses distinct from HBV induce dissemination of hepatitis D virus *in vivo*” by Jimena Perez-Vargas, Fouzia Amirache, Bertrand Boson, Chloé Mialon, Camille Sureau, Floriane Fusil, and myself, which we would like to publish in *Nature Communications* as a Research Article.

We greatly appreciated the Editor and Reviewers’ helpful and constructive comments, which we have all taken into account to improve our manuscript by performing additional experiments. Overall, we believe that we have succeeded to provide a more detailed description of these novel HDV particles and to clarify most issues raised by all Reviewers in this revised version of our manuscript.

We have revised the manuscript accordingly (see manuscript copy with changes underlined) and we provide a point-by-point response to these comments below (in blue).

The additional results, as per Reviewers’ requests, are:

- Northern blot analysis of HDV particles produced with unconventional GPs (Figure 1C) and of cells infected with these particles (Figure 3D).
- Determination by strand-specific RT-PCR of HDV RNA unit size in HDV particles produced with unconventional GPs (Figure 1B, Figure 1H), with live viruses (Figure 6), and in sera of co-infected animals (Supplemental Figure 7).
- Western blot analysis of HDV particles produced with HBV, VSV and HCV glycoproteins (Figure 1D) and of cells infected with these particles (Figure 3E).
- Electron microscopy analysis of HDV particles produced with HBV, VSV and HCV glycoproteins (Figure 1F and Supplemental Figure 3).
- Quantitative analysis of HDV intracellular and extracellular RNAs by strand-specific RTqPCR assays that detect genomic and antigenomic RNAs (Figure 3 and Supplemental Figure 1).
- Use of Lonafarnib in production (and subsequent infection) experiments (Figure 3A, B).
- Time-course analysis of genomic vs. antigenomic HDV RNAs and of L-HDAg and S-HDAg forms in infected cells (Figure 3C, D).
- Assessment of co-infection of cells by HDV and live helper viruses (HBV, HCV and DENV) by immuno-fluorescence assays (Figure 5D and Supplemental Figure 5).
- Demonstration that HDV particles can be formed with non-HBV glycoproteins both *via* transfection of pSVLD3 plasmid and *via* infection with “helper-free” HDV particles in GP-expressing cells (Supplemental Figure 6).

The other important changes in our revised manuscript are:

- Statistical analysis of the data.
- Assessment of production of HDV particles by HDV/DENV-co-infected mosquito cells (Supplemental Figure 6).
- Demonstration that identical production of HDV particles can be achieved from cells cultured in media containing, or not, 2% DMSO (Supplemental Figure 2).
- Results of co-infection by HDV and HCV in a second cohort of human liver mice (N=24; Supplemental Figure 8).

- Reorganization of the manuscript text, figures and supplementary figures to address, on the whole, all comments of the Reviewers.

We thank you very much for your interest and time in considering our revised manuscript for publication in *Nature Communications*.

Sincerely yours,

A handwritten signature in blue ink, consisting of several fluid, overlapping loops and strokes, positioned above the printed name.

Dr. FL Cosset

Point-by-point Reply (see literature cited at the end of this document)

Reviewer #1 (Remarks to the Author):

Hepatitis delta virus (HDV) has long been known to co-infect people in a manner dependent on the hepatitis B virus and, indeed, was discovered based on its association with severe hepatitis in HBV patients. This dependence is due to the need for the hepadnavirus envelope to release infectious particles containing the HDV RNA and protein enveloped by the hepadnavirus surface antigen. Perez-Vargas et al describe results indicating that HDV might be able to use the envelope proteins of other viruses to produce infectious particles. The observations involve combinations of cell culture based experiments in which infectious HDV was found to be released from cells co-expressing the envelope of other viruses besides HBV, as well as experiments using mice with “humanized” livers in which HDV spread occurred via HCV rather than HBV, although at much lower levels. The authors findings not only have the potential to dramatically expand our understanding of the egress of HDV RNA-protein complexes from cells but also imply that HDV might affect the pathogenesis of numerous other viruses, as it is known to do for Hepatitis B virus. Thus, the potential impact of this study is quite large. However, given this potential impact, it is imperative that several weaknesses in the cell-culture based experiments several be addressed to convincingly demonstrate that the authors’ conclusions are correct. These weaknesses (addressed specifically below), in addition to inconsistencies in some of the data and the use of somewhat unorthodox cell culture conditions undermine confidence in the robustness of the experimental results.

Major points

1. The conclusion that infectious HDV particles are secreted from cells expressing VSV or HCV glycoproteins is indeed suggested by the results in Figs. 1 and 2; however, there are concerns. The biggest is that the purported secreted viral particles are not characterized sufficiently and the characterization that is provided - immunoprecipitation – raises questions about their identity. The immunoprecipitation of the particles is very inefficient – less than 10%. This inefficiency is masked by the log representation of the graph in Fig. 1B. There is no need for a log representation in this figure; it should be changed. It seems possible that the observed release of what are presumed to be enveloped particles might be just HDV RNPs. Further analysis of the particles, in particular determining whether the RNA is genome, antigenome or some combination of both, would help to conclude one way or the other. In addition, in Fig. 1B, the authors suggest a very unusual HDAg composition for the HDV particles released from cells co-expressing different virus glycoproteins (even for regular “HDV”). Numerous studies of HDV particles obtained from cells, infected animals and patients consistently show similar amounts of S-HDAg and L-HDAg. The authors, from labeling of the immunoblot, propose that the particles consist mostly of L-HDAg, with very little S-HDAg present (except following immunoprecipitation with anti-VSV G antibody). There is no discussion of this highly unusual HDAg composition. On the other hand, without showing specific L-HDAg and S-HDAg controls on the immunoblot, it is possible the electrophoresis is not resolving the two species (that is, the labeling is incorrect) and that it is not possible to determine the relative amounts of S-HDAg and L-HDAg from the blot shown.

Reply: We have addressed these points and we are happy to provide a more detailed characterization of VSV- Δ p and HCV- Δ p particles, as described below :

1 - Demonstration that HDV RNAs in particles are genomes rather than antigenomes. We used a strand-specific RTqPCR assay (Li et al., 2006) to quantify HDV genomic RNA (gRNA) and antigenomic RNA (agRNA) in lysates and supernatants of transfected and/or infected cells (see new Supplemental Figure 1A). The enrichment of HDV gRNAs (panel A) in secreted particles is reflected by the gRNA/agRNA ratios (panel C), which were up to 800-fold higher in HDV, VSV- Δ p or HCV- Δ p particles than in the lysates of their corresponding producer cells. As shown in panels B and E, we noted no significant increase over time post-transfection of the low amounts of HDV agRNAs detected in the supernatants, in sharp contrast to the extracellular HDV gRNAs that increased by up to 1,000-fold (panels A and D). Owing to the high sensitivity of the RTqPCR assay, these low levels HDV agRNAs could be due to some background of cell death induced by the combination of GP transfection and extended culture conditions of these cells (up to 9 days). Note that identical extracellular HDV agRNAs levels were detected for VSV- Δ p and HCV- Δ p particles as compared to “normal” HDV particles (*i.e.*, with HBV GPs). We believe that these new results show that HDV particles generated with unconventional GP incorporate full-length genomic RNA.

2 - Improvement regarding the detection of HDAg species present in viral particles. We replaced the HDAg co-IP analysis, which was not possible to improve at this stage, by a Western blot analysis of

the different types of HDV particles that were purified by ultracentrifugation on a sucrose cushion. The results clearly show that both L-HDAg and S-HDAg are incorporated at similar levels and ratios in the purified viral particles generated with HCV and VSV GPs as compared to “normal” HDV particles produced with HBV GPs.

3 – Concerning the RNA colP that precipitated 5 to 11% of HDV RNAs, we do not expect that the efficiency could be higher because of the competition exerted by the SVPs for either type of particles that outnumber the infectious particles. We respectfully request to keep the log representation of the graph in Figure 1E, in order to better show the results of the Flow through RTqPCR values.

2. A second major concern is that the authors have not conclusively shown that the particles they have obtained are actually infectious. Several additional experiments are necessary to prove that the authors are observing actual infections rather than, for example, adherence of material to cells. A time course showing accumulation of HDV RNA and protein over several days following incubation would be more convincing than a single time point on day 7. Also more convincing would be demonstration of antigenomic RNA accumulation (assuming that the released RNA is genome) and an increase with time in the amount of L-HDAg, which only occurs during replication.

Reply: We have performed all these experiments. The panels C-E of the new Figure 3 provides a time course analysis in infected cells over several days following inoculation. Using a strand-specific RTqPCR assay for HDV RNA, we show that not only genomic HDV RNAs but also antigenomic RNAs are amplified from day 3 to day 9 post-infection and accumulate in infected cells (panel C). Likewise, we confirm by Northern blot analysis of these infected cells that HDV RNAs accumulate in these cells (Panel D). Finally, we show that HDAg protein levels also increase with a progressive appearance of L-HDAg, which marks productive infection (panel E).

In addition to the other pieces of evidence such as i) inoculation of cell expressing vs. not expressing the receptors (now Figure 4A), ii) co-infection and transmission assays with live helper viruses (now Figure 6 and Supplemental Figure 6) and iii) propagation in experimentally infected animals (now Figure 7 and Supplemental Figures 7 & 8), we believe that altogether, these results convincingly show that the particles are infectious.

3. The authors included 2% DMSO in the cell cultures used to produce HDV particles and for infection experiments. The stated purpose was to retard cell growth. However, this treatment is unnecessary (2% DMSO is not typically included in experiments used to produce HDV nor to analyze infection in Huh 106 cells) and its use here raises questions about the generality of the results. Perhaps 2% DMSO is somewhat toxic (it does retard cell growth) and leads to the release of HDV from cells stressed by expression of certain viral glycoproteins. At least some of the production and infection experiments should be repeated in the absence of DMSO.

Reply: We used Williams E-based medium for production or infection with HDV particles in Huh-7-derived cells (including Huh-106 and Huh-7.5 cells). While this Reviewer is correct to say that DMSO-containing medium is not typically included in such experiments, we supplemented our medium with 2% DMSO in this study since, when we started the project, the current procedures to grow hepatocyte-derived cell lines for several days recommended such media both to maintain cell differentiation (Bauhofer et al., 2012, Sainz & Chisari, 2006) and to induce or maintain NTCP expression (Watashi et al., 2014, Yan et al., 2012). For example, it was shown that DMSO-containing media strongly increase HDV and HBV infection efficacy in HepG2^{NTCP} and Huh-7^{NTCP} cells, as compared to DMSO-free media (Iwamoto et al., 2014, Ni et al., 2014).

Importantly, as requested by this Reviewer, we now show in the new Supplemental Figure 2, first, that 2% DMSO does not induce more cell toxicity as compared to cell cultures grown in DMSO-free medium (panel A) and, second, that omitting DMSO does not change the production levels and infectivity of HDV, VSV-Δp and HCV-Δp particles (panels B and C).

Additional points

1. There was considerable variability between some similar experiments, or unexplained inconsistencies. In Fig. 3, for example, the levels of HDV RNA detected in mock infected cells varied by almost 10-fold between panel A and panel B. While the RNA analyses suggest that HDV obtained from cells expressing VSV G replicates to 10-fold higher levels than HDV with an HBV envelope (Fig 2A), the immunofluorescence analysis shows approximately 5 times more cells positive for HDV with the HBV envelope (Fig. 2C).

Reply: The previous immunofluorescence analysis of Figure 2C was displayed to provide a qualitative assessment of HDAg nuclear localization upon infection. As requested by this Reviewer, we have

repeated the experiment and we provide in the revised Figure 2B images that are more consistent with the quantification of infectivity (now shown in Figure 2C) and that include nuclei staining with Hoechst. As for the variability between panel A and panel B of previous Figure 3 (now Figure 4), *i.e.*, there is 3- to 5-fold differences in the HDV RNA RTqPCR results obtained for the mock-treated supernatants for panel A vs. panel B. This is explained by the fact that either experiment type (*i.e.*, neutralization in panel A and receptor blocking in panel B) was performed at different sessions of the study, which induces experimental variations. Yet, we had made sure that the sizes of the HDV, VSV- Δ p and HCV- Δ p particles inputs in either panel A or panel B were identical in order to provide accurate comparisons between conditions in each panel.

2. Page 3, second paragraph, second sentence. The statement that HDV does not meet the criteria for the definition of a virus is overstated. HDV is a satellite virus, with HBV as the only known helper.

Reply: We have removed this sentence as requested.

3. Figure 5. The legend describes black and gray bars, there are only solid black and hashed bars.

Reply: We have corrected the legend in this Figure (now revised Figure 6).

4. Supplemental Fig. 1; Group 9. According to the table in Fig. 6, only 4 animals were in this group, yet there are about 9 lines on the graph. There is no indication of what the colors represent in this graph nor on any of the others in this figure.

Reply: We thank this Reviewer for pointing this. Like for the “Mocks” group (Group #10), but also in other groups (not shown, for sake of clarity), we tested the samples for all three viruses (HBV, HCV and HDV) in Group #9, whose mice were infected with HDV only, and this is now indicated in the revised legend with the indicated color codes (blue: HBV; black: HCV; red: HDV). Note that one animal died after week 8 (P4), which explains that there are 9 lines after P4 (12 lines until P4) in this graph.

Reviewer #2 (Remarks to the Author):

Perez-Vargas et al. report that hepatitis D virus (HDV), which was thought to be a cognate satellite virus of hepatitis B Virus (HBV), may be enveloped by the surface glycoproteins (GPs) from a variety of viruses for its assembly and the release. The authors also found that the production and infection of HDV is not restricted to liver cells, but is restricted by the GPs enveloping HDV and the corresponding receptors expressed on cells. The authors performed various cell culture and animal experiments to support their observations. Co-expression of HDV RNPs and individual viral GP (HBV, VSV, HCV, etc) in hepatoma cell lines led to release of infectious HDV particles. The infection of different GP-enveloped HDV could be blocked by antibodies to the corresponding viral envelop proteins. Notably, in both HBV or HCV infected mice HDV viremia was detected, confirming the observations in a physiologically relevant experimental system.

Based on these lines of evidence, the authors propose that HDV may have an origin independent of HBV, and could potentially be propagated by viruses other than HBV. The authors observation is surprising, given the scarcity of literature hinting HDV infection in the absence of an HBV infection. The authors have carved a unique angle to investigate the HDV propagation and provided both cell culture and animal evidences to support their hypothesis, which if proven true will enrich our understanding of HDV origin and the interplay of different viruses. However, several issues need to be addressed to further validate their hypothesis.

Major issues:

1. In figure 1 and figure 4, the key plasmid pSVLD3 was first developed in the Taylor lab (Kuo, et al, 1989, J. Virol) as a trimer of HDV genome and used for HDV replication. However, as it was indicated later (Taylor, 2006, Curr Top Microbiol Immunol), that the unit-length genomic or antigenomic HDV RNA was mostly DNA-directed rather than RNA-directed, and since this does not recapitulate the authentic HDV replication, an improved construct was made to have slightly larger than one unit length to produce RNA-derived transcripts (Lazinski & Taylor, 1994, J. Virol). The data produced in Figure 1 and 4 may not hold if the production of HDV RNPs is formed in way that deviates from the authentic mechanism. Two methods could be used: 1) NTCP expressing cells/cell lines expressing various viral GPs is infected by recombinant HBV enveloped HDV virus to test if infectious HDV particles is secreted, and 2) use the improved constructs to validate the findings.

Reply: We thank this Reviewer for pointing out the original reference to this key construct, which is duly cited now (Kuo et al., 1989). Regarding his/her specific point, we had used in Figure 6 a variation of the

method #1 he/she suggested. Accordingly, following infection of naïve cells with VSV- Δ p particles (*i.e.*, “helper-free” VSV-G enveloped HDV particles), the cells were superinfected with live HCV, HBV or DENV viruses. The results show that we could rescue infectious HDV particles, indicating that both pSVLD3 transfection and “helper-free” HDV infection (such as VSV- Δ p) processes leads to expression of HDV RNA that can be transmitted as infectious particles. Note that a similar conclusion can be deduced from the mouse infection data since these animals were inoculated with “helper-free” HBsAg-enveloped HDV virus before, after or concomitantly with live HCV or HBV (Figure 7).

Finally, we show in the new Supplemental Figure 6 the results of transmission experiments using both Huh-7.5 human hepatoma and C6/36 mosquito cells that were infected with supernatants from HDV/DENV co-infected cells. We found that these secondary HDV/DENV-infected Huh-7.5 and C6/36 cells could replicate, assemble and transmit infectious HDV particles to tertiary cells.

In our opinion, these results also demonstrate that HDV RNA can be transmitted *via* processes that involve authentic HDV replication.

2. In figure 1a, the release of virus through cell death should be ruled out.

Reply: We now provide indirect evidence to address this point, which is very difficult to formally rule out since most of the GPs studied here can intrinsically cause cell death (albeit through different pathways). We evaluated the cytotoxicity in transfected cells at different time points of collection of HDV, VSV- Δ p, and HCV- Δ p particles as well as in No GP (*i.e.*, pSVLD3-transfected cells) and non-transfected control cells. Using the Pierce Cytotoxicity Assay Kit, we obtained similar levels of LDH release for both VSV- Δ p or HCV- Δ p particles and “normal” HDV particles but also for the No GP control and the non-transfected condition as shown at day 6 post-transfection in the new Supplemental Figure 2. Thus, we conclude that while the combination of long-term culture and transfection procedure is somehow harmful to cells, the release of particles may not occur through cell death first, since otherwise, the No GP control (transfected with pSVLD3 only) would induce secretion of HDV RNAs from these cells, and second, since one may conclude that “classical” HDV particles would also be released through cell death. Note that slightly increased cytotoxicity levels were obtained when producing VSV- Δ p particles; this was expected owing to the previously known fusogenic activity of VSV-G (see *e.g.*, (Arai et al., 1998) for VSV-G-pseudotyped lentiviral vectors), which, ultimately, does not preclude production of such vectors.

Minor issues:

1. Figure 1b, the VSV- Δ p 41A1 has a different pattern, *e.g.*, much more s-HDAg and a 55 kDa band. A discussion of the difference, cause, and implication would be helpful.

Reply: We agree with this issue of this Reviewer, which was also pointed out by the two other Reviewers. Accordingly, we have replaced this HDAg co-IP analysis, which was difficult to improve, by a Western blot analysis of the different types of HDV particles that were purified by ultracentrifugation on a sucrose cushion. The results unambiguously show that both L-HDAg and S-HDAg are incorporated at similar levels and ratios in the purified viral particles generated with HCV and VSV GPs as compared to “normal” HDV particles produced with HBV GPs.

2. Figure 2c should include light-field or nuclei staining.

Reply: As requested by this Reviewer, we have repeated the experiment and we provide in the revised Figure 2B images that show nuclei staining (Hoechst) in inoculated cells.

3. Figure 5, it is not clear what is the HDV-RNA expressing cell, what construct is used to drive HDV-RNA expression?

Reply: We infected these cells with VSV-G-coated HDV particles (VSV- Δ p). Cells were then superinfected with the indicated live viruses (see our reply to Major issue #1 of this Reviewer).

4. Is there any explanation why the HDV infection is not reported to be dependent on HCV, if HCV propagates HDV indeed rather efficiently?

Reply: We are deeply interested by finding an explanation to this question, which is also raised by Reviewer #3. Indeed, one of our future plans is to attempt detection of HCV-dependent HDV propagation in selected patient cohorts, which is difficult clinically and logistically. As for tentative explanation, it is possible that direct or indirect (*e.g.*, immune-mediated) interference mechanisms may impede in the long term HDV/HCV co-infections *in vivo*, though they may occur in different contexts. For example, HDV-induced activation of the innate immune response, which is known to have little/no effect on HDV itself (Alfaiate et al., 2016, Zhang et al., 2018), may impact several markers of co-infection, such as for HCV that is interferon-sensitive in contrast to HBV (Lutgehetmann et al., 2011, Mutz et al., 2018).

Thus, overall, we propose that what might determine eventual successful vs. sporadic transmission and propagation of HDV with non-HBV helper viruses would reside in the balance between biochemical/virological HDV RNP compatibility with the GP of these helper viruses vs. potential (immunological) mechanisms of interference, though the immune status of individuals, such as immune-suppression, may favor transmission of such HDV co-infections. This putative explanation is included in the revised Discussion.

5. At numerous occasions the authors refer to “data not shown”. This reviewer regards it as important to show all data relevant to the study in the manuscript

Reply: We have complied with the request of this Reviewer and we now display these data not shown in Figure 3 (kinetics of HDV replication in infected cells), in Figure 5 (results of infectivity for all HDV/GP combinations), in Supplemental Figure 5 (assessment of co-infection by IF), in Supplemental Figure 6 (infection of mosquito cells), and in Supplemental Figure 8 (results of infection from a second cohort of HuHep mice). The only results that are not shown are the FAH staining of humanized livers, as they have been published previously by us (Calattini et al., 2015) and others (Bissig et al., 2010).

6. Page 4: “While HDV was expressed...” rephrase as RNA is not expressed but transcribed or in this case replicated. Proteins are expressed.

Reply: We have changed this sentence to “While HDV RNA accumulated...”

7. Page 8, line: please correct/spell out the mutant alleles in the FRG mice: fumarylacetoacetate hydrolase (fah^{-/-}), recombinase activating gene 2 (rag2^{-/-}), interleukin 2 receptor gamma chain (IL2Rg^{NULL})

Reply: We have also modified this sentence accordingly (revised Material and Methods).

8. Page 12: subheading, delta particle NOT particles

Reply: We have introduced the requested change in this subheading.

Reviewer #3 (Remarks to the Author):

The origin of HDV attracts many interesting speculations. Current study proposed it coming from cellular circular RNAs that captured by HBV envelopes, so it is possible other viruses also enabling the packaging of naked HDV RNPs. They tested several viruses, such as HCV, dengue, HIV, et al, and showed HCV, dengue and WNV, among others, could package the HDV RNPs into their envelope proteins and pass the HDV into next round of infections in cell cultures or in human hepatocyte chimera mice.

Though the results appeared to be interesting, their validation of pseudo-typed HDV and its infections is incomplete and many basic HDV RNA and proteins analysis are missing.

The comments are for authors' reference.

1. The claimed of packaging of HDV RNP by HBV Surface proteins, or by VSV or HCV GPs are interesting by in vitro co-transfection. This finding is supported by their immune-precipitation of these pseudo-typed HDVs, using anti-HBs or anti-VSV or anti-HCV GP. However, the validation of these packaged HDV falls far behind. To confirm the packaged HDV RNP, the authors only showed an ambiguous detection of so-called HDV large HDAg, but not HDV RNA. It is essentially to include a HDV virus packaged by HBV surface protein as a positive control. Such virion has to contain the HDV small delta antigen, and genomic HDV RNA, other than the so-called large HDAg. A Northern blot to confirm an intact, full-sized HDV RNA is required. The RT-PCR quantitation cannot distinguish the viral genomic vs. antigenomic HDV RNAs, either about the size. (In fact, the large HDAg detected in western blot appeared to be suspicious. Other HDAg-specific antibody is required, as it is difficult to understand why no small HDAg is co-packaged).

Reply: We have performed these experiments and we provide in this revised manuscript a more detailed characterization of VSV- Δp and HCV- Δp particles :

1 – Incorporation of genomic HDV RNA in viral particles.

First, we provide in revised Figure 1C a result of Northern blot that confirm the presence of an intact, full-sized HDV RNA in pellets of particles purified by ultracentrifugation on a 30% sucrose cushion.

Second, we used a strand-specific RTqPCR assay (see revised Material and Methods) to quantify HDV genomic RNA (gRNA) and antigenomic RNA (agRNA) in lysates and supernatants of transfected and/or

infected cells (see new Supplemental Figure 1A). The enrichment of HDV gRNAs (panel A) in secreted particles is reflected by the gRNA/agRNA ratios (panel C), which were up to 800-fold higher in HDV, VSV- Δ p or HCV- Δ p particles than in the lysates of their corresponding producer cells.

Third, we designed a RT-PCR strand-specific “banding” assays with primers that allow amplification of the HDV genomic RNA. We found that HDV particles contains HDV RNA at the expected size of 1.7 kb, whether they were produced by transfection with pSVLD3 and GP-expression plasmids (Figure 1B, 1H) or by co-infection with live HCV, HBV or DENV *in vitro* (Figure 6) and in experimentally-infected animals (Supplemental Figure 7).

Fourth, showing that VSV- Δ p and HCV- Δ p form particles, we performed Electron Microscopy analysis of particles (Figure 1C and Supplemental Figure 3), which were obtained from cell supernatants purified with heparin beads, as discussed below in Point #3.

2 - Detection of HDAg species present in viral particles. We replaced the HDAg co-IP analysis, which was not possible to improve, by a Western blot analysis of the different types of HDV particles that were pelleted by ultracentrifugation on a sucrose cushion. The results (Figure 1D) clearly show that both L-HDAg and S-HDAg are incorporated at similar levels and ratios in the purified viral particles generated with HCV and VSV GPs as compared to “normal” HDV particles produced with HBV GPs.

2. The packaging of HDV RNP by HBsAg required specific isoprenylation of large HDAg. Do the rescue of HDV RNPs require the same modification or not ? This can be easily studied by using isoprenylation inhibitor currently available.

Reply: We have performed the requested experiment and we show, in Figure 3A & B, that Lonafarnib, an isoprenylation inhibitor that prevents HDV assembly and secretion (Bordier et al., 2003), could readily inhibit production and hence, transmission and replication of HDV RNA from HDV, VSV- Δ p and HCV- Δ p particles, suggesting a shared pathway of the early assembly process leading to production of all HDV particle types.

3. The authors tried to band the VSV or HCV GP-packaged HDV virions by CsCL gradient analysis. They succeeded in identifying the putative pseudo-typed HDV in unique density fractions. Again, their only data based upon RT-PCR assay for HDV RNA. Northern and western blots to show HDV genomic RNA and both large and small delta antigens are essential. Finally, as the HDV virions are so abundant, it is necessary to do a simple EM study for these fractions to visualize the size, distribution of these pseudo-type HDV particles.

Reply: We performed the requested experiment but failed to detect HDV RNA by Northern blot in that specific case, owing to their insufficient concentrations in fractions from density gradients. Indeed, the HDV RNA copy number required to perform Northern blots ($>10^7$ copies/lane – *i.e.*, 20 μ l loaded – are needed) allowed detection of full-sized HDV RNA in the 100-fold pelleted viral particles shown in Figure 1C but not in the fractions from iodixanol density gradients, owing to dilution of the sample in the gradient. Note that the aim of this latter experiment was to performed density gradient analysis from unprocessed, crude supernatants (in order to maintain native state of the sample) and that these supernatants contain *ca.* 4×10^7 copies /mL for HCV- Δ p particles (thus, the most HDV RNA-enriched fraction contain less than 2×10^5 copies/20 μ l, which is below the threshold level). As for detection of L-HDAg and S-HDAg, while we concentrated the fractions with methanol/acetone, the signals were not of sufficient quality for being displayed in Figure 1 owing to BSA levels that interfered with migration in SDS-Page.

To overcome these technical issues and address the request of this Reviewer regarding the packaging of full-sized HDV RNA, we used the above-mentioned RT-PCR banding assays and we show that the RTqPCR-positive fractions contain HDV RNA at the expected genomic size of 1.7 kb (Figure 1G).

As for EM studies, we provide in Figure 1F and Supplemental Figure 3 images of particles which were obtained from cell supernatants purified with heparin beads. We observed two types of spheres with diameters of 35-40 and 25-30 nm (Gudima et al., 2007). The small spheres likely corresponded to sub-viral particles since they were also detected when VSV-G and HCV-E1E2 were expressed alone, similar to HBV GPs (Supplemental Figure 3C & D) whereas the large spheres, that were only detected when HDV RNA were co-expressed with either GP (Supplemental Figure 3A & B), could correspond to VSV- Δ p and HCV- Δ p particles. While the concentration of these particles appeared insufficient to allow simple EM studies from the fractions of density-gradients, we believe that this consolidate the characterization of these novel HDV particles.

4. In their co-infection experiments, though HCV or other viruses appeared able to rescue the intracellular HDV RNPs and resulted in efficient next round infections, the data are not comprehensive. The authors relied only HDV RNA quantification by RT-PCR, however, they failed to provide either

northern blot or western blot to show the simultaneous presence of HDV RNA or delta antigens. These are easily to show, as the HDV RNA titers are so high by their data. Besides, it is important to document the co-presence of HDAg and HCV antigen or dengue virus antigen in the same human hepatocytes from the chimera mice. Without these collaborating data, the HDV RNA RT-PCR seems shaky. It should be pointed that currently there is no approved HDV RNA assays, and many in-house assays suffer from varying or inconsistent performance.

Reply: We show in the revised set of figures a more detailed characterization of these co-infection experiments.

First, regarding the presence of full-sized HDV RNA, using the above-mentioned RT-PCR banding assays, we show that cells co-infected with HDV and HCV or HBV or DENV express and secrete RNAs at the expected genomic size of 1.7 kb, which matches the detection of these RNAs by RTqPCR.

Second, we performed an immunofluorescence (IF) analysis of these co-infected cells to document the co-presence of HDAg with HCV, HBV or DENV antigens in the same human hepatocytes. As shown in the revised Figure 6 and new Supplemental Figure 5, in addition to cells that were mono-infected by either virus type, we could readily detect cells co-expressing the antigens of either virus combinations (HDAg with HBV core, HDAg with HCV NS5A or HDAg with DENV E), which indicates that cells were co-infected by HDV and HCV, HBV or DENV.

Third, regarding the chimera mice, we performed an IF analysis of liver sections from the co-infected animals. While we could readily detect mono- and co-infected hepatocytes in HBV/HDV co-infected mice, as shown previously by others (Lutgehetmann et al., 2012), the IF analysis of HDV/HCV infected animals was more difficult (see Figure below) and displayed rare co-infected cells with dull HDAg immunofluorescence, which may be explained at this stage by the following reasons. First, as the levels of HCV RNAs in this human liver mouse model are typically *ca.* 10-30 fold less elevated than for HBV, the propagation of HDV is less favorable with HCV helper virus than with HBV and results in a smaller proportion of infected hepatocytes. Second, at the time these animals were sacrificed (*i.e.*, at week 14 post-infection (Figure 7A)), the levels of HDV RNAs had decreased by over two-logs as compared to previous time-points (see *e.g.*, week 8 for Group#8 in Figure 7), which made the analysis difficult to do. Third, we think that HDV and HCV interfere with each other, perhaps in a stronger manner than the previously known HDV/HBV interference (Alfaiate et al., 2016, Lutgehetmann et al., 2012), and this will be the subject of a further study of our team. Indeed, it is possible that direct or indirect (*e.g.*, immune-mediated) interference mechanisms may impede in the long term HDV/HCV co-infections *in vivo*, though they may occur in different contexts. For example, HDV-induced activation of the innate immune response, which is known to have little/no effect on HDV itself (Alfaiate et al., 2016, Zhang et al., 2018), may impact several markers of co-infection, such as HCV that is interferon-sensitive in contrast to HBV (Lutgehetmann et al., 2011, Mutz et al., 2018). Thus, **if this is acceptable, we respectfully request to this Reviewer that we do not display the IF results from the infected mice** as they warrant further studies beyond the scope of this first study. We also believe that the results IF analyses of co-infection *in vitro* requested by this Reviewer are meaningful to establish the co-presence of HDV and live helper viruses.

Finally, using the above-mentioned PCR banding assays, we show that sera from mice co-infected with HDV and HCV or HBV contain RNAs at the expected genomic size of 1.7 kb, in agreement with the presence these RNAs by RTqPCR, which supports our conclusion that the unconventional HDV particles can be secreted and propagated *in vivo*.

5. Finally, the HCV or dengue virus infections in humanized chimera mice took a lot of effort and showed intriguing results. Other than insufficient virological data as mentioned in point 3, the authors may need to study the natural HCV/HDV coinfection in human intravenous drug abusers who frequently co-infected by HBV/HDV/HCV. Do these patients carry HDV RNA within HCV envelope ?

Reply: This is clearly a highly important and interesting question that we wish to pursue in the follow up work of this pioneer study. Indeed, how to best address this and reach statistical significance, given that natural HCV/HDV coinfections in human must be very rare in our opinion, is the subject of on-going discussions with clinicians who may collaborate with us on this issue. Yet, identifying and forming the different patient cohorts (*e.g.*, from human intravenous drug abusers, as proposed by this Reviewer) or just accessing to collections of samples will require time, not only because we do not yet know exactly which are the best types of individuals to screen but also because getting the necessary ethical permits (and funding) is a difficult enterprise, particularly when it deals with countries where HDV is currently prevalent, like Mongolia and South America in the Amazonian basin. Finally, while Western countries, particularly Italia, have been severely hit by HDV infection in the 80's, recovering the collections of specimens from infected patients and their complete clinical description is difficult and will also take several months.

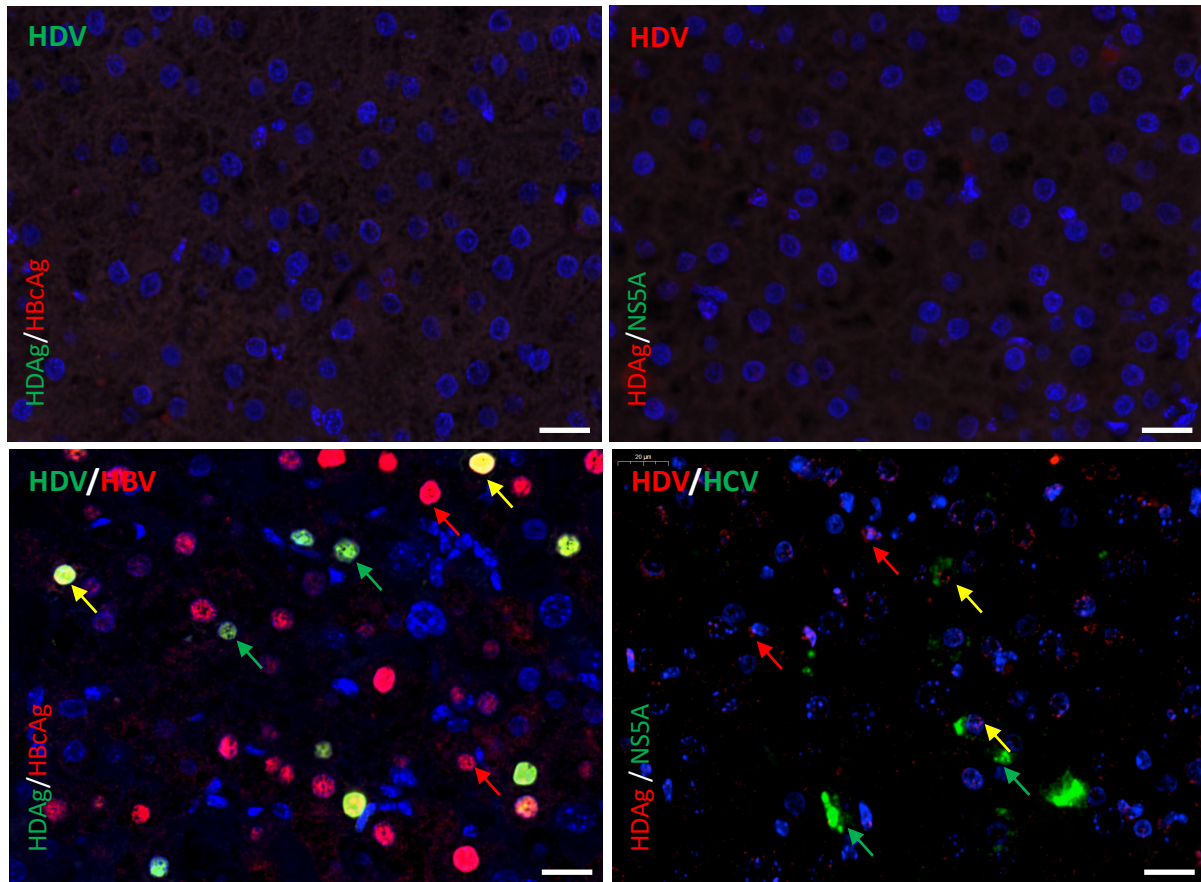


Figure 1. Immunohistochemistry of livers from HDV/HCV co-infected HuHep mice. 4-8 weeks old NOD-FRG mice were engrafted with primary human hepatocytes (PHH). After ca. 2-3 months, the animals displaying HSA levels >15 mg/mL were split in different groups that were infected with HDV alone (10^7 GE/mouse) (**top panels**), with HDV and HBV (10^8 GE/mouse) (**lower left panel**), or with HDV and HCV (1.5×10^5 FFU/mouse) (**lower right panel**). Tissue samples of animals sacrificed at week 14 post-infection (see Figure 7A) were fixed in 10% buffered formalin and embedded in paraffin. 4 μ m-thick tissue sections of formalin-fixed, paraffin-embedded tissue were prepared according to conventional procedures.

For immunofluorescence, sections were incubated with a rabbit anti-HDAg antibody, then the OmniMap Detection Kit was used with a FITC kit (**lefts panels**) or with a rhodamine kit (**right panels**). After stripping of the first antibody, sections were incubated with a human anti-HBcAg with an OmniMap Detection Kit and rhodamine kit (**lower right panel**) or with a mouse anti-NS5A 9E10 with an OmniMap Detection Kit and a rhodamine kit (**lower left panel**). Dapi were used for counterstaining. The slides were scanned with a panoramic scan II (3D histech, Hungary). Scale bars represent 20 μ m.

Note that livers of animals infected with HDV alone did not display HDAg-positive cells, owing to the late time point at sacrifice and probable extinction of HDV RNA replication in the absence of helper virus. In contrast, cells mono-infected by HDV (**green arrows in left panel and red arrows in right panel**), by HBV (**red arrows in lower left panel**) or HCV (**green arrows in lower right panel**), or co-infected could be detected (**yellow arrows in lower panels**). Note that the number of HDV/HCV co-infected cells is significantly lower than for HDV/HBV co-infection, in line with the lower viremia of the former (see Figure 7B and Supplemental Figures 7 & 8), and that HDV/HCV HDAg immunofluorescence is less bright than for the latter, which denotes negative interference between the two viruses.

Literature cited in this rebuttal document

- Alfaiate D, Lucifora J, Abeywickrama-Samarakoon N, Michelet M, Testoni B, Cortay JC, Sureau C, Zoulim F, Deny P, Durantel D (2016) HDV RNA replication is associated with HBV repression and interferon-stimulated genes induction in super-infected hepatocytes. *Antiviral Res* 136: 19-31
- Arai T, Matsumoto K, Saitoh K, Ui M, Ito T, Murakami M, Kanegae Y, Saito I, Cosset FL, Takeuchi Y, Iba H (1998) A new system for stringent, high-titer vesicular stomatitis virus G protein-pseudotyped retrovirus vector induction by introduction of Cre recombinase into stable prepackaging cell lines. *J Virol* 72: 1115-21
- Bauhofer O, Ruggieri A, Schmid B, Schirmacher P, Bartenschlager R (2012) Persistence of HCV in quiescent hepatic cells under conditions of an interferon-induced antiviral response. *Gastroenterology* 143: 429-38 e8
- Bissig KD, Wieland SF, Tran P, Isogawa M, Le TT, Chisari FV, Verma IM (2010) Human liver chimeric mice provide a model for hepatitis B and C virus infection and treatment. *J Clin Invest* 120: 924-30
- Bordier BB, Ohkanda J, Liu P, Lee SY, Salazar FH, Marion PL, Ohashi K, Meuse L, Kay MA, Casey JL, Sebti SM, Hamilton AD, Glenn JS (2003) In vivo antiviral efficacy of prenylation inhibitors against hepatitis delta virus. *J Clin Invest* 112: 407-14
- Calattini S, Fusil F, Mancip J, Dao Thi VL, Granier C, Gadot N, Scoazec JY, Zeisel MB, Baumert TF, Lavillette D, Dreux M, Cosset FL (2015) Functional and Biochemical Characterization of Hepatitis C Virus (HCV) Particles Produced in a Humanized Liver Mouse Model. *J Biol Chem* 290: 23173-87
- Gudima S, He Y, Meier A, Chang J, Chen R, Jarnik M, Nicolas E, Bruss V, Taylor J (2007) Assembly of hepatitis delta virus: particle characterization, including the ability to infect primary human hepatocytes. *J Virol* 81: 3608-17
- Iwamoto M, Watashi K, Tsukuda S, Aly HH, Fukasawa M, Fujimoto A, Suzuki R, Aizaki H, Ito T, Koiwai O, Kusahara H, Wakita T (2014) Evaluation and identification of hepatitis B virus entry inhibitors using HepG2 cells overexpressing a membrane transporter NTCP. *Biochem Biophys Res Commun* 443: 808-13
- Kuo MY, Chao M, Taylor J (1989) Initiation of replication of the human hepatitis delta virus genome from cloned DNA: role of delta antigen. *J Virol* 63: 1945-50
- Li YJ, Macnaughton T, Gao L, Lai MM (2006) RNA-templated replication of hepatitis delta virus: genomic and antigenomic RNAs associate with different nuclear bodies. *J Virol* 80: 6478-86
- Lutgehetmann M, Bornscheuer T, Volz T, Allweiss L, Bockmann JH, Pollok JM, Lohse AW, Petersen J, Dandri M (2011) Hepatitis B virus limits response of human hepatocytes to interferon-alpha in chimeric mice. *Gastroenterology* 140: 2074-83, 2083 e1-2
- Lutgehetmann M, Mancke LV, Volz T, Helbig M, Allweiss L, Bornscheuer T, Pollok JM, Lohse AW, Petersen J, Urban S, Dandri M (2012) Humanized chimeric uPA mouse model for the study of hepatitis B and D virus interactions and preclinical drug evaluation. *Hepatology* 55: 685-94
- Mutz P, Metz P, Lempp FA, Bender S, Qu B, Schoneweis K, Seitz S, Tu T, Restuccia A, Frankish J, Dachert C, Schusser B, Koschny R, Polychronidis G, Schemmer P, Hoffmann K, Baumert TF, Binder M, Urban S, Bartenschlager R (2018) HBV Bypasses the Innate Immune Response and Does Not Protect HCV From Antiviral Activity of Interferon. *Gastroenterology* 154: 1791-1804 e22
- Ni Y, Lempp FA, Mehrle S, Nkongolo S, Kaufman C, Falth M, Stindt J, Koniger C, Nassal M, Kubitz R, Sultmann H, Urban S (2014) Hepatitis B and D viruses exploit sodium taurocholate co-transporting polypeptide for species-specific entry into hepatocytes. *Gastroenterology* 146: 1070-83
- Sainz B, Jr., Chisari FV (2006) Production of infectious hepatitis C virus by well-differentiated, growth-arrested human hepatoma-derived cells. *J Virol* 80: 10253-7
- Watashi K, Urban S, Li W, Wakita T (2014) NTCP and beyond: opening the door to unveil hepatitis B virus entry. *Int J Mol Sci* 15: 2892-905
- Yan H, Zhong G, Xu G, He W, Jing Z, Gao Z, Huang Y, Qi Y, Peng B, Wang H, Fu L, Song M, Chen P, Gao W, Ren B, Sun Y, Cai T, Feng X, Sui J, Li W (2012) Sodium taurocholate cotransporting polypeptide is a functional receptor for human hepatitis B and D virus. *Elife* 1: e00049
- Zhang Z, Filzmayr C, Ni Y, Sultmann H, Mutz P, Hiet MS, Vondran FWR, Bartenschlager R, Urban S (2018) Hepatitis D virus replication is sensed by MDA5 and induces IFN-beta/lambda responses in hepatocytes. *J Hepatol* 69: 25-35

Reviewers' Comments:

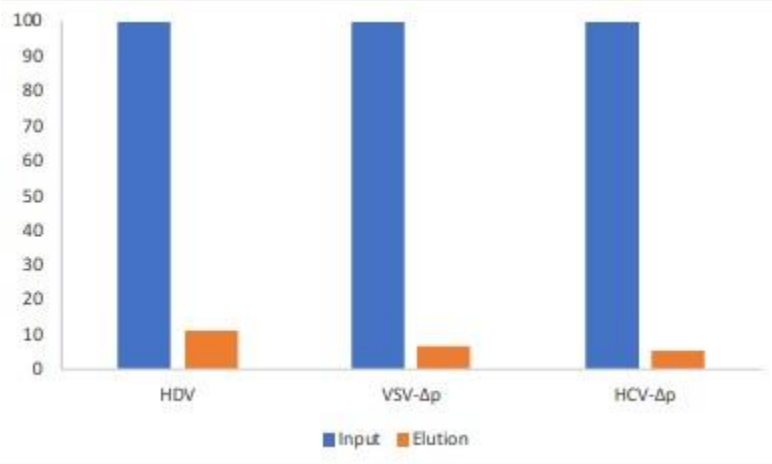
Reviewer #1:

Remarks to the Author:

This is a frustrating process. The authors are proposing potentially very interesting and important results. Their overall proposal may well fit very nicely with recent observations that viruses closely related to HDV exist in other species in the absence of any hepadnavirus (Wille, 2018; Hetzel, 2018 - the authors would do well to incorporate this information in their discussion). However, and unfortunately, the manuscript still has problems.

1. Fig. 1D – the image appears to have been manipulated. The right hand side of the HDV, VSV- Δ p and HCV- Δ p lanes has been cropped in the same manner. Furthermore, on close inspection, all three of these “lanes” appear to be identical!!

2. Fig. 1E The immunoprecipitation experiment is still not sufficiently described. How was the elution performed? How did the authors control for non-specific immunoprecipitation/elution? One good way to do this would be to use each of the antibodies against each of the supernatants. Furthermore, it is unimpressive to see that the efficiency of the IP is under 10%. I have taken the liberty to graph the data without the log representation:



3. The EM results are nice, but the authors should purify the particles by immunoprecipitation rather than heparin and should compare particles produced with and without HDV – otherwise, how do we know that the particles observed have anything to do with HDV?

4. There are several problems with the description of the strand-specific assay described on lines 497 – 514. The primers listed are opposite the sense that they should be; that is, the primer 5'-CCCGGCTAC..., is genomic sense and would be appropriate for detecting the antigenome, not the genome. Likewise for the other primer, which for some reason contains two mismatches to the HDV sequence. Moreover, without more information about the RNAs used as standards (presumably they are linear), it is not possible to evaluate the strand-specificity. Mis-priming during the RT step on circular HDV RNA can decrease strand-specificity in ways that would not be detected using linear RNA templates. One might get around this problem by using RNAs of dimer or greater length.

5. The RT-PCR results showing detection of full-length HDV RNA must include controls run without RT. Amplification of the full-length HDV RNA by RT-PCR is difficult and this reviewer is not aware of other reports to have done so. Although the authors certainly may have succeeded in this task, because HDV replication was initiated by transfection of an HDV trimer plasmid DNA, it is possible – even likely – that the plasmid was not completely eliminated by the DNase digestion and that the assay is simply

detecting the HDV plasmid.

6. Is the cytotoxicity really about 40% (Fig. S2A)?? If so, we are all wasting our time.

Reviewer #2:

Remarks to the Author:

The authors have carefully addressed the points that I had raised during the first round of review. Please check the manuscript carefully regarding any references of "expressed HDV", e.g. line 240 "As control, we performed HBV infection assays in Huh-106 cells expressing HDV". This should be corrected throughout.

Congratulations on this very nice, intriguing body of work!

Reviewers' comments:

Reviewer #1 (Remarks to the Author):

This is a frustrating process. The authors are proposing potentially very interesting and important results. Their overall proposal may well fit very nicely with recent observations that viruses closely related to HDV exist in other species in the absence of any hepadnavirus (Wille, 2018; Hetzel, 2018 - the authors would do well to incorporate this information in their discussion). However, and unfortunately, the manuscript still has problems.

Reply: We feel sorry about this comment. The revision of our work and manuscript was very intense and, we believe, allowed incorporation of all the points raised by this Reviewer as well as of most points of the other Reviewers. As for the remaining issues, we have done our best to address them in this new revised manuscript.

We have incorporated in the revised Introduction (page 4) the recent observations that viruses closely related to HDV exist in other species in the absence of any hepadnavirus, which indeed gives strong credit to our observations that HDV can be transmitted by hepadnavirus-unrelated viruses.

1. Fig. 1D – the image appears to have been manipulated. The right hand side of the HDV, VSV- Δ p and HCV- Δ p lanes has been cropped in the same manner. Furthermore, on close inspection, all three of these “lanes” appear to be identical!!

Reply: We are humbly asking to accept our most sincere apologies for not having detected the problem with this image, which obviously shows that the three lanes (HDV, VSV- Δ P, HCV- Δ P in our Fig 1D) are absolutely identical. After careful examination of the image, it appears that the 4 lanes (*i.e.*, with the positive control (*Ctrl* in Fig 1D)) are the same. We are sorry to say that we have been too quick, owing to the intensity of the revision work and we should have been able to immediately detect this absurd occurrence. In addition, we are most grateful with this Reviewer for detecting the mistake.

We truly do not understand what happened. The only bit of explanation that we think about would be a bizarre event generated with a Bio-Rad ChemiDoc™ Imager that seems to have replicated part of the image (likely part of the *Ctrl* lane). I must say that I have never come across such a situation during my career. Actually, we usually use in most of our work (including this study) the Odyssey Imaging System from LI-COR Biosciences as it allows linear integration of signals on scales of several logs which is essential when dealing with quantifications (see, for example, the Western blot image of Fig 3E that was generated with this system). However, because of a breakdown of this equipment that occurred during the revision period and of its subsequent repairing time, we had to use a Bio-Rad ChemiDoc™ Imager for the image of Fig 1D. We thus believe that either we did not use it properly or, alternatively, that something got wrong in the system, but the situation is this one: we were happy when we saw the three pairs of bands corresponding to the exact sizes of L-HDAg and S-HDAg, and we did not - and I apologize for this - think further than this.

We feel deeply sorry with the confusion it may have generated, or worse, with the possible opinion of this Reviewer who may think that the image would have been manipulated. I am respectfully asking to believe that it is certainly not the case and I trust that my professional reputation based on over 30 years of academic research in molecular virology confirms my intellectual honesty and that of my team colleagues.

Meanwhile, we have redone this Western blot using the original samples (and processed them with our Odyssey Imaging System), which is now displayed in the new revised Figure 1D.

Once again, please accept our apologies and, above everything, please be convinced of our scientific integrity.

2. Fig. 1E The immunoprecipitation experiment is still not sufficiently described. How was the elution performed? How did the authors control for non-specific immunoprecipitation/elution? One good way to do this would be to use each of the antibodies against each of the supernatants. Furthermore, it is unimpressive to see that the efficiency of the IP is under 10%. I have taken the liberty to graph the data without the log representation:

Reply: We provide a better description of the method used for this immunoprecipitation experiment in our revised manuscript (page 16). To address the concerns of this Reviewer, we now provide the results of immunoprecipitation experiments that were controlled as per his/her request, *i.e.*, using each of the antibodies against each of the supernatants (new Figure 1e). As also suggested by this Reviewer, we now display the data without the log representation. We have also worked to optimize the

antigen/antibody ratio in order to improve the recovery of HDV particles (now, of over 15%). Yet, we propose that the relatively low efficiency of this immunoprecipitation reflects the strong competition by HBV, HCV and VSV subviral particles that outnumber the HDV RNA-bearing particles.

3. The EM results are nice, but the authors should purify the particles by immunoprecipitation rather than heparin and should compare particles produced with and without HDV – otherwise, how do we know that the particles observed have anything to do with HDV?

Reply: We thank this Reviewer for his/her positive appreciation of these EM results that were performed as part of our reply to Comment #3 of Reviewer #3 who suggested to provide “a simple EM study (...) to visualize the size, distribution of these pseudo-type HDV particles”. Rather, owing to the presence of contaminants detected *via* simple EM studies (data not shown), we undertook a more sophisticated EM study of particles purified with heparin beads (Figure 1F and Supplemental Figure 3) with the help of the EM facility on our campus.

We respectfully request to this Reviewer that we can keep the EM results as they are in this report for the following reasons. Indeed, the purification of the particles by immunoprecipitation with viral surface GP antibodies may potentially improve the analysis but would not allow distinguishing HDV particles from the subviral particles of either helper virus as they both share the same surface antigen. Furthermore, we are concerned that such a study for which we would have to determine and optimize many conditions for 3 different viruses investigated simultaneously (HDV, HCV- Δ P, VSV- Δ P) would require a tremendous effort, of largely over a year, and would not provide incremental results relative to the set of data in this report. Particularly, from our own experience, eluting antibody-captured particles from beads or equivalent material is technically a very difficult issue and also depends on variable antigen/antibody affinities between the three virus types. Given the uncertainty of these outcomes, we think that this is beyond what is reasonably needed to characterize these novel particles for which we believe we have provided multiple and convergent evidence with different biochemical and functional *in vitro* or *in vivo* assays in this report. Finally, that we did not detect particles when pSVLD3 was expressed alone (Figure 1F), that we detected HDV particles in addition to subviral particles when pSVLD3 and GP-expression plasmids were co-expressed (Figure 1F and Supplemental Figure 3) but that we only detected subviral particles when GP-expression plasmids were individually expressed (Supplemental Figure 3) argues that the particles observed are HDV particles.

4. There are several problems with the description of the strand-specific assay described on lines 497 – 514.

Reply: We thank this Reviewer for inviting us to clarify our methodologies that have been modified in the Methods section of our new revised manuscript. The strand-specific RTqPCR method utilized in the present study to discriminate and quantify genomic and antigenomic HDV RNA consists in reverse transcription reactions with strand-specific primers (opposite polarity as compared to the template) followed by qPCR reaction. We address below the five concerns of his/her comment.

Concern #1: *The primers listed are opposite the sense that they should be; that is, the primer 5'-CCCGGCTAC....., is genomic sense and would be appropriate for detecting the antigenome, not the genome.*

Reply: We apologize for our sentence “... RNAs were reverse transcribed ... using strand-specific oligonucleotides primers for genomic RNA 5'-CCGGCTACTTCTTTCCCTTCTCTCGTC and for antigenomic RNA 5'-CACCGAAGAAGGAAGGCCCTGGAGAACAA” that was unclear. It has been replaced by “..., extracted RNAs were reverse transcribed ... by using specific primer: genomic primer 5'-CCGGCTACTTCTTTCCCTTCTCTCGTC for genomic-sense cDNA synthesis and antigenomic primer 5'-CACCGAAGAAGGAAGGCCCTGGAGAACAA for antigenomic-sense cDNA synthesis” in the revised Methods (page 15).

Concern #2: *Likewise for the other primer, which for some reason contains two mismatches to the HDV sequence.*

Reply: For this primer (5'-CACCGAAGAAGGAAGGCCCTGGAGAACAA), which detects the genomic HDV RNA and allows amplification of antigenomic-sense cDNA, its two mismatches to the HDV sequence in Genbank M21012 are due to the fact that when we sequenced the pSVLD3 plasmid from the EBV-Rev primer (1551-1570 on pSVLD3 Addgene sequence), we detected these mismatches at positions 1754 and 1768 in the pSVLD3 Addgene sequence. We therefore decided to synthesize this primer in order to best match our sequence and also because the identical primer was used in a previous description of the HDV RNA strand-specific RTqPCR assay by Li et al., (2006).

Concern #3: Moreover, without more information about the RNAs used as standards (presumably they are linear), it is not possible to evaluate the strand-specificity.

Reply: We have improved in our revised Methods section the description of the genomic and antigenomic HDV RNAs used as standards for this strand-specific RTqPCR assay (page 15). They were obtained by *in vitro* transcription of a set of HDV DNA amplicons flanked by T7 promoters using a commercially available kit according to manufacturer's instructions (RiboMAXTMExpress T7, Promega). The full-length linear RNAs were treated with RNase-free-DNase, followed by RNA purification (GeneJET RNA purification kit, Thermo Fisher Scientific) and quantified using a Nanodrop device (Thermo Fisher Scientific). The genomic or antigenomic HDV RNA calibration standards were diluted in RNase-free water and stored at -80°C in single use aliquots. The characterization of genomic and antigenomic RNA standards (artificial RNA) with the correct primer and the respective opposite primer were performed as described previously by Giersch et al. 2017; Freitas et al 2012; Gudima et al 2007.

Concern #4: Mis-priming during the RT step on circular HDV RNA can decrease strand-specificity in ways that would not be detected using linear RNA templates.

Reply: Mis-priming is defined as non-specific DNA-primer binding and extension during reverse transcription. Regarding HDV genomic and antigenomic HDV RNA, since both molecules display high degree of intramolecular base pairing it must be considered two types of mispriming: within the same molecule (intramolecular mis-priming) or within a molecule of reverse polarity (intermolecular mis-priming). Strand specific cDNA synthesis was carried out using specific primers (to minimize RT priming at multiple points as with random primers) using a reverse transcriptase with impaired/reduced ribonuclease-H activity under a significantly low temperature incubation, two factors shown to reduce significantly the potential of template switch events during reverse transcription. Using RNaseH⁻ RTs, during elongation of the nascent DNA chain, the RNA template is not degraded and remains as a double stranded DNA/RNA molecule of high stability disfavoring the dissociation of the RT from the template. In other words, as the nascent cDNA remains complexed to the RNA template, it is unlikely to find and bind a different acceptor RNA to allow template switching and production of chimeric cDNAs or cDNAs carrying internal deletions.

The possibility of intermolecular mis-priming was experimentally checked and the results obtained, as presented in the Supplemental Figure 1F indicate that intermolecular mis-priming is a very rare event. Specifically, it is as low as 0.000001% using 10¹¹ copies of genomic RNA as template and a primer of the same polarity and even lower when reverse transcription was carried out using 10¹¹ copies of antigenomic HDV RNA as template and a primer of antigenomic polarity, suggesting that in our experimental conditions, the primer of genomic polarity almost exclusively detects antigenomic HDV RNA and *vice-versa*.

Intramolecular mispriming, defined as non-specific binding of the DNA-primer to the same molecule was evaluated by assessing the linearity of the reverse transcription step. We foresee that mispriming upstream of the specific primer-binding site would not interfere with specific primer binding and extension (cDNA synthesis) and quantification by qPCR. The reverse scenario, mispriming downstream the specific primer-binding site could have a more important impact, although almost impossible to predict, on the kinetics of primer extension and qPCR detection sensitivity. To determine the efficiency of RNA-to-cDNA conversion we analyzed the linearity and range of the designed RTqPCR assay. We performed cDNA synthesis using a 10-fold serial dilution ranging from 10¹¹ to 10 copies of the *in vitro* synthesized genomic and antigenomic HDV RNA and the results show an efficient and RNA dose-dependent cDNA synthesis that results in a qPCR standard calibration curve with a slope of -3.3 ± 10% reflecting an efficiency close to 100%. It is our opinion that the linearity of the RT reaction over this wide range suggests rare intramolecular mispriming events. We also carefully analyzed the dissociation curves of the products obtained from qPCR and there is no indication of any extra subproduct being produced other than the expected correct amplicon of less than 100bps with a single dissociation temperature.

Concern #5: One might get around this problem by using RNAs of dimer or greater length.

Reply: Unit length linear HDV RNA standards should closely mimic the circular HDV RNA, the only type of HDV RNA molecules incorporated into particles that are secreted from the cells. The major difference is that HDV genome inside the particles has no end. Our data strongly suggests that our strand specific genomic and antigenomic HDV RNA quantification by RT-qPCR is not significantly biased by inter or intramolecular mispriming. We anticipate that the number of mispriming events between a linear and a circular RNA molecule of the same size would be similar. Therefore, only one concern remains, strand displacement during cDNA synthesis resulting in HDV cDNA concatemers that would lead to an over-estimation of the input RNA by qPCR. Because, RTs have limited processivity (Mohr et al., 2013), this consideration is likely to have little effect on large circRNAs (Szabo and Salzman, 2016). For the reasons

explained above, it is our opinion that there would be no advantage or significant improvement in our assays from using dimeric or greater length RNA standards.

Finally, we wish to recall that there is not a standard protocol for quantification of HDV RNA by RTqPCR though several groups regularly use one-step RT-qPCR assays (e.g., Ferns et al., 2012; Scholtes et al., 2012; Karatayli et al., 2014). Likewise for calibration standards, there are no recognized calibration standards available for HDV RNA quantification and the quantitative data generated by different laboratories are produced by different RTqPCR protocols that use HDV plasmid DNA (Le al., et al 2005; Hofmann et al., 2010; Mederacke et al., 2010; Zachou et al., 2010) or *in vitro*-transcribed genomic or antigenomic HDV RNA standards (Freitas et al., 2012; Gudima et al., 2007; Giersch et al., 2017) for calibration of assays. Interestingly, despite their differences, these protocols give comparable results for the HDV RT-qPCR assays.

5. The RT-PCR results showing detection of full-length HDV RNA must include controls run without RT. Amplification of the full-length HDV RNA by RT-PCR is difficult and this reviewer is not aware of other reports to have done so. Although the authors certainly may have succeeded in this task, because HDV replication was initiated by transfection of an HDV trimer plasmid DNA, it is possible – even likely – that the plasmid was not completely eliminated by the DNase digestion and that the assay is simply detecting the HDV plasmid.

Reply: We provide in the revised Figure 1B the controls run without RT and/or without DNase treatment. These data indicate that we could detect full-length HDV RNA from replicated RNAs but not from HDV trimer plasmid DNA. Please note that the “No GP” control, which does not yield full-length HDV RNA detection in the transfected cells supernatants, as well as the detection of full-length HDV RNA in the gradient (Figure 1G), in the supernatants of co-infected cells (Figure 6B, F & J) or in the sera of co-infected animals (Supplemental Figure 7B) also indicate that this method detects replicated and secreted HDV RNA. Furthermore, no PCR signal could be detected in the supernatants using a genomic primer during the reverse transcription step before PCR amplification, indicating absence of antigenomic HDV RNA secretion

6. Is the cytotoxicity really about 40% (Fig. S2A)?? If so, we are all wasting our time.

Reply: We thank this Reviewer for pointing out this mistake in the display of this Fig. S2A. Indeed, to experimentally address the Point #3 of this Reviewer and the Point #2 of Reviewer #2 (“2. In figure 1a, the release of virus through cell death should be ruled out.”) of our previous revision, we had tested several variations from our HDV production protocol, including production in media with or without 2% DMSO, OptiMEM, DMEM+FBS (different FBS doses) and daily change of media vs. 6 day-long conditioned media. However, by error, the previous Fig. S2A showed the toxicity results from supernatants of cells transfected with the indicated constructs and cultivated using the latter condition, *i.e.*, harvested at day 6 post-transfection without daily changing of the media, which we generally do not use in our experiments and which raises cytotoxicity levels.

In our standard conditions (adapted from Ref #29), *i.e.*, for which transfected cells are maintained in a daily-changed William’s E medium supplemented with 2% FBS +/- 2% DMSO, the average cytotoxicity at day 6 is below 15%, as shown in the revised Fig. S2A, and is similar to that of non-transfected cell cultured in parallel. Note that this mistake only concerns Fig. S2A but not the other panels. We have corrected this figure in the revised manuscript and we apologize for the inaccuracy.

Reviewer #2 (Remarks to the Author):

The authors have carefully addressed the points that I had raised during the first round of review. Please check the manuscript carefully regarding any references of “expressed HDV”, e.g. line 240 “As control, we performed HBV infection assays in Huh-106 cells expressing HDV”. This should be corrected throughout.

Reply: We thank this Reviewer for his/her positive appreciation of our revised manuscript and for pointing out these sentences that are corrected throughout in the new revised manuscript.

Congratulations on this very nice, intriguing body of work!

Reply: We thank this Reviewer for his/her nice comment on our study!

Reviewers' Comments:

Reviewer #1:

Remarks to the Author:

The authors have adequately addressed the concerns raised in the prior reviews. The authors' findings are very interesting and important for the HDV field, and, as I mentioned in the previous review, provide an intriguing fit with recent reports (some published), based on metagenomic analysis, that viruses very closely related to HDV exist in other species in the absence of any detectable hepadnavirus.

Reviewers' Comments:**Reviewer #1 (Remarks to the Author):**

The authors have adequately addressed the concerns raised in the prior reviews. The authors' findings are very interesting and important for the HDV field, and, as I mentioned in the previous review, provide an intriguing fit with recent reports (some published), based on metagenomic analysis, that viruses very closely related to HDV exist in other species in the absence of any detectable hepadnavirus.

Reply: We thank this Reviewer for his/her positive appreciation of our revised manuscript and comment on our study.